A NUMERICAL MODEL FOR FLOW AND SEDIMENT TRANSPORT IN ALLUVIAL-RIVER BENDS

by

Tatsuaki Nakato, John F. Kennedy, and John L. Vadnal

Sponsored by

U.S. Army Engineer Waterways Experiment Station
Vicksburg, Mississippi

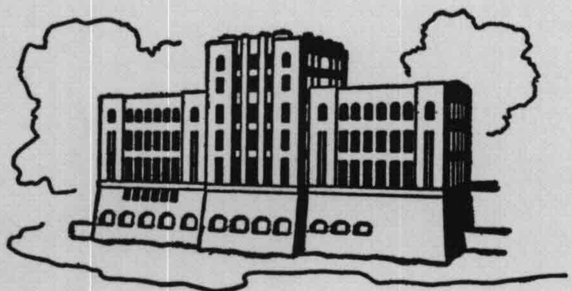

IIHR Report No. 271

Iowa Institute of Hydraulic Research
The University of Iowa
Iowa City, Iowa 52242

December 1983

Final Report

A NUMERICAL MODEL FOR FLOW AND SEDIMENT TRANSPORT IN ALLUVIAL-RIVER BENDS

by

Tatsuaki Nakato, John F. Kennedy, and John L. Vadnal

Sponsored by

U.S. Army Engineer Waterways Experiment Station
Vicksburg, Mississippi

IIHR Report No. 271

Iowa Institute of Hydraulic Research
The University of Iowa
Iowa City, Iowa 52242

December 1983

Final Report

PREFACE

The investigation reported herein was conducted for and sponsored by the U.S. Army Engineer Waterways Experiment Station (WES, Contract No. DACW39-80-C-0129). The numerical aspects of the investigation served as the basis for the Ph.D. thesis of Mr. John Vadnal. The companion, experimental investigation has been reported by Odgaard and Kennedy[3]. The numerical model developed in this phase of the investigation analyzes and predicts flow and sediment-transport distributions in alluvial-channel bends. The authors wish to acknowledge their gratitude to Mr. Steve Maynord of WES for his continuing encouragement and assistance during the course of this study.

CONTENTS

CONVERSION FACTORS, U.S. CUSTOMARY TO METRIC(SI) UNITS OF MEASUREMENT

U.S. customary units of measurement used in this report can be converted to metric (SI) units as follows:

Multiply	By	To Obtain
inches	0.0254	meters
feet	0.3048	meters
feet per second	0.3048	meters per second
cubic feet per second	0.02831685	cubic meters per second
miles (U.S. statute)	1.6093	kilometers
pounds (mass)	0.4535924	kilograms
pounds (force) per square inch	6894.757	pascals
tons (short) per foot per day	2.9763	tons per meter per day

A NUMERICAL MODEL FOR FLOW AND SEDIMENT TRANSPORT IN ALLUVIAL-RIVER BENDS

PART I: INTRODUCTION

Background

1. Two of the most striking and intriguing features of natural alluvial streams are their tendency to meander, and the downstream migration of the meanders. In addition to being a fascinating natural phenomenon and posing some of the most nettling problems in the whole of river mechanics, river meandering, and in particular the bank erosion attendant to the growth and migration of the meander loops, has become a major international problem. According to the final report on work conducted under the Streambank Erosion Control Evaluation and Demonstration Act of 1974[1] (Section 32, Public Law 32-251, submitted in December 1981), approximately 142,000 bank-miles of streams and waterways are in need of erosion protection. The cost to arrest or control this erosion by means of conventional bank-protection methods currently available is estimated to be in excess of $1 billion annually. For the Upper-Mississippi River basin alone, the cost was estimated to be in excess of $21 million annually. These figures exceed the benefits derived by a large margin, thereby rendering many of the bank-erosion-control projects uneconomical on a cost/benefit basis. As a result, most bank-erosion losses continue unabated. Attempts to halt the erosion are often limited to piecemeal protection along isolated bank reaches, at public or private facilities on streambanks, or at highway crossings. However, as such facilities increase in value and as the consequences of failure become greater, the threshold level of acceptable risk becomes smaller. At the same time, traditional channel-stabilization measures have become extremely expensive and are not acceptable to environmentalists in many instances.

2. Nowhere has the problem come to sharper focus than along the Sacramento River, California. The Sacramento River Valley contains the

Nation's finest (and most rapidly disappearing) agricultural land. According to Brice[2], river-bank erosion along the unprotected stretches of the approximately 200-mile-long reach of the Middle and Lower Sacramento River is producing an average annual loss of nearly two acres of farmland per mile. Even when evaluated against current inflated land values, traditional means of bank protection (for example rock riprap) are so expensive that they cannot be justified economically. The problem is compounded by some of the material eroded from the banks being transported to the dredged navigation channels of the Lower Sacramento River system and San Francisco Bay. Bank protection along the upper reaches by traditional means can be justified economically only if it can be demonstrated that the reduced erosion will result in less dredging for navigation-channel maintenance. Thus, the problem poses two general questions: (1) Will it be possible to develop alternative bank-protection measures that are effective, environmentally acceptable, and economically justifiable when evaluated against land values alone?; and (2) Will reduced bank erosion upstream be reflected in reduced downstream dredging (and how much, and when), or is the material eroded from the banks being deposited at other locations (e.g., on point bars) along the river?

3. It is against this backdrop that the Institute of Hydraulic Research at The University of Iowa entered into a contract with the Army Corps of Engineers, Sacramento District, in 1980 to conduct an investigation directed at developing improved, "unconventional" bank-protection methods for application along the Sacramento River. It was realized that the investigation should also include laboratory testing of the techniques or the devices proposed, and development of an analytical model, likely a computer-based one, for routing of flow and sediment through channel bends. Funds for conduct of the laboratory investigation and development of the routing model were not available from the Sacramento District, but were provided by the Waterways Experiment Station.

4. A report describing the new bank-protection method developed under the contract with the Sacramento District (Contract No. DACW05-80-C-0083) and the laboratory testing supported jointly by the Sacramento District and the Waterways Experiment Station (Contract No. DACW39-80-C-0129) was submitted in May 1982[3]. The present report is concerned solely with the second phase of the WES-sponsored project: development of a numerical model for analysis and prediction of flow and sediment-transport characteristics in the bends of meandering alluvial channels.

Analytical Strategy

5. The point of departure for development of the numerical model is the analytical work reported by Falcon and Kennedy[4]. The manuscript of this paper is included herewith as Appendix A, and is to be considered an integral part of this report. An understanding of the analysis presented in PART II requires considerable familiarity with the Falcon-Kennedy analysis described in Appendix A.

6. The principal stumbling blocks encountered in the analysis of river-bend flow are the interdependency of the bed topography, flow distribution, and sediment-discharge distribution. The interaction of the vertically nonuniform distribution of streamwise velocity and channel curvature produces a secondary flow which spirals about the channel-section axis and moves the higher velocity, near-surface fluid toward the outside of the bend and the near-bed fluid toward the inside. The radially inward bed shear-stress transports bed sediment radially inward until the bed becomes inclined such that the radial-plane shear stress is balanced by the component of the moving bed layer's weight radially outward along the bed. The resulting warping of the channel bed, which produces larger depths near the outer bank, as shown in figure 1, leads to a redistribution of the streamwise flow, and produces much larger velocities, boundary shear stress, and unit discharge near the outer bank. This, in turn, affects the lateral distribution of unit sediment discharge. It is emphasized that the

secondary flow itself has a relatively minor impact on the distribution of flow and sediment transport in a channel bend. It is the bed warping produced by the secondary flow that is primarily responsible for the redistributions outlined above.

7. In the case of fully developed flow in a uniform curved channel (i.e., one of whose channel axis is circular in plan view), the torque generated about the channel axis by the interaction of the velocity profile and channel curvature is balanced almost exclusively by boundary shear stress. In the case of channels with nonuniform planform curvature, as occurs in meandering streams, it is necessary in the calculation of the secondary-flow strength to include the nonuniformity of the flux of moment-of-momentum (or, more simply, the torsional inertia of the flowing fluid) in the torque balance. The inclusion of the inertial effects in this case leads to a phase shift between local channel curvature and local secondary-current strength and transverse bed slope.

8. A hallmark of the numerical flow and sediment routing model developed in PART II is a partial uncoupling of the secondary flow from the distributions of primary flow and sediment transport. The principal steps in the development of the analytical framework for the numerical model are summarized with annotation as follows:

i. The strength of the secondary flow is computed for any section along a channel of nonuniform curvature. The integral-form analysis of conservation of moment-of-momentum (or torsion) is performed for a channel of rectangular cross section with depth equal to that of the same flow in a straight rectangular channel of equal slope.

ii. It is assumed that the bed topography can be adequately represented by an inclined straight line passing through the mid-width point of the equivalent rectangular channel utilized in step i, above. It is further argued that the transverse slope of the channel bed varies linearly with the strength of the secondary current. The force equilibrium of the bed layer is analyzed to relate the mean bed slope to the secondary-flow strength.

iii. The depth-integrated differential equations of continuity and of conservation of streamwise momentum then are employed to calculate the velocity field. It is assumed that the secondary-flow velocity has linear vertical distribution at any point across the channel, and the magnitude of the secondary-flow velocity is obtained from the analysis presented in Appendix A. A radial, mass-shift velocity is also included to account for the movement of fluid across the channel as the channel curvature and transverse bed slope change and even reverse. The mass-shift velocity is assumed to be uniformly distributed over the depth.

iv. The lateral distribution of unit sediment discharge across the channel at any section is computed on the basis of a power law using the local flow properties computed in step iii.

9. The analysis is limited to steady flow in channels with constant width and centerline streamwise slope. Utilization of the model requires an estimate of the stream's friction factor using some other method, such as that of Alam and Lovera[5]. The model does not allow for transverse variations of local friction factor, due to the lateral variations of local depth and velocity, nor does it compute sediment discharge by size fraction. However, the computer program is structured to accommodate these features.

PART II: ANALYTICAL MODEL

Secondary Flow in Rectangular Channels with Nonuniform Curvature

10. As indicated above, the secondary-flow calculation will be made for a rectangular channel that is "equivalent" to the warped sections. Because the analysis is of the integral form, and considers only the streamwise and lateral fluxes, over the whole channel section, of the quantities of interest, neglect of the lateral variations of the primary and secondary currents that occur in a warped channel is not judged to be a major limitation. Support for this conclusion is provided by the generally good agreement between measured transverse bed slopes and those calculated on the basis of the radial bed shear stress in the "equivalent" rectangular channel (see figure 4A).

11. The control volume to be utilized in the moment-of-momentum analysis is depicted in figure 2, and the coordinate system is defined in figure 3. The control volume can be envisioned as the central region (see figure 1) of the flow as it existed before the bed became warped by the secondary current. The primary-flow velocity profile will be described by the power law,

$$\frac{v}{V} = \frac{n+1}{n} \left(\frac{y}{d}\right)^{1/n} \tag{1}$$

where, in addition to the quantities defined* in figures 1 and 2, V = depth-averaged flow velocity and n = reciprocal of the power-law exponent. The secondary-flow velocity distribution will be approximated by a linear profile,

$$\frac{u}{U} = 2 \left(\frac{y}{d} - \frac{1}{2}\right) \tag{2}$$

---

*For convenience, symbols and unusual abbreviations are listed and defined in the Notation (Appendix C).

In general, n is greater than about 4, and figure 2A indicates that (2) is an adequate representation of the profiles for an integral analysis, in which small deviations between the actual and formulated profiles have relatively small effects. The equation expressing conservation of moment-of-momentum (torque) about the centroid of the control volume shown in figure 2 is

$$\rho \int_0^d \int_{r_i}^{r_o} \frac{v^2}{r} \left(y - \frac{d}{2}\right) dr\, dy\, r d\phi - W\rho \frac{d}{d\phi} \left[\int_0^d uv \left(y - \frac{d}{2}\right) dy\, d\phi \right.$$

$$- \tau_{or} \frac{d}{2} (r_o^{\,2} - r_i^{\,2}) \frac{d\phi}{2\pi} = 0 \qquad (3)$$

in which τ_{or} = radial component of the bed shear stress. The radial shear force exerted on the bed results principally from the velocity profile just above the bed being skewed by the secondary-flow velocity. The secondary velocity itself is relatively small compared to the primary velocity, and alone produces a minor increase in the total shear stress. It appears reasonable to assume, therefore, that it is the skewing of the primary-flow bed shear stress that produces the radial component of the bed shear, and that the latter is proportional to the skewing of the velocity profile. This will be expressed as

$$\frac{\tau_{or}}{\tau_{os}} = \beta \frac{U}{\overline{V}} \qquad (4)$$

where β = proportionality factor to be determined from measured rates of streamwise development of secondary flow in curved channels, and $\overline{V}$ = mean streamwise flow velocity. The quantity τ_{os} (hereinafter denoted simply as τ_o) will be related to the local mean velocity by means of the Darcy-Weisbach equation,

$$\tau_o = \frac{f}{8} \rho \overline{V}^2 \qquad (5)$$

where f = Darcy-Weisbach friction factor. Substitution of (1), (2), (4), and (5) into (3) and carrying out the indicated integrations yields

$$\frac{d_c}{r_c}\frac{dU}{d\phi} + g_1 U = \frac{d_c}{R_c} g_2 \overline{V} \tag{6}$$

in which

$$R_c = \frac{1}{2}(r_i + r_o) \tag{7}$$

$$g_1 = \frac{(3n+1)(2n+1)}{2n^2+n+1}\frac{\beta f}{8} \tag{8}$$

and

$$g_2 = \frac{(3n+1)(2n+1)(n+1)}{n(n+2)(2n^2+n+1)} \tag{9}$$

Equation 6 is a linear, ordinary differential equation which has for its solution

$$U(s) = U(s_o) + g_2\overline{V} \exp\left[-g_1\left(\frac{s-s_o}{d}\right)\right] \int_{s_o}^{s} \frac{d_c}{R_c(s)} \exp\left[g_1\left(\frac{s-s_o}{d}\right)\right] ds \tag{10}$$

where the change of variable $ds = R_c\, d\phi$ has been made. Note that the subscript c is used hereinafter to refer to centerline values. The quantity $U(s_o)$ is the secondary-current strength at $s = s_o$. In a field application, the centerline curvature, $1/R_c(s)$, would be determined from a map or survey and, in the case of complex channel lineament, the quadrature appearing in (10) likely would have to be evaluated numerically. This poses no problem inasmuch as the governing equation themselves must be treated numerically.

Bed Topography

12. To determine the bed topography, and therefrom the streamwise and transverse distributions of flow depth for utilization in the

numerical solution of the equations of continuity and motion of the fluid, two assumptions will be made, as follows:

i. The transverse bed profile is a straight line at every channel section. Figures 4A and 6A, and also the results presented by Zimmermann and Kennedy[6], demonstrate that the deviations of both measured and more accurately computed transverse profiles from a straight line are relatively small.

ii. The transverse bed slope varies linearly with U. This is consistent with (4) and the bed-layer equilibrium analysis presented in Appendix A, where it is shown that the local bed slope varies linearly with the local stress (14, App. A). In terms of the mean transverse bed slope, S_T(= sin β in (14, App. A)), this equation reads

$$\tau_{or} = y_b(1-p)\ \Delta\rho\ g\ S_T \qquad (11)$$

where p = bed-layer porosity; $\Delta\rho = \rho_s - \rho$, in which ρ_s = particle density and ρ = fluid density; and g = gravitational constant. Substitution of (4), (5), and (10), (15, App. A), (16, App. A), and (17, App. A), into (11) yields

$$S_T = \frac{\beta}{\alpha(1-p)} \sqrt{\frac{f}{8}}\ \frac{\sqrt{\theta_c}}{\sqrt{g \frac{\Delta\rho}{\rho} D_{50}}}\ U \qquad (12)$$

where θ_c = Shields parameter defined by (16, App. A) and α = proportionality constant between the bed-layer thickness, y_b (see figure 1), and shear velocity, u_*, used by Karim[7]. Equation (12) can be simplified to the following expression:

$$S_T = g_3 \frac{U}{V} \tag{12A}$$

where

$$g_3 = \frac{\beta}{\alpha(1-p)} \sqrt{\frac{f}{8}} \frac{\sqrt{\theta_c}}{\sqrt{g \frac{\Delta\rho}{\rho} D_{50}}} V \tag{12B}$$

Note that n and f are related by Nunner's relation (17, App. A), which is

$$n = 1/\sqrt{f} \tag{13}$$

13. It will be assumed further that the depth changes across any section due to curvature-induced inclination of the water surface are very small compared to those due to bed warping. (Note, however, that the effect of radial water-surface inclination is retained initially in the equations of motion developed in the next section, but is then shown to be negligible in the streamwise momentum equation for most meandering river situations.) The depth at any point across the channel is then given by

$$d(r,s) = d_c \pm S_T r \tag{14}$$

where the sign, ±, is adopted according as R_c (see figure 3) is positive or negative. The bed elevation at any point in the channel then is given by

$$h(r,s) = h_c(0,s_o) - S_c(s-s_o) \pm S_T r \tag{15}$$

in which, again, the sign is chosen to be the same as that of R_c.

Equations for Fluid Motion

14. The steady-flow, depth-integrated conservation equations for mass and for radial and streamwise momenta, expressed in radial coordinates, will be used for calculation of the velocity field. The continuity equation is

$$\frac{\partial}{\partial s}[V(H-h)] + \frac{1}{r}\frac{\partial}{\partial r}[r\,\overline{U}(H-h)] = 0 \qquad (16)$$

in which $\overline{U}$ = shift velocity (see figure 1) which accounts for the transverse mass shift that occurs in channels with nonuniform curvature (e.g., along meandering channels as the thalweg moves from the vicinity of one bank to the other).

15. The radial-momentum equation is

$$[\int_h^H \rho\frac{v^2}{r}\,dr\,dy]\,rd\phi + \frac{\partial}{\partial r}[\frac{1}{2}\rho g(H-h)^2 rd\phi]dr$$

$$+\frac{1}{2}\rho g(H-h)^2 dr\,d\phi - \rho g(H-h)\,dr\,rd\phi\,\frac{\partial h}{\partial r} + \tau_{or}\,rd\phi\,dr =$$

$$\frac{\partial}{\partial \phi}[\int_h^H \rho(u+\overline{U})v\,dr\,dy]d\phi + \frac{\partial}{\partial r}[\int_h^H \rho(u+\overline{U})^2 rd\phi\,dy]dr \qquad (17)$$

Substitution of (1) and (2) into (17) yields for the depth-integrated radial-momentum equation

$$\frac{(n+1)^2}{n(n+2)}\frac{(H-h)}{r}V^2 - \frac{f}{8}V(\overline{U}-U) - g(H-h)\frac{\partial H}{\partial r} =$$

$$\frac{\partial}{\partial s}[V(H-h)(\overline{U} + \frac{U}{2n+1})] + \frac{1}{r}\frac{\partial}{\partial r}[r(H-h)(\frac{U^2}{3} + \overline{U}^2)] \qquad (18)$$

16. The corresponding equation expressing conservation of streamwise momentum is

$$\frac{\partial}{\partial \phi}[\frac{1}{2}\rho g(H-h)^2 dr]d\phi - \rho g(H-h)\,rd\phi\,dr\,\frac{1}{r}\frac{\partial h}{\partial \phi} + \tau_o\,rd\phi\,dr =$$

$$\frac{\partial}{\partial\phi}\left[\int_h^H \rho v^2 dr\ dy\right]d\phi + \frac{\partial}{\partial r}\left[\int_h^H \rho v(u+\overline{U}) r d\phi\ dy\right]dr \qquad (19)$$

which, after introduction of the velocity distributions adopted for this analysis, (1), (2), and the uniformly distributed transverse shift velocity, yields the following depth-integrated streamwise-momentum equation:

$$-\ g(H-h)\frac{\partial H}{\partial s} - \frac{f}{8}V^2 =$$

$$\frac{1}{r}\frac{\partial}{\partial r}\left[rV(H-h)(\overline{U} + \frac{U}{2n+1})\right] + \frac{(n+1)^2}{n(n+2)}\frac{\partial}{\partial s}\left[V^2(H-h)\right] \qquad (20)$$

The numerical treatment of these equations is described in PART III.

Sediment-Discharge Relation

17. The local sediment discharge will be calcualted on the basis of the local streamwise velocity using a power-law relation,

$$q_t = a\ V^b \qquad (21)$$

in which q_t = total sediment discharge per unit width; and the coefficient a and exponent b are to be determined on the basis of a sediment-discharge predictor or data on the channel under consideration for its particular flow regime, bed-material size, etc., etc. The numerical program is structured such that other sediment-discharge relations can be incorporated into it. In particular, it is envisioned that the future development might utilize a formulation such as that recently developed by Karim[7], which uses an iterative procedure to calculate sediment discharge and friction factor as interdependent variables. This would permit incorporation of laterally nonuniform friction factor into the program, and calculation of the sediment discharge of each bed-material size fraction. However, time and funds did not permit undertaking of this rather major effort in the present study.

18. It is recognized that the nonlinearity of (21) can lead to calculated streamwise variations in the sediment discharge along a nonuniformly curved channel with warped bed. A correction procedure is incorporated into the numerical model which compensates for this artifact in the following way:

i. The sediment discharges computed from (21) for radial computational increments across each computation section are summed to obtain the computed total sediment discharge for the section.

ii. The sediment discharge in each radial computational increment is corrected by a factor equal to the ratio of the sediment discharge into the bend divided by the computed total sediment discharge across the section.

This insures that sediment continuity is preserved along the channel bend.

PART III: NUMERICAL MODEL

Numerical Strategy

19. The three governing equations, (16), (18), and (20), contain three unknowns: the depth-integrated streamwise velocity, $V(r,s)$; the shift velocity, $\overline{U}(r,s)$; and water-surface elevation, $H(r,s)$. The secondary-flow velocity $U(s)$, was calculated from the torsion-balance analysis and is given by (10), and the bed elevation, $h(r,s)$, was obtained from the computed average radial bed slope and expressed by (15). Numerical solution of these three strongly coupled equations proved to be quite difficult, but was greatly simplified by introducing the following restriction. Note that in (16) and (20), H appears only in the combination $(H-h)$, which is the local depth given by (14), except in the first term of (20). The streamwise water-surface slope comprises two parts: one due to the friction slope, which is of order

$$\left(\frac{\partial H}{\partial s}\right)_f = O\left(f \frac{\overline{V}^2}{8gd_c}\right) \qquad (22)$$

and a second resulting from the centrifugally-induced superelevation of the water surface and of order

$$\left(\frac{\partial H}{\partial s}\right)_s = O\left(\frac{\overline{V}^2}{gR_c} \frac{W}{L/2}\right) \qquad (23)$$

in which L = characteristic length of the curve (say, the half-wavelength of a meander). The second of these can be neglected compared to the first if

$$16 \frac{Wd_c}{R_c L} \ll f \qquad (24)$$

which is satisfied by most natural, sand-bed, meandering streams flowing in the ripple- or dune-bed regimes. If (24) is satisfied, $\frac{\partial H}{\partial s}$ in (20) may be replaced by

$$\frac{\partial H}{\partial s} = - S_c \frac{R_c}{R_c + r} \quad (25)$$

which states that the water-surface elevation is constant across all sections. Substitution of (25) into (20) yields an equation which, together with (16) forms a pair of simultaneous equations for the two velocities of interest, $\overline{U}$ and V.

20. It is convenient for numerical analysis to simplify (16) and (20) as much as possible. The radial coordinate, r, is first replaced by $R_c + r$ in (16) and the expressions for d(r,s) and $S_T(s)$, (14) and (12), are introduced, which yields

$$F_1\overline{U} + F_2V + d_cF_4 \left(\frac{\partial\overline{U}}{\partial r} + \frac{\partial V}{\partial s}\right) = 0 \quad (26)$$

where

$$F_1 = S_T(s) + \frac{d_c + S_T(s)r}{R_c + r} \quad (27)$$

$$F_2 = g_2g_3 \frac{r}{R_c} - g_1 \frac{r}{d_c} S_T(s) \quad (28)$$

and

$$F_4 = 1 + \frac{r}{d_c} S_T(s) \quad (29)$$

The flow-continuity equation (26) is normalized using the following variables:

$$\overline{U}' = \frac{\overline{U}}{\overline{V}}; \; V' = \frac{V}{\overline{V}}; \; R_c' = \frac{R_c}{W}; \; d_c' = \frac{d_c}{W};$$

$$r' = \frac{r}{W}; \text{ and } s' = \frac{s}{W} \quad (30)$$

The normalized expression of (26) becomes, after dropping the prime superscripts,

$$F_1\overline{U} + F_2V + d_cF_4 \left(\frac{\partial\overline{U}}{\partial r} + \frac{\partial V}{\partial s}\right) = 0 \quad (26A)$$

Similarly, substitution of (14) into (20) and nondimensionalization of the equation yields

$$F_1\overline{U}V + d_cF_4 \frac{\partial}{\partial r}(\overline{U}V) + \frac{U}{2n+1}[F_1V + d_cF_4 \frac{\partial V}{\partial r}]$$

$$+ [\frac{(n+1)^2}{n(n+2)} F_2 + \frac{f}{8}] V^2 + \frac{(n+1)^2}{n(n+2)} d_cF_4 \frac{\partial V^2}{\partial s} =$$

$$\frac{1}{F_r^2} S_cF_4 \frac{R_c}{R_c+r} \qquad (31)$$

where

$$F_r^2 = \frac{\overline{V}^2}{gd_c} \qquad (32)$$

21. It is also advantageous in the numerical treatment of the equations to avoid computing small derivatives of the dependent variables. Because the shift velocity is much smaller than the depth-averaged streamwise velocity, the term, $\partial\overline{U}/\partial r$ in (31) will be eliminated by the use of (26A), with the result

$$d_cF_4[\overline{U} + \frac{U}{2n+1}] \frac{\partial V}{\partial r} + \frac{F_1}{2n+1} UV$$

$$+ d_cF_4 [\frac{1}{n(n+2)} + \frac{1}{2}] \frac{\partial V^2}{\partial s} + [\frac{F_2}{n(n+2)} + \frac{f}{8}] =$$

$$\frac{1}{F_r^2} S_cF_4 \frac{R_c}{R_c+r} \qquad (31A)$$

22. The numerical strategy employed to solve for $\overline{U}$ and V proceeded as follows:

i. The local depth-averaged velocity was approximated by the Darcy-Weisbach equation,

$$V = \sqrt{\frac{8gdS}{f}} \qquad (33)$$

in which d is given by (14) and S by

$$S = S_c \frac{R_c}{R_c + r} \qquad (34)$$

which expresses continuity of energy slope across the channel.

ii. The velocity V given by (33) was substituted into (16) which was then integrated numerically to obtain the first estimate for $\overline{U}$.

iii. The value of $\overline{U}$ was substituted into (31A) which was integrated to obtain the next estimate for V.

iv. The V computed in step iii was substituted into (16) and a new estimate of $\overline{U}$ obtained.

v. The iteration procedure between (16) and (31A) was continued until satisfactory convergence, as measured by the differences between successive values of $\overline{U}$ and V, was obtained.

Further details are presented below.

Numerical Solutions for $\overline{U}$

23. In order to solve (26A) and (31A) numerically for the two unknown variables, $\overline{U}$ and V, a backward finite-difference scheme was employed. Figure 4 shows the coordinate-grid layout that was utilized. The indicies i and j represent the streamwise and radial positions, respectively. Note that the origin of the transverse coordinate was taken at the channel centerline. In discretizing both radial and streamwise derivatives of an arbitrary variable F, the following backward finite-difference scheme was utilized:

$$\frac{\partial F}{\partial r} \simeq \frac{F_{i,j} - F_{i,j-1}}{r_j - r_{j-1}} \qquad (35)$$

and

$$\frac{\partial F}{\partial s} \simeq \frac{F_{i,j} - F_{i-1,j}}{s_{i,j} - s_{i-1,j}} \qquad (36)$$

24. An approximate solution for $\overline{U}$ can be obtained from the flow-continuity equation, (16), by introducing the Darcy-Weisbach relationship and (34):

$$V^2 = \frac{8gdS_c}{f}\frac{R_c}{R_c+r} \qquad (37)$$

Substitution of (37) into (16), use of (14) and (12A), and subsequent discretization yields the following explicit expression for $\overline{U}_j$:

$$\overline{U}_j = \overline{U}_{j-1}\frac{d(R_c+r)|_{j-1}}{d(R_c+r)|_j} - 3g_2g_3\sqrt{\frac{2gS_c}{f}}\,\frac{\exp[-g_1\frac{s_i-s_{i-1}}{d_c}]}{d(R_c+r)|_j}\,T \qquad (38)$$

where

$$T = 2R_c^2(R_cS_T - d_c)[\frac{(R_cS_T-d_c)T_1}{4} + \frac{(5R_cS_T-d_c)T_2 - (d_c + 3R_cS_T)T_3}{8R_cS_T}] \qquad (39)$$

$$T_1 = \frac{t}{(t^2-R_cS_T)^2}\Big|_{j-1}^{j} \qquad (40)$$

$$T_2 = \frac{t}{t^2-R_cS_T}\Big|_{j-1}^{j} \qquad (41)$$

$$T_3 = \begin{cases} \dfrac{1}{2\sqrt{R_cS_T}}\,\ln\left|\dfrac{t-\sqrt{R_cS_T}}{t+\sqrt{R_cS_T}}\right| : & R_cS_T > 0 \\ \dfrac{1}{\sqrt{-R_cS_T}}\tan^{-1}\left[\dfrac{t}{\sqrt{-R_cS_T}}\right] : & R_cS_T < 0 \end{cases} \qquad (42)$$

and

$$t = \sqrt{\frac{R_c(d_c + S_T r)}{R_c + r}} \tag{43}$$

Note that the boundary condition $\overline{U} = 0$ was imposed at the inside (convex) bank. Equation 38 gives the approximate solution for $\overline{U}$ which can be substituted into the streamwise-momentum equation, (31A), to solve for V.

25. Once V is computed at Section I = i, the flow-continuity equation can be again utilized to solve for $\overline{U}_{i,j}$ in the iterative process without utilizing the Darcy-Weisbach relationship. The final discretized form of (16) in terms of V is

$$\overline{U}_j = \overline{U}_{j-1} \frac{d(R_c+r)|_{j-1}}{d(R_c+r)|_j} - \frac{(V_{i,j}d_{i,j} - V_{i-1,j}d_{i-1,j})}{2(s_{i,j} - s_{i-1,j})} \frac{[(R_c+d)^2|_j - (R_c+d)^2|_{j-1}]}{d(R_c+r)|_j} \tag{44}$$

Numerical Solution for V

26. Discretization of the streamwise-momentum equation, (31A), yields the following quadratic equation for $V_{i,j}$:

$$AV_{i,j}^2 + BV_{i,j} + C = 0 \tag{45}$$

where

$$A = \frac{F_2}{n(n+2)} + \frac{f}{8} + \frac{d_c F_4}{s_{i,j} - s_{i-1,j}} \left[\frac{1}{n(n+2)} + \frac{1}{2}\right] \tag{46}$$

$$B = \frac{d_c F_4}{r_j - r_{j-1}} \left[\overline{U}_{i,j} + \frac{U_{i,j}}{2n+1}\right] + \frac{F_1}{2n+1} U_{i,j} \tag{47}$$

and

$$C = \frac{-d_c F_4}{r_j - r_{j-1}} \left[\overline{U}_{i,j} + \frac{U_{i,j}}{2n+1}\right] V_{i,j-1}$$

$$- \frac{d_c F_4}{s_{i,j} - s_{i-1,j}} \left[\frac{1}{n(n+2)} + \frac{1}{2}\right] V_{i-1,j}^2 - \frac{1}{F_r^2} S_c F_4 \frac{R_c}{R_c + r_j} \tag{48}$$

It should be noted that the total water discharge calculated with the computed transverse distribution of V did not equal the imposed total discharge due to discretization errors. Therefore, an adjustment was made to V at each cross section by multiplying $V_{i,j}$ by the ratio of the imposed water discharge to the computed water discharge. This ratio was typically of the order of 1.0005.

Boundary Conditions

27. The streamwise velocity, V, was specified at the inlet section ($s = s_0$) and along the inside bank of the computational reach by the Darcy-Weisbach relationship, (37). Along the inside bank, the shift velocity, $\overline{U}$, was set equal to zero.

Computer Program

28. The program PR-SEG6 consists of a main program, four subroutines, and seven sub-subroutines. Listings of the main program, the subroutines, a sample input file, and a sample output file are included in Appendix B. Note that the sample input and output shown in Appendix B are for the idealized two-bend model which is discussed in PART IV.

29. The main program first reads the common input variables from the input file called SEGDAT: $\overline{V}$, d_c, W, S_c, ρ, ρ_s, and NSEG (number of channel segments in the reach that requires new input parameters). The program, then reads the following parameters at each new channel segment: a, b, M (number of radial positions), N (number of streamwise positions), R_c, s_o, s_1 (centerline streamwise coordinate of the

downstream end of the segment), α, β, θ_c, D_{50}, and NSTEPS (number of cross sections into which the channel segment is divided). The program computes the boundary values of U and V across the inlet section using (10) and (37), and the transverse distribution of $\overline{U}$ is subsequently computed from (38). The program then advances to the next downstream section, and computes $\overline{U}$ and V according to the iterative scheme described in paragraphs 22, 24, 25, and 26.

30. Subroutine PQN was used to determine the total water discharge for a given cross section with computed transverse distributions of streamwise velocity and depth. Subroutine PG determines the g-parameters defined by (8), (9), and (12B). Subroutine EVAL evaluates the shift velocity, $\overline{U}$, given by (38).

31. The main program writes the following outputs in the output file, called OUTT, for each cross section: S_T, U_c, number of iterations required to compute satisfactory convergence of $\overline{U}$ and V, and transverse distributions of $\overline{U}$, V, d, U + $\overline{U}$, and q_t.

Sensitivity Analysis

32. The effects of the specified error tolerance for $\overline{U}$, the grid size, the transverse derivative of U, and parameters α and β on $\overline{U}$ and V were tested using the basic hydraulic and sediment parameters that were utilized in the Oakdale flume experiments conducted at the Iowa Institute of Hydraulic Research, The University of Iowa, by Odgaard and Kennedy[3]. The basic parameters were: $\overline{V}$ = 1.56 ft/s, d_c = 0.505 ft, W = 8.0 ft, R_c = 43 ft (see figure 5), S_c = 0.00104, p = 0.4, ρ_s/ρ = 2.65, $\nu = 1.21 \times 10^{-5}$ ft^2/s, D_{50} = 0.3 mm, and θ_c = 0.032.

33. The relative errors for $\overline{U}$ and V computed at each cross section were defined by

$$E_{\overline{U}} = \frac{\sum_{J=2}^{M} \frac{|\Delta\overline{U}|}{(M-1)}}{|\overline{U}|} \text{ and } E_V = \frac{\sum_{J=2}^{M} \frac{|\Delta V|}{(M-1)}}{V} \qquad (49)$$

where $\Delta\overline{U}$ and ΔV are changes in $\overline{U}$ and V between adjacent radial positions, respectively. Because $\overline{U}$ was typically at least two orders of magntiude smaller than V, the error tolerance for $\overline{U}$ was selected to be an order of magnitude larger than that for V. In the sensitivity tests, parameters α and β were set equal to 1.0 and 3.35, respectively, and a grid size of 6 in. was used. For E_V of 0.1%, two tests were run for $E_{\overline{U}}$ values of 2% and 0.4%. There were no discernible differences between two sets of values computed. An additional run with $E_{\overline{U}}$ equal to 0.2% demonstrated that this criterion was not able to be satisfied with single-precision computations. Note that E_V was of the order of 10^{-5} between successive iterations for V. It was concluded that satisfactory results could be obtained with the error tolerances of $E_{\overline{U}}$ and E_V equal to approximately 2% and 0.1%, respectively.

34. Sensitivity tests were run for different square-grid sizes. The grid size was reduced step by step until no significant changes in estimates of $\overline{U}$ and V resulted. As shown in figures 6 and 7, grid sizes of 4 in. and 6 in. yielded quite similar transverse distributions of $\overline{U}$ and V; in fact, the two sets were almost identical at the downstream end of the channel bend. From the sensitivity analysis, it was concluded that the grid size should be approximately equal to the mean flow depth. Note that the mean flow depth of the Oakdale flume was about 6 in. (see figure 5).

35. In obtaining the simplified streamwise momentum equation, (31), the secondary-flow velocity, U, was treated as a function of only s because of the assumption of constant transverse bed slope, as given by (12). However, in computing V by means of (45), the computer program utilized a radially-varied secondary-flow velocity distribution derived by Falcon and Kennedy[4]

$$\frac{U}{U_c} = \left(\frac{V}{V_c}\right)\left(\frac{d}{d_c}\right)\left(\frac{R_c}{R_c+r}\right) \qquad (50)$$

was utilized. When (50) is substituted into (20), the discretized streamwise-momentum equation, (45), yields coefficients A, B, and C that are slightly different from those given by (46), (47), and (48). In order to ascertain the validity of the computational scheme, a special test run was made with the term, $\partial U/\partial r$, retained in the streamwise momentum equation. The computed distributions of $\overline{U}$ and V are compared in figures 8 and 9 with those obtained using (45), which was developed without the term, $\partial U/\partial r$. As can be seen in these figures, the effects of the term, $\partial U/\partial r$, on overall estimates of $\overline{U}$ and V are minor.

36. The parameters α and β control the transverse bed slope, S_T, and the development rate of the secondary-flow velocity, respectively, as can be seen from (12), and (8) and (10). Figures 10 and 11 show the effects of α on the transverse distributions of $\overline{U}$ and V. As can be seen in these figures, the smaller α resulted in larger S_T, and consequently in much larger shift velocities along the initial entrance reach of the bend. The smaller α also resulted in much smaller streamwise velocities along the inside bank, because the larger S_T decreased the flow depth there. Similar effects of β on $\overline{U}$ and V are seen in figures 12 and 13. The smaller β resulted in a slower development rate of the secondary-flow velocity, and reduced the rate of the development of the transverse nonuniformity in V.

PART IV: RESULTS OF NUMERICAL SIMULATIONS

Oakdale Flume

37. The Oakdale flume shown in figure 5 is a 1:48-scale, highly idealized, undistorted model of the Sacramento River bend lying between R.M. 188 and 189, approximately. Experimental data on the streamwise distribution of the equilibrium transverse bed slope and transverse distributions of the depth-averaged streamwise velocity reported by Odgaard and Kennedy[3] were compared with the computer-simulated results. The basic hydraulic and sediment parameters described in paragraph 32 were utilized in the simulation. Additional parameters specified were: $\alpha = 1.00$, $\beta = 3.35$, grid size = 6 in., $n = 4.24$, $E_{\overline{U}} = 2\%$, and $E_V = 0.1\%$.

38. Figures 14 and 15 demonstrate generally good agreements between the measured and computed transverse distributions of the flow depth and the depth-averaged streamwise velocity, respectively, at $\phi = 20°$. The results for $\phi = 114°$ are shown in figures 16 and 17, in which the observed streamwise velocities are seen to be somewhat larger than the computed values in the outside portion of the channel. The larger measured velocities near the outside bank are believed to be attributable to the very low roughness of the exposed plywood bank of the trapezoidal flume section. Note that the friction factor was kept constant in the whole flow field in the numerical model. Figure 18 depicts extremely good agreement between the measured and computed transverse bed profiles for $\phi = 146°$.

Sacramento River

39. The Sacramento River bend between R.M. 188 and 189 shown in figure 19 was simulated for two water discharges (Q = 9,000 cfs and 25,800 cfs). Basic field data were collected in the reach in 1979 and

1980 by the U.S. Geological Survey (USGS) (Odgaard and Kennedy[3]). As can be seen in table 1, both the hydraulic and sediment parameters varied widely along the bend. Therefore, average values of the various quantities listed in table 1 were utilized for the numerical simulations.

40. The transverse distributions of the measured and computed flow depth and streamwise velocity for Q = 9,000 cfs are shown for ϕ = 80° and 126° in figures 20 and 21, and figures 22 and 23, respectively. Note that at ϕ = 80°, velocities and depths were measured at only four verticals across the channel, while they were measured at ten verticals at ϕ = 126°. Despite the fact that averaged input data were adopted for the simulation, the numerical model reproduced the field distributions surprisingly well for the low river discharge of 9,000 cfs. The distributions obtained for the higher discharge of 25,800 cfs are shown in figures 24 through 27. The agreements between the measured and predicted values are seen to be not as good as those for Q = 9,000 cfs; however, it is believed that during high flows the channel bed had not attained an equilibrium configuration. For example, the measured transverse bed slopes shown in figures 22 for Q = 9,000 cfs and figure 26 for Q = 25,800 cfs are entirely different. The field transverse bed slope was, paradoxically, much smaller during the high flow, resulting in the decreasing streamwise velocity toward the outside bank, as seen in figure 27. This type of abnormal transient phenomenon likely is a consequence of the rapidly changing flow conditions, and cannot be simulated by a steady-state numerical model. It should be noted that each Sacramento River simulation required approximately 0.7 second CPU time per 100-grid points using the PRIME-750 computer at The University of Iowa.

Idealized Single-Bend Model with Gradually Varying Radius of Curvature

41. The numerical results presented in paragraphs 37 through 40 for the Oakdale flume and the Sacramento River were obtained using constant centerline curvature. In order to demonstrate the ability of the computer program to handle nonuniform curvature, two simulations were made for single bends with gradually varying centerline curvature. These numerical simulations were made also to illustrate the behavior of flow in idealized, nonuniform river bends.

42. The first simulation was for a four-segment channel bend with stepped decreases in curvature in the downstream direction, as depicted in figure 28. The centerline radius of the first segment was 2,000 ft, and this value was increased by 2.5% for each of the subsequent three segments, resulting in a total channel length of 7,400 ft. It was found that a 5% increase in R_c produced such large transverse-bed-slope changes, which appear as sloped steps in the bed elevation, that the program would not run. Therefore, in cases in which R_c increases along a bend, the curve should be subdivided into sufficiently short subreaches that the increments in R_c are less than about 2.5%, although, as discussed in the next example, the model can accommodate larger changes in the case of decreasing R_c. The basic hydraulic and sediment parameters used were identical to those for the Sacramento River at high flow, listed in table 1. A grid size of 14.5 ft was used, and the parameters α and β were set at 0.86 and 7.13, respectively. The computed longitudinal and transverse distributions of the normalized shift velocity are shown in figures 29 and 30, respectively. In figure 29, the shift velocities computed for sections 65, 193, 321, and 449 are connected by straight lines. The shift velocity developed rapidly in the first segment, with its maximum values occurring near r/W equal to -0.25, and diminished gradually after section 193. At section 385, the shift velocity along r/W equal to -0.25 became negative, and remained so until section 469. This flow redistribution directed radially inward

was a consequence of the increased R_c. Figures 31 and 32 depict the longitudinal and transverse distributions of the depth-averaged streamwise velocity, respectively. Along the inside bank, the streamwise velocity decreased initially; however, it increased farther downstream as the larger radii of curvature produced less steep transverse bed slopes. The values of S_T at sections 1, 65, 193, 321, 449, and 513 were 0, 0.058, 0.063, 0.062, and 0.060, respectively.

43. The second idealized case simulated was a single bend with radius of curvature that decreased 10% between curve subreaches. The numerical results are not presented herein, because the qualitative characteristics are very similar to those for the two-bend curve with decreasing radius of curvature presented in the following section.

Idealized Two-Bend Model with Gradually Decreasing Radius of Curvature

44. An idealized two-bend model, shown in figure 33, was tested. The two-bend reach consisted of four segments with equal centerline length of 67.5 ft. The centerline radius of curvature of the first segment was 43.0 ft, and was reduced by 10% for each subsequent subreach. The sign of R_c was reversed after the second subreach. The simulation was made on the basis of the principal parameters used in the Oakdale flume simulation. These parameters are described in paragraph 37, except that α = 1.42 and β = 3.28 were used in the present simulation. Figures 34 and 35 show the longitudinal and transverse distributions of the normalized shift velocity, $\overline{U}/\overline{V}$, respectively. The shift velocity increased rapidly in the first segment and decreased gradually toward the end of the first bend. Once the flow entered the second bend, a mass shift took place toward the right bank due to the change in sign of the channel curvature. Note that in figure 34, the computed data points at sections 69, 205, 341, 477, and 545 are connected by straight lines. As shown in figure 35, the maximum value

of the shift velocity across the cross section was closer to the convex side of the bend. Figures 36 show the transverse distributions of the depth-averaged streamwise velocity computed at sections 1, 205, 341, and 545. The transverse location of the maximum V gradually shifted radially outward in the first segment, and reached the outside bank at section 71. The maximum V remained along the left bank until section 273, after which the flow became concentrated near the right bank. The maximum V reached the right bank at section 417 in the second bend. Because the streamwise velocity at the left bank at section 273 was much larger than that at section 1, a larger streamwise distance was required to attain redistribution of the flow in the second bend.

45. Figure 37 shows the transverse distributions of the unit total-load discharge, q_t, computed at various cross sections. The sediment-transport coefficients a and b in (21) were taken to be 0.108 and 4.0, respectively. Note that the units of V and q_t are ft/s and tons/ft/day, respectively. These coefficients yielded a mean total-load concentration of 300 mg/l (or about 5 tons/day) for the Oakdale flume. The distribution curves shown in this figure are seen to be generally congruent with those transverse distributions of the streamwise velocity shown in figure 36, because of the sediment-transport relation adopted being a power function of V.

PART V: SUMMARY AND CONCLUSIONS

Conclusions

46. The principal features of the numerical model developed herein for calculation of flow and sediment-transport distributions in alluvial-river bends may be summarized as follows:

i. The secondary-flow strength and the bed topography are uncoupled from the calculation of distributions of lateral shift velocity and streamwise velocity. This is accomplished by, first, calculating the secondary-flow strength on the basis of conservation of flux of moment-of-momentum, and, second, determining the bed topography on the basis of radial force equilibrium of the moving bed layer.

ii. The distributions of lateral shift velocity and depth-averaged streamwise velocity are calculated, for the warped channel determined as described in step i above, from the depth-integrated equations expressing conservation of mass and momentum. It was concluded that for flows which satisfy (24), it is not necessary to include the third conservation equation, that for radial-direction momentum, or to iterate among three equations to obtain a solution. The numerical scheme utilizes the backward finite-difference method, and evaluates transverse and streamwise distributions of the radial mass-shift velocity and the depth-averaged streamwise velocity.

47. Numerical simulations utilizing the model developed were made for one laboratory flow, two Sacramento River flows, and three different idealized channel bends. The principal conclusions obtained from the simulations are as follows:

i. Generally satisfactory agreement between computed and measured results was obtained by utilizing error tolerances of E_U and E_V of 2% and 0.2%, respectively. In the absence of better information, it is recommended that $\alpha = 1.00$ and $\beta = 3.50$ be utilized. In instances where actual field data are available on the rate of development and equilibrium values of S_T, α and β should be adjusted on the basis of the data.

ii. The most cost-effective square-grid size is approximately equal to the mean flow depth.

iii. The computer program is capable of simulating flow in multiple-bend channels with stepwise-varying radius of curvature. On the basis of the numerical simulations, it was found that the maximum permissible stepwise change of centerline curvature for which the program will run is about 2.5% in the case of increasing R_c, and about 10% for decreasing R_c.

48. Further development and improvement of the model should include the following:

i. More complete and modern sediment-discharge and friction-factor models should be incorporated into the model. In particular, it is recommended that Karim's[7] model be incorporated into the program to permit calculation of lateral and streamwise variations of friction factor based on local flow depth, velocity, and sediment discharge. Karim's model is unique in that it formally takes into account the interdependence between sediment discharge and friction factor, an interdependency which appears to be very important in channel-bend flows.

ii. A further refinement of the flow calculation would involve incorporation of the radial-momentum equation, (18). This would permit application of the model to bends with relatively short radius of curvature. However, the numerical model would become much more complex, and would require significantly more computer time. The model developed herein is believed to be adequate in its flow-calculation aspects for most natural alluvial-channel bends.

iii. An effort should be made to incorporate features into the model to permit prediction of the occurrence and characteristics of point bars and their effects on the flow field. It is believed that this likely will require incorporation of the radial-momentum equation and a more refined sediment-discharge predictor, as described above.

iv. As is generally the case in river-flow analysis, there is a pressing need for detailed, diagnostic-quality data on the distributions of velocity and sediment discharge from both natural and laboratory streams.

v. After some experience is gained with the model, the computer program should be reviewed, made more compact and concise where possible, and a user's manual for the program should be prepared.

REFERENCES

1. U.S. Army Corps of Engineers, Final Report on the Streambank Erosion Control Evaluation and Demonstration Act (Section 32, Public Law 93-251), U.S. Government Printing Office, Dec., 1981.

2. Brice, B.J., "Lateral Migration of the Middle Sacramento River, California," U.S. Geological Survey, Water-Resource Investigations, 77-43, U.S. Department of the Interior, July 1977.

3. Odgaard, A.J., and Kennedy, J.F., "Analysis of Sacramento River Bend Flows, and Development of a New Method for Bank Protection", IIHR Report, No. 241, Iowa Institute of Hydraulic Research, The University of Iowa, Iowa City, Iowa, May 1982.

4. Falcon, M. and Kennedy, J.F., "Flow in Alluvial-River Curves," accepted for publication in Journal of Fluid Mechanics, Jan., 1983.

5. Vanoni, V.A., (ed.), Sedimentation Engineering, American Society of Civil Engineers, Manuals of Engineering Practice, No. 54, 1975.

6. Zimmermann, C. and Kennedy, J.F., "Transverse Bed Slopes in Curved Alluvial Stream," Journal of the Hydraulic Division, ASCE, Vol. 104, No. HY1, Jan., 1978.

7. Karim, M.F., "Computer-Based Predictors for Sediment Discharge and Friction Factor of Alluvial Streams," Ph.D. thesis submitted to the Department of Mechanics and Hydraulics, The University of Iowa, December 1981 (Also available as IIHR Report No. 242, Iowa Institute of Hydraulic Research, The University of Iowa.)

Table 1

Hydraulic and Sediment Parameters Used in Simulating the Sacramento River

Parameter	Low Flow		High Flow	
	Measured Range	Average Value Used	Measured Range	Average Value Used
Q (cfs)	7,800-9,900	9,000	24,000-28,400	25,800
A (ft^2)	3,190-4,340	3,960	6,370-7,600	6,950
$\bar{V}$ (ft/s)	2.12-2.60	2.28	3.15-4.00	3.72
d_c (ft)	5.6-15.2	10.28	8.6-23.1	15.0
R_c (ft)	1,800-3,920	2,540	1,800-3,920	2,430
W (ft)	263-570	385	275-778	463
n	6.3-10.5	8.2	5.8-12.5	8.6
D_{50}(mm)	0.7-6.3	1.0	0.7-10.8	1.3
S_T*	0.01-0.15	0.053	0.018-0.145	0.065
α		0.374		0.711
β		2.39		3.82
Θ_c		0.045		0.050
Grid Size (ft)		9.6		9.6
$E_{\bar{U}}$ (%)		0.1		0.1
E_V (%)		1.0		1.0

* Maximum equilibrium transverse bed slope

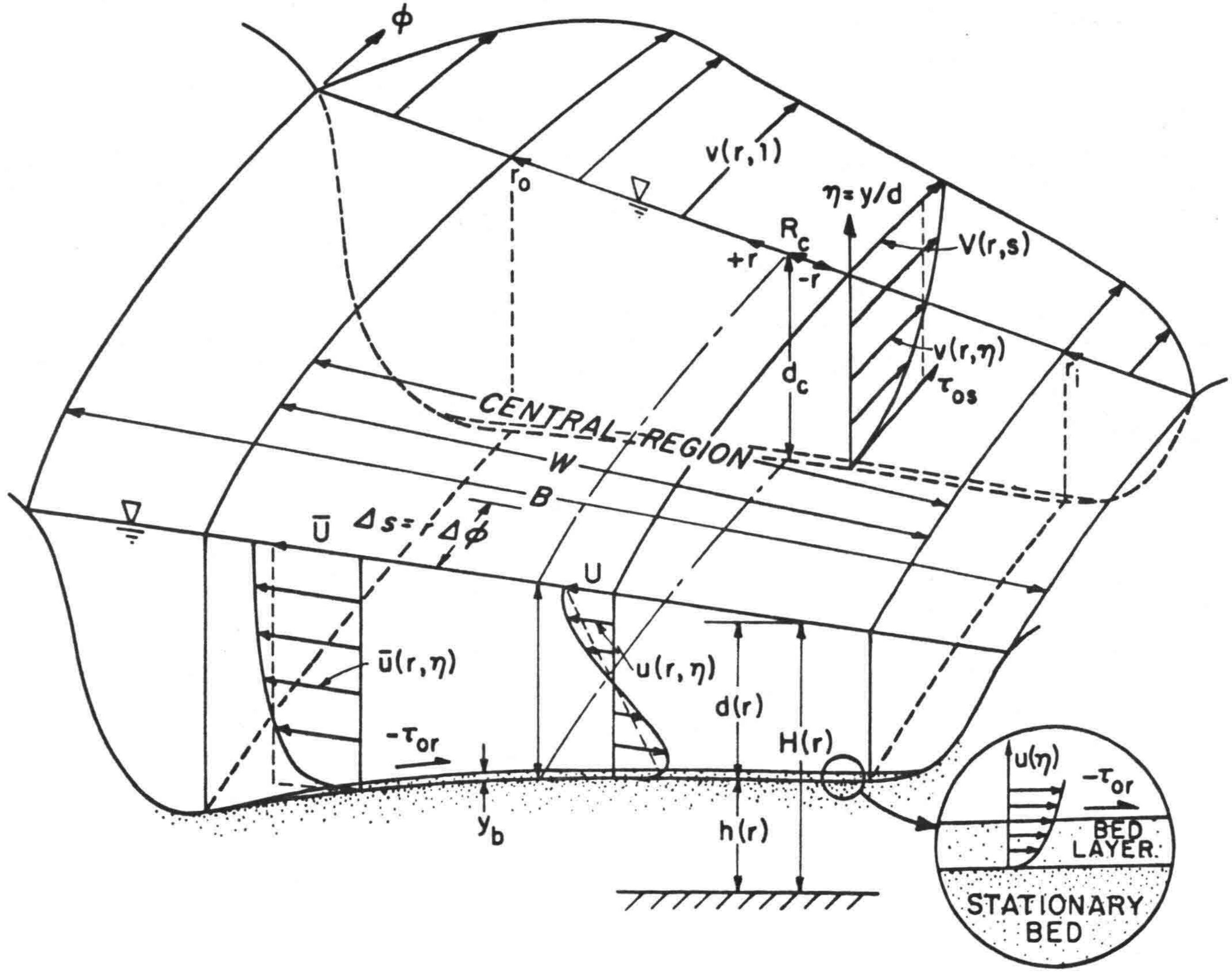

Figure 1 Definition sketch of flow in river bends

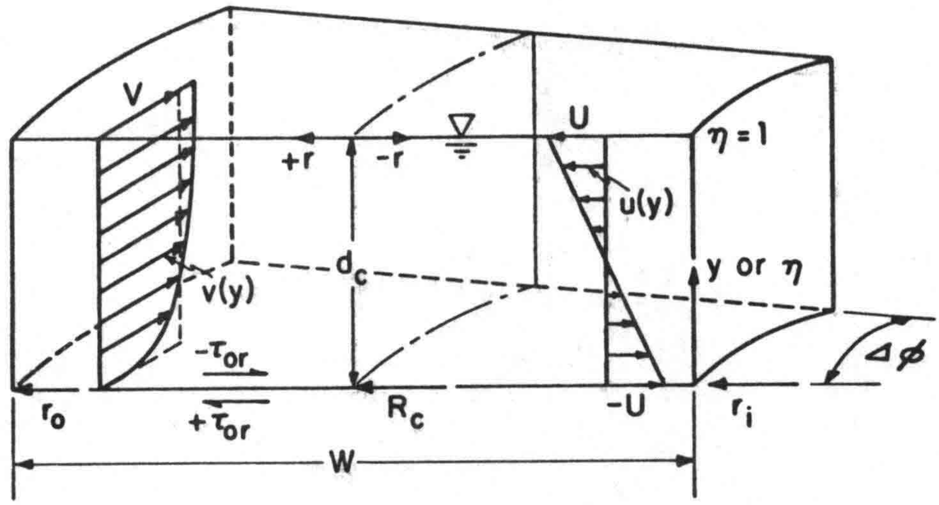

Figure 2 Control volume used in analysis of secondary flow in channels with nonuniform curvature

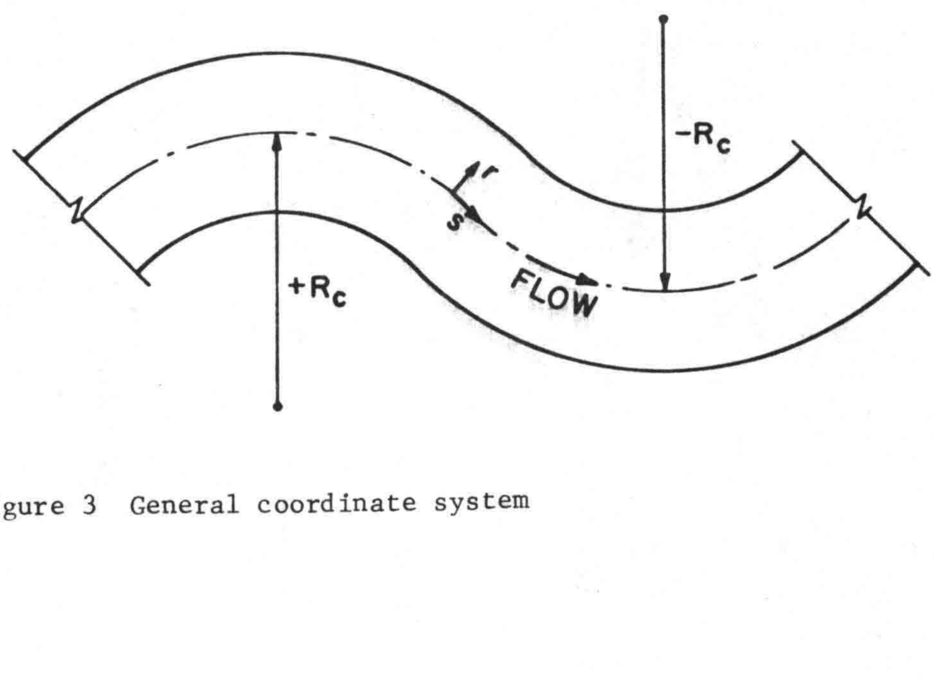

Figure 3 General coordinate system

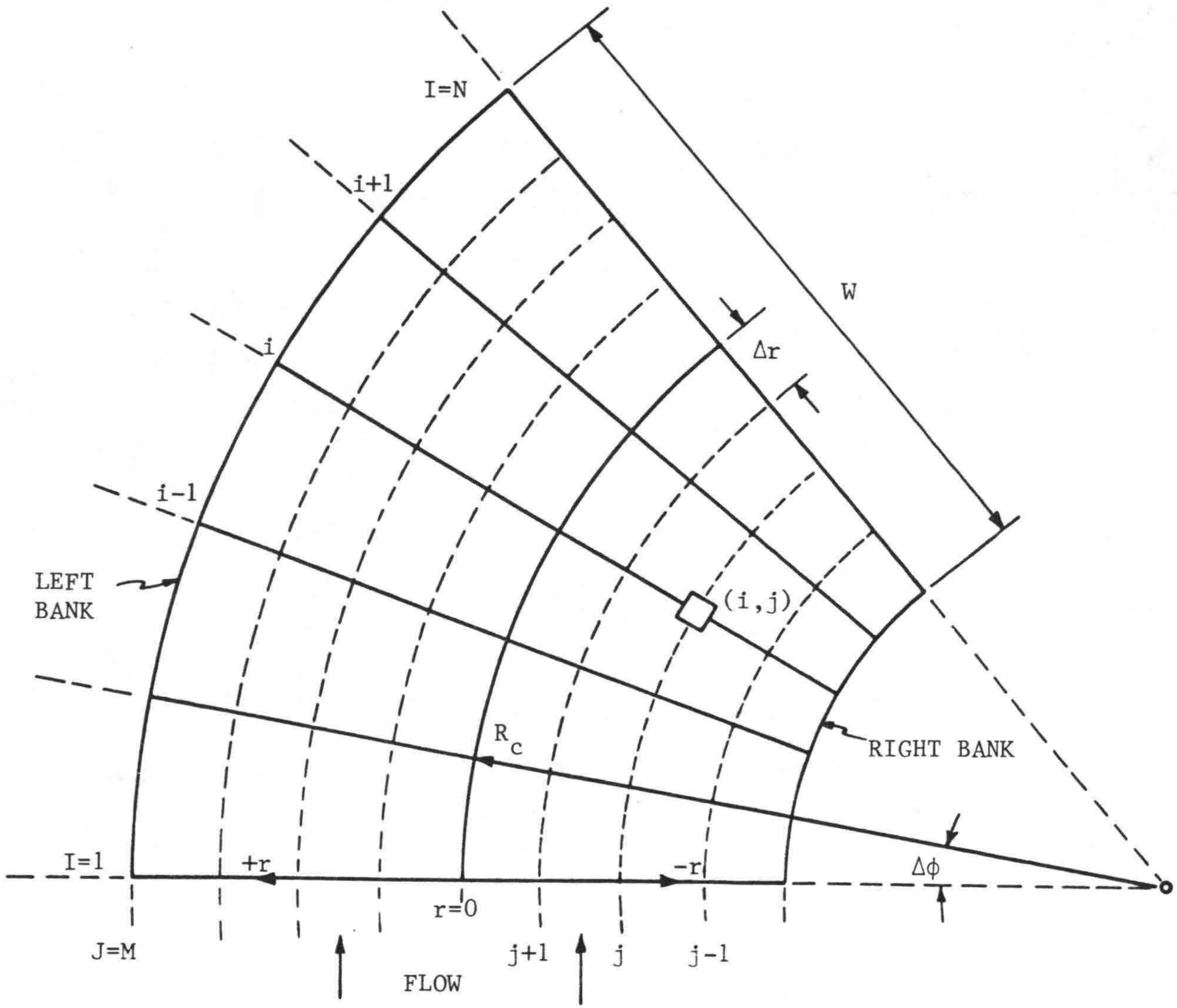

Figure 4 Coordinate-grid layout for numerical analysis

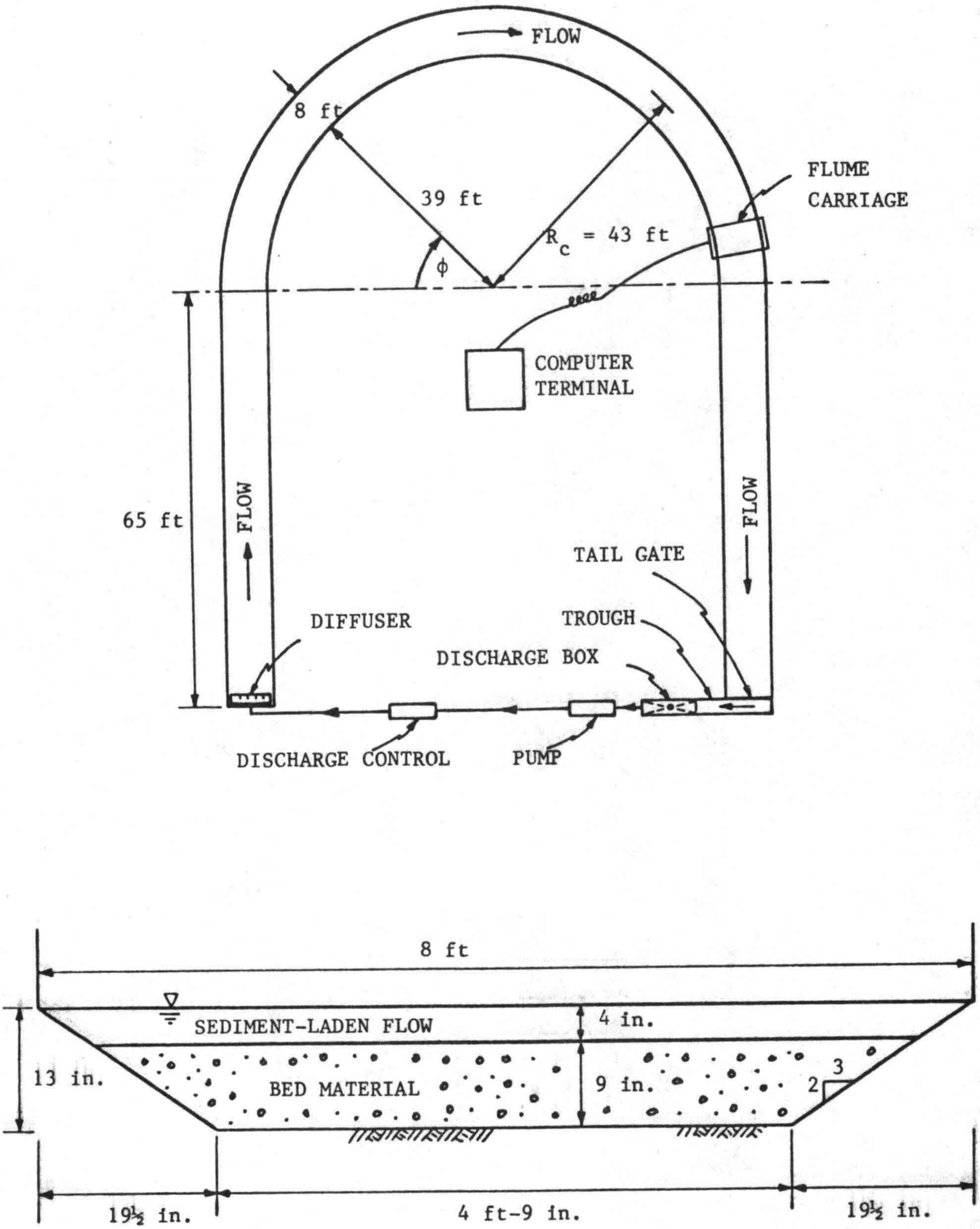

Figure 5 Plan and section views of the Oakdale flume

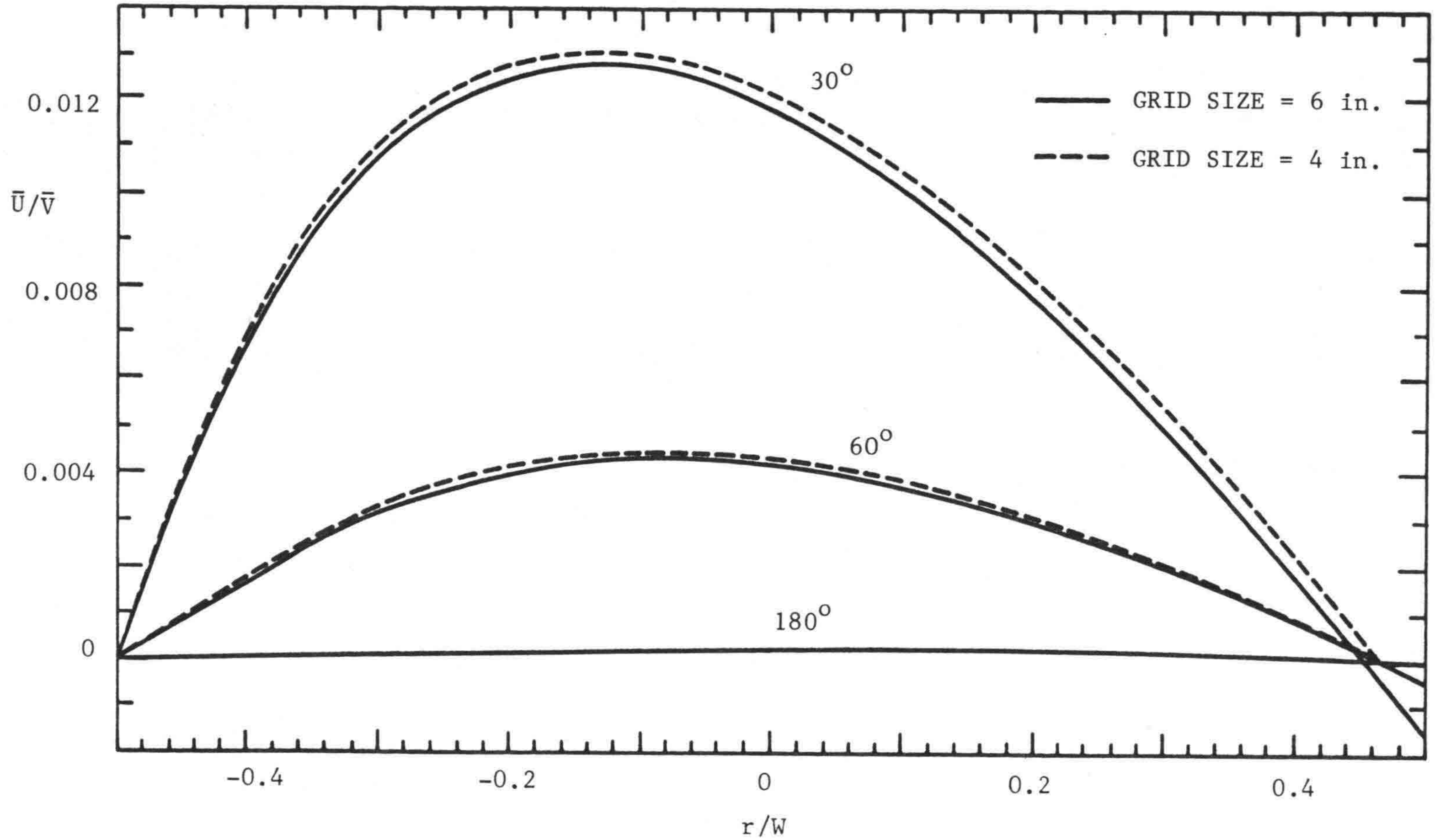

Figure 6 Transverse distributions of $\bar{U}/\bar{V}$ for different grid sizes

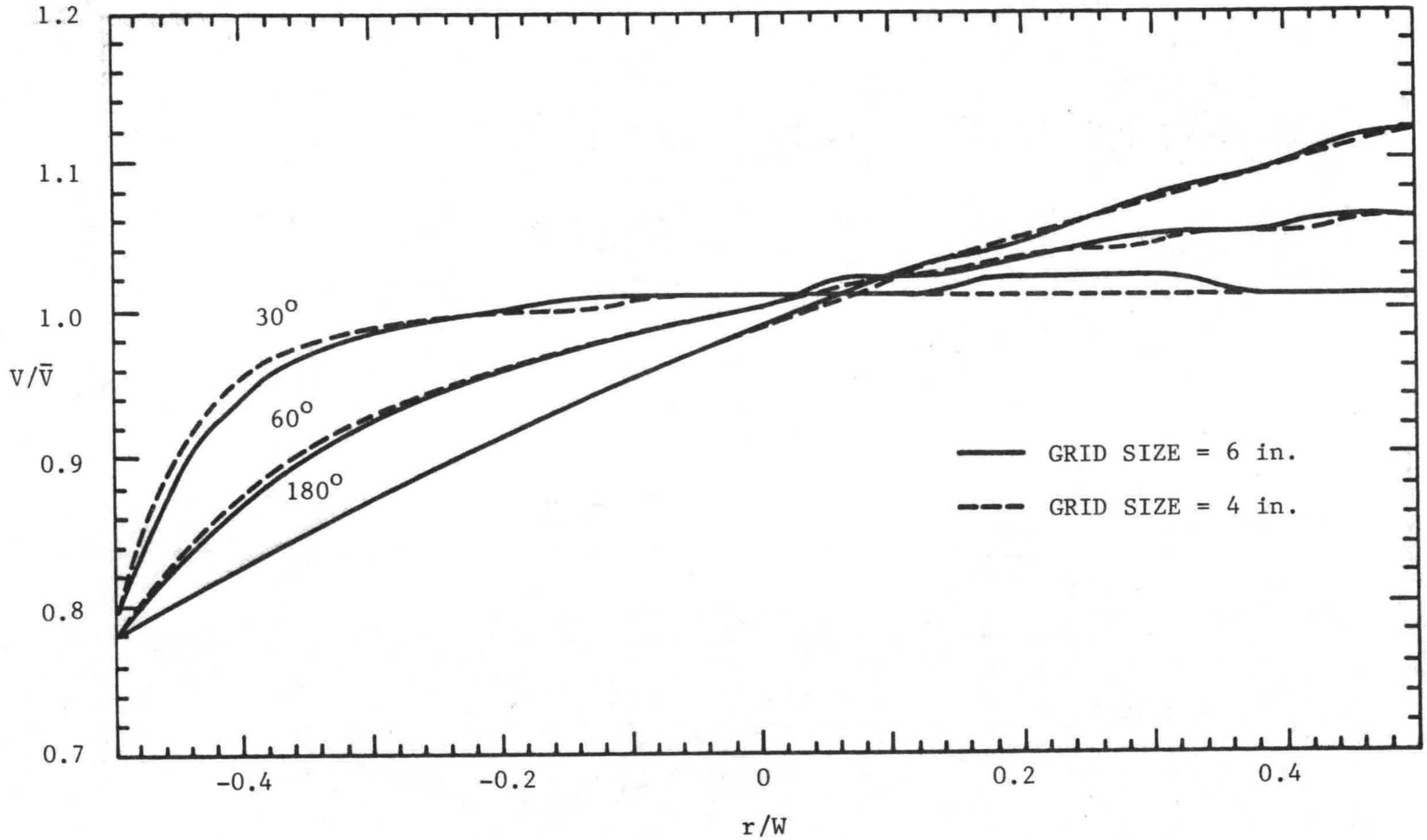

Figure 7 Transverse distributions of $V/\bar{V}$ for different grid sizes

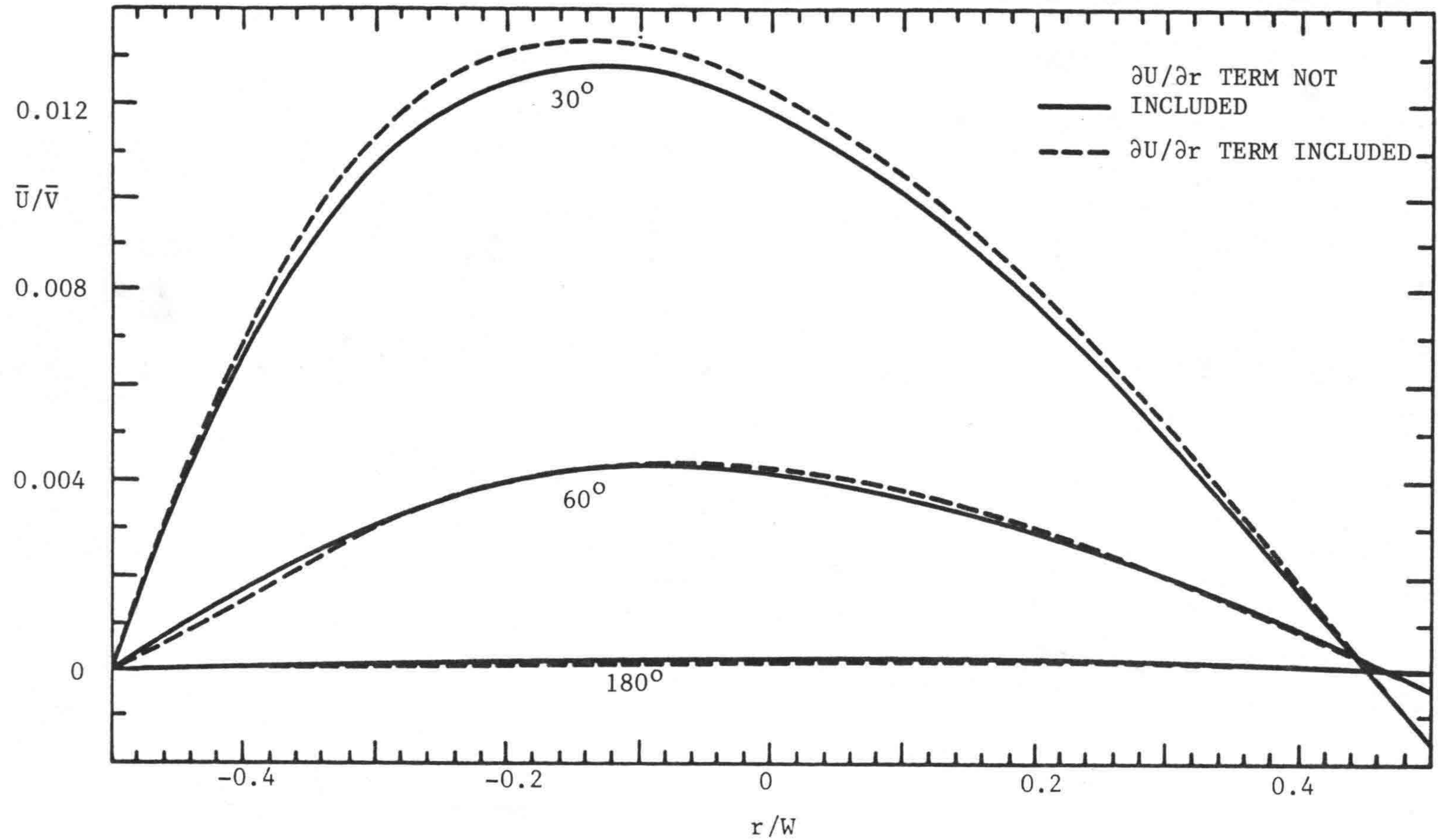

Figure 8 Transverse distributions of $\bar{U}/\bar{V}$ for cases with and without $\partial U/\partial r$ term in the streamwise momentum equation

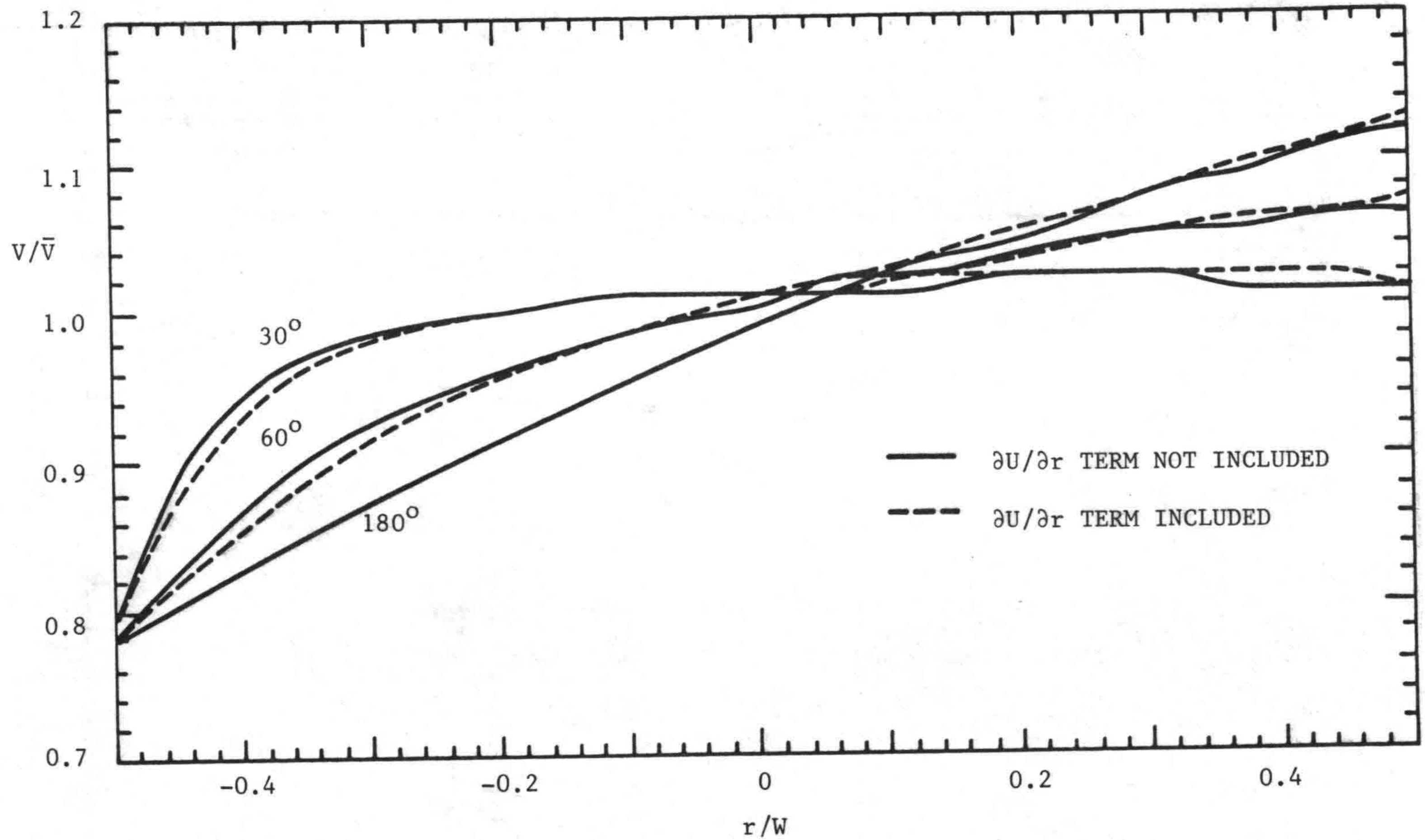

Figure 9 Transverse distributions of $V/\bar{V}$ for cases with and without $\partial U/\partial r$ term in the streamwise momentum equation

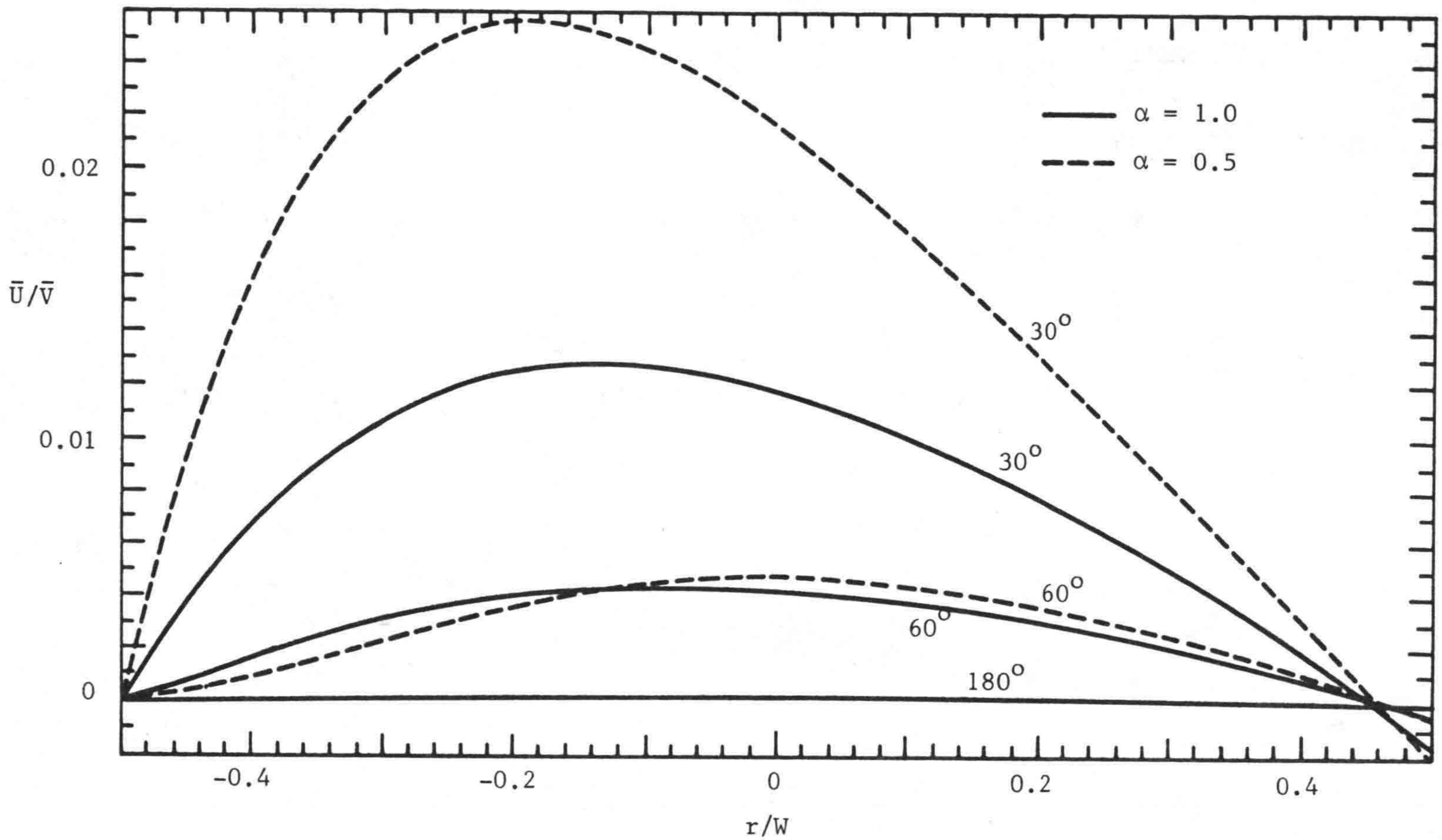

Figure 10 Transverse distributions of $\bar{U}/\bar{V}$ for different α values

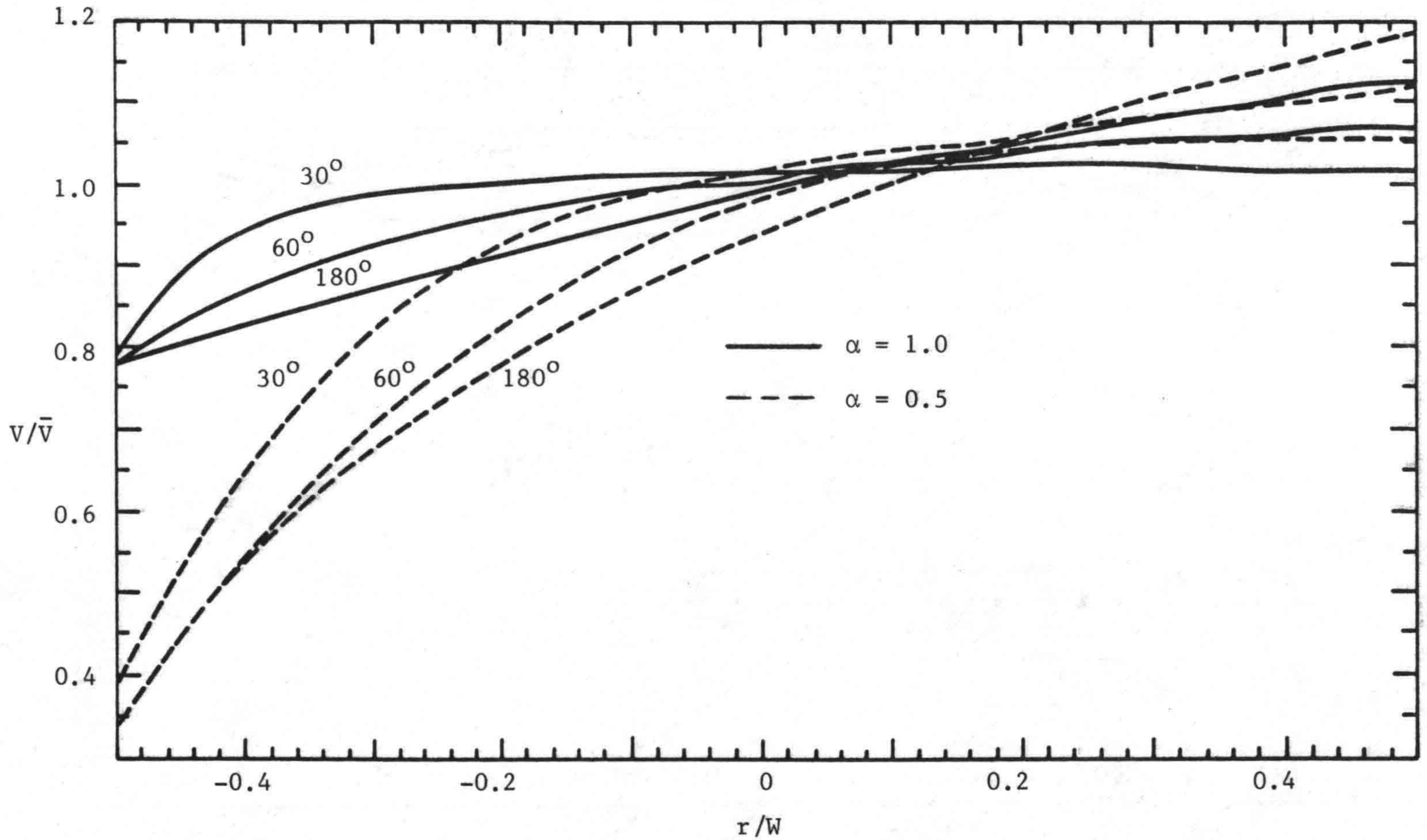

Figure 11 Transverse distributions of $V/\bar{V}$ for different α values

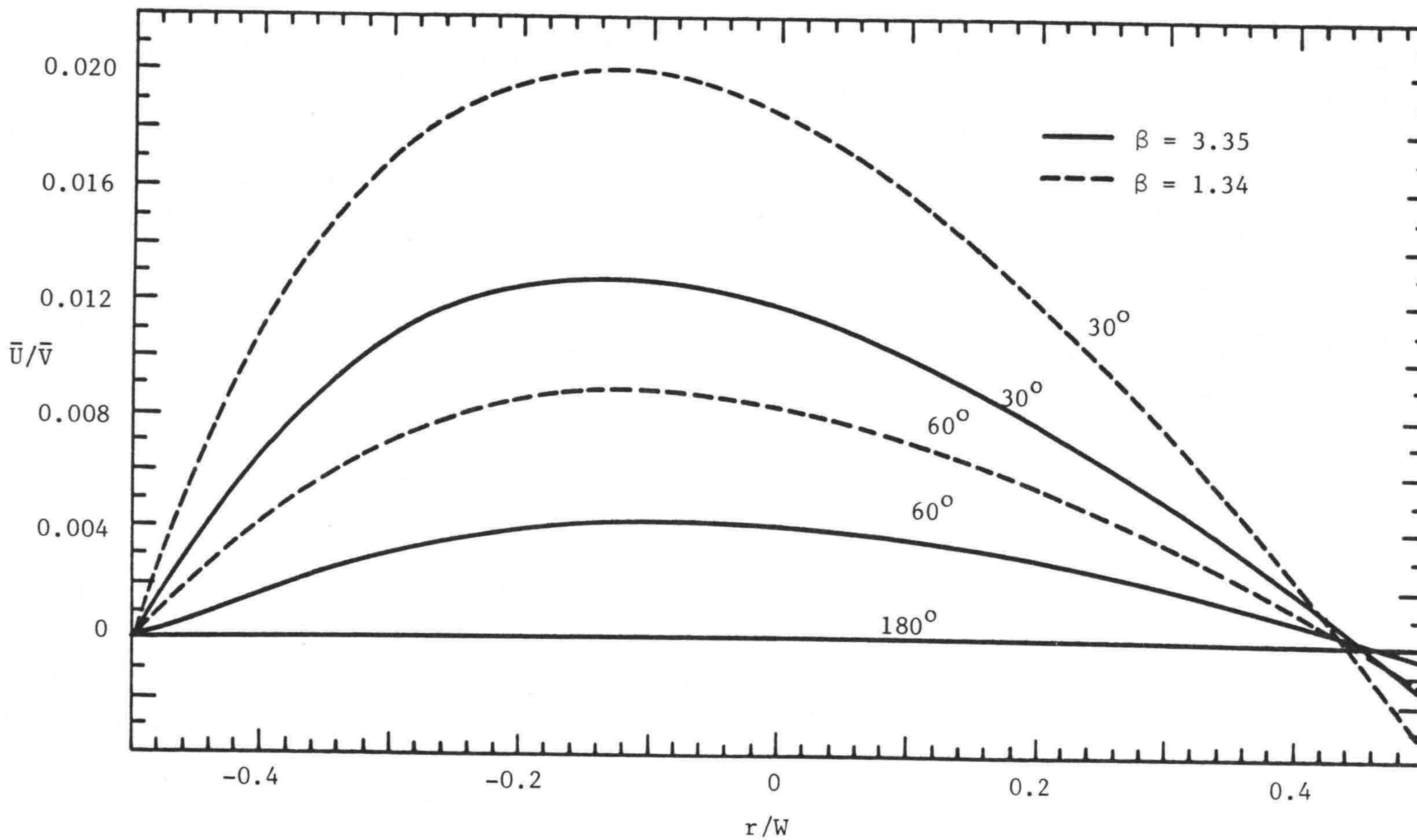

Figure 12 Transverse distributions of $\bar{U}/\bar{V}$ for different β values

THIS SHEET INTENTIONALLY BLANK

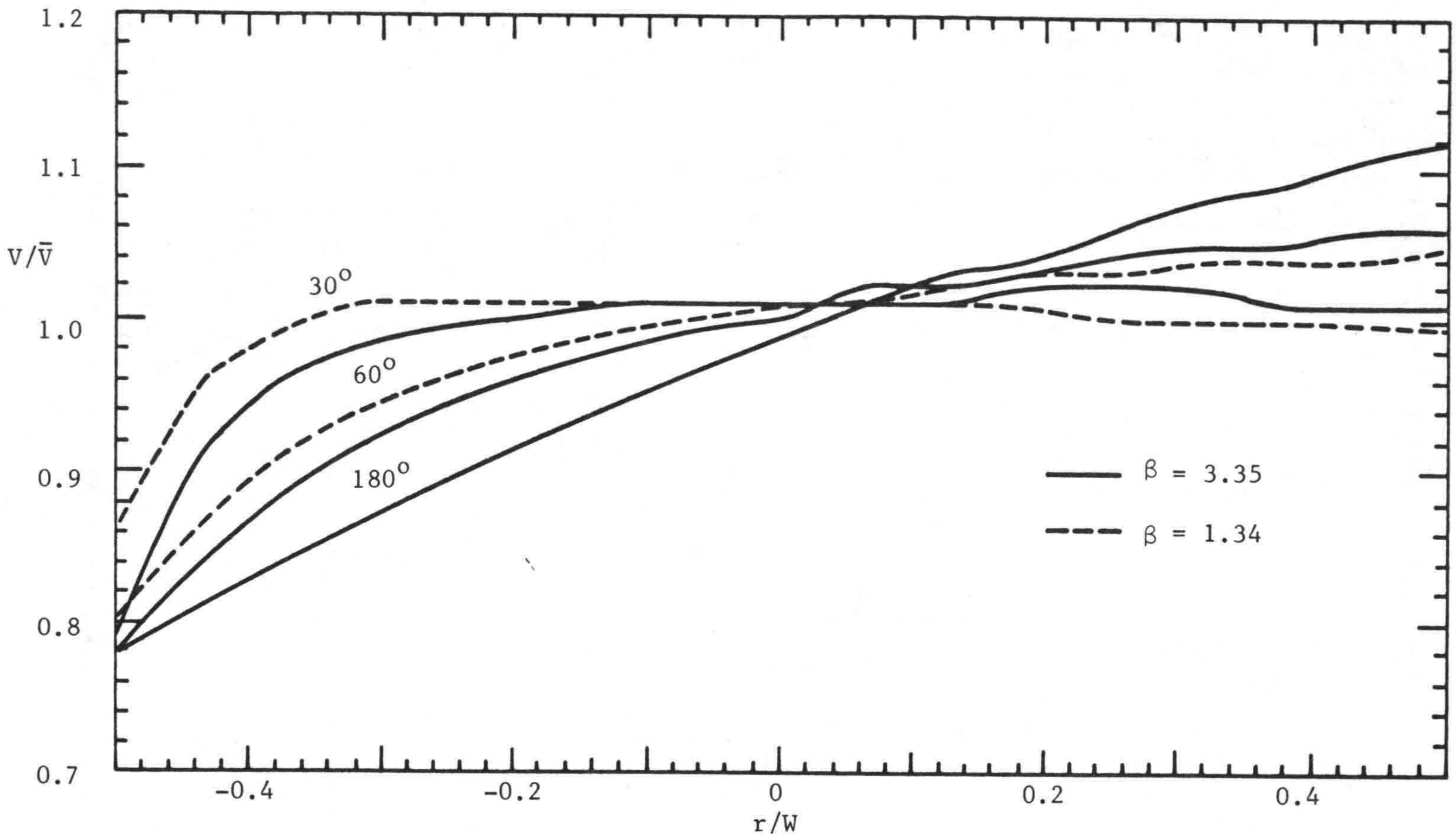

Figure 13 Transverse distributions of $V/\bar{V}$ for different β values

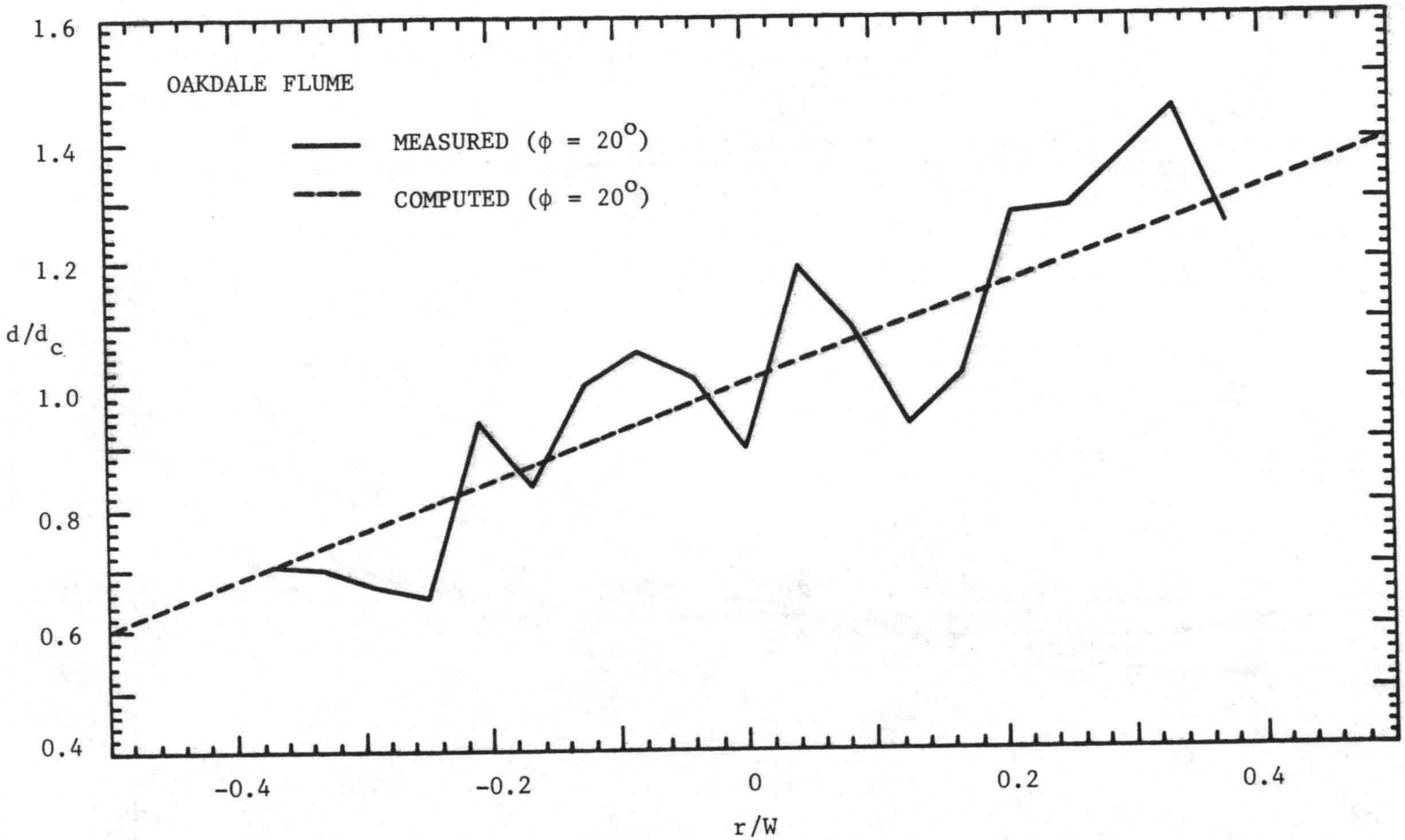

Figure 14 Transverse distributions of measured and computed d/d_c for the Oakdale flume ($\phi = 20^o$)

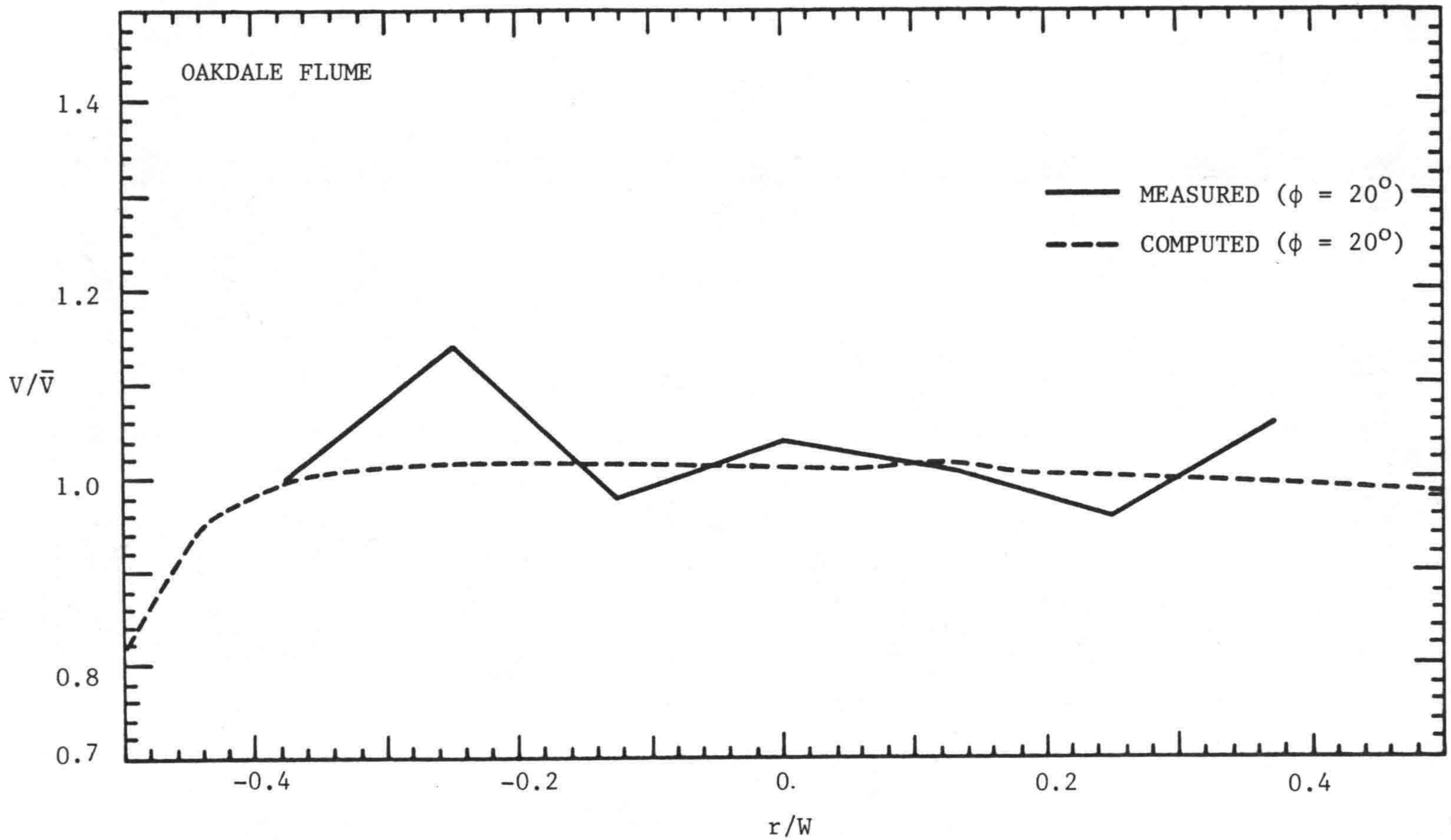

Figure 15 Transverse distributions of measured and computed $V/\bar{V}$ for the Oakdale flume ($\phi = 20^{o}$)

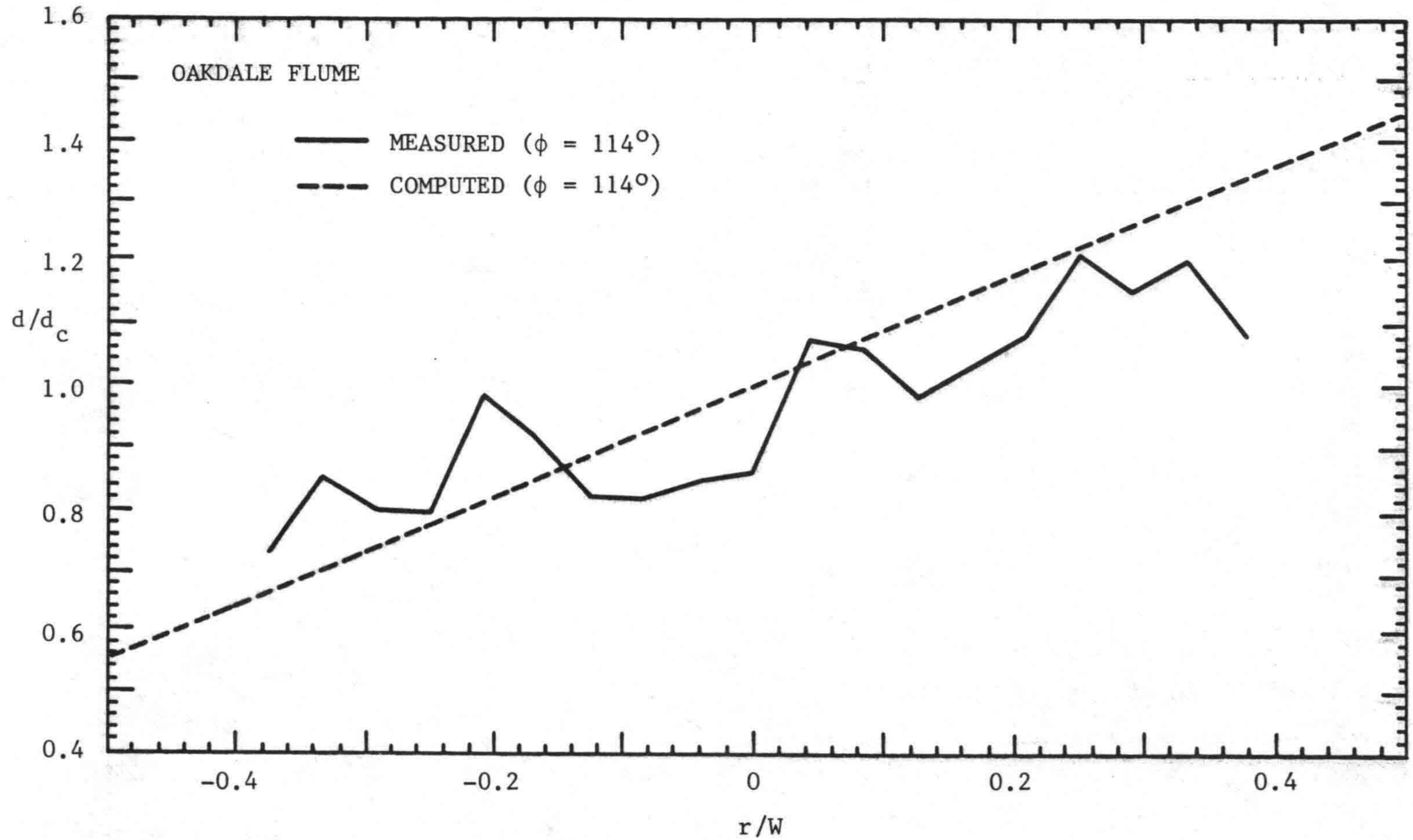

Figure 16 Transverse distributions of measured and computed d/d_c for the Oakdale flume ($\phi = 114^{\circ}$)

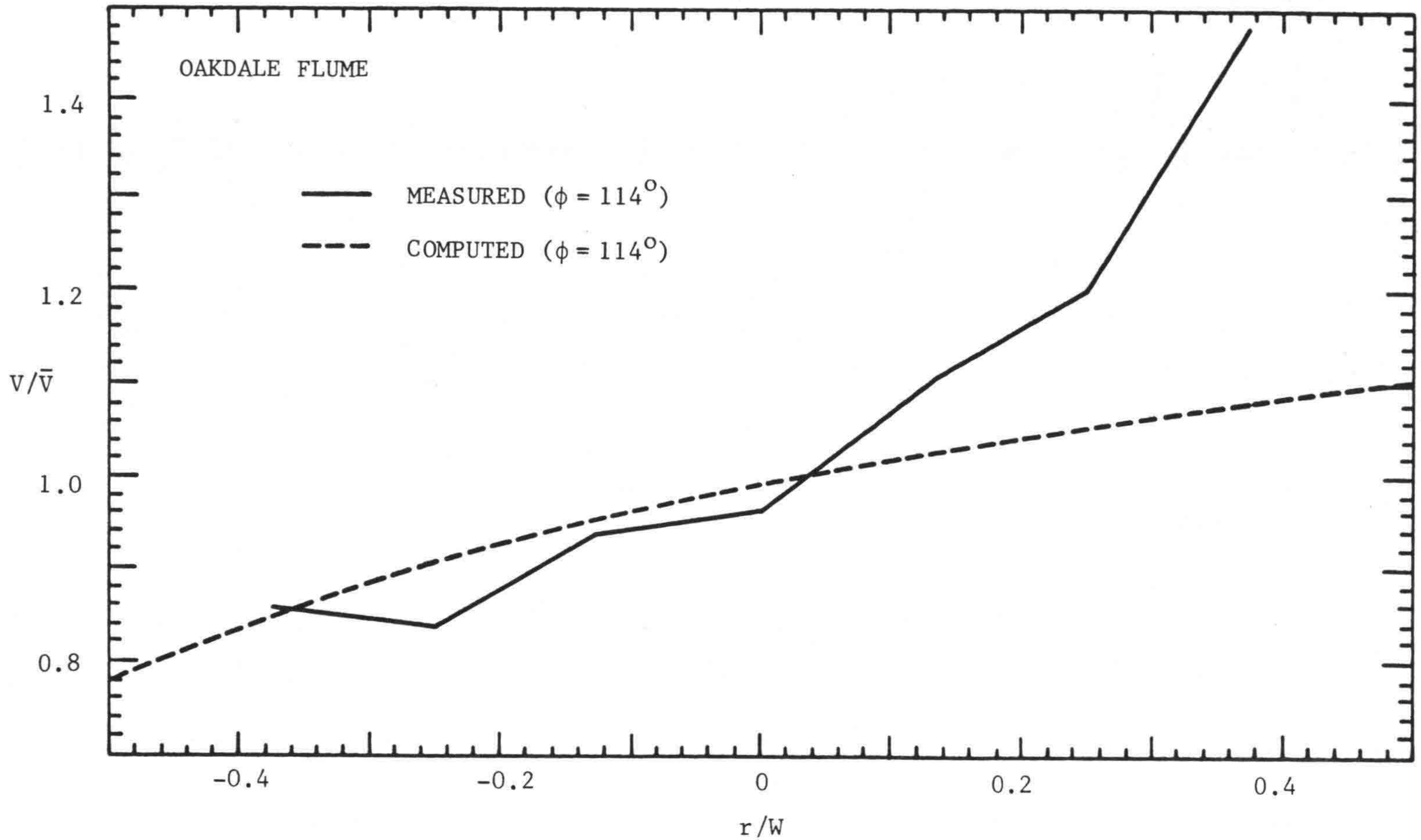

Figure 17 Transverse distributions of measured and computed $V/\bar{V}$ for the Oakdale flume ($\phi = 114^{\circ}$)

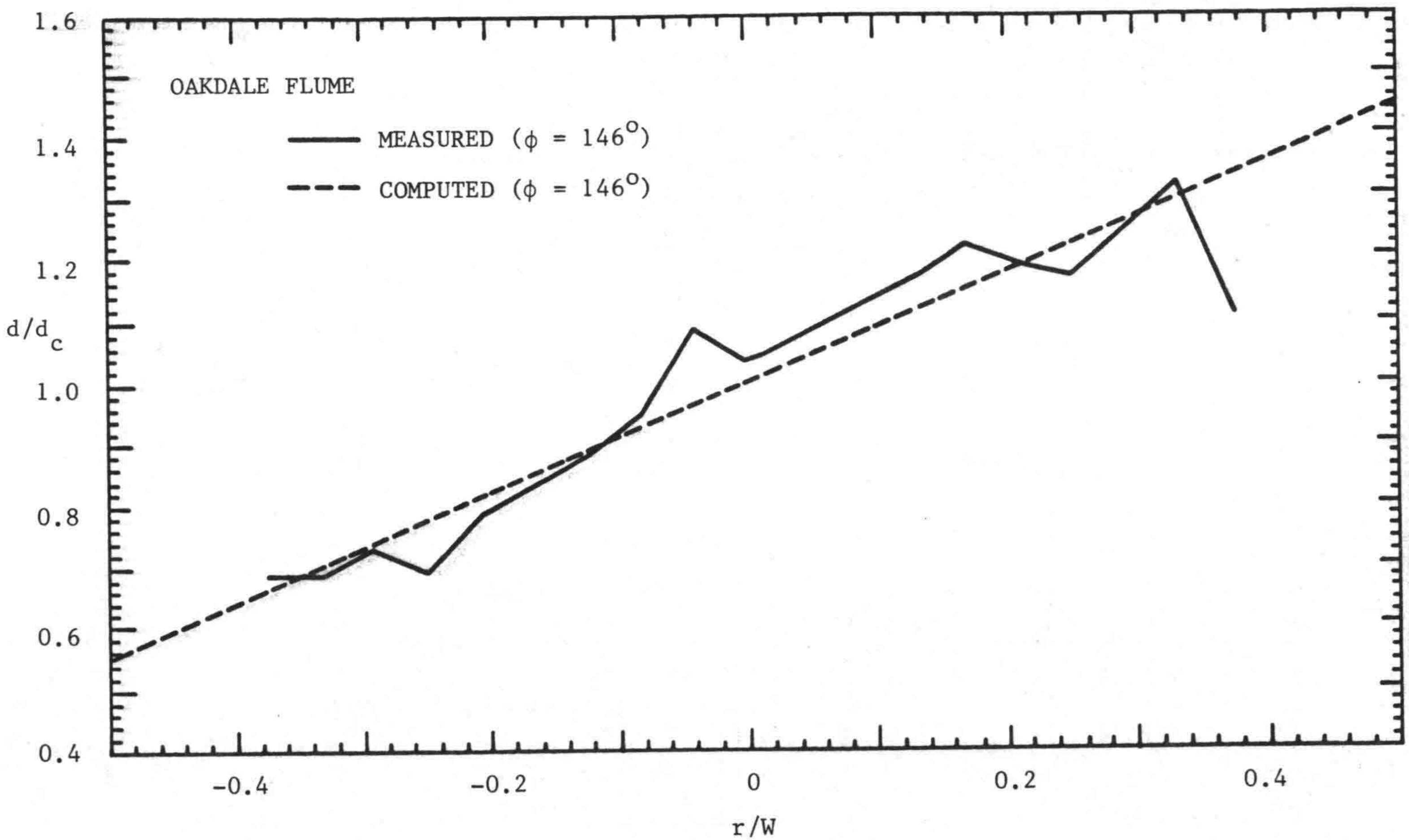

Figure 18 Transverse distributions of measured and computed d/d_c for the Oakdale flume ($\phi = 146^o$)

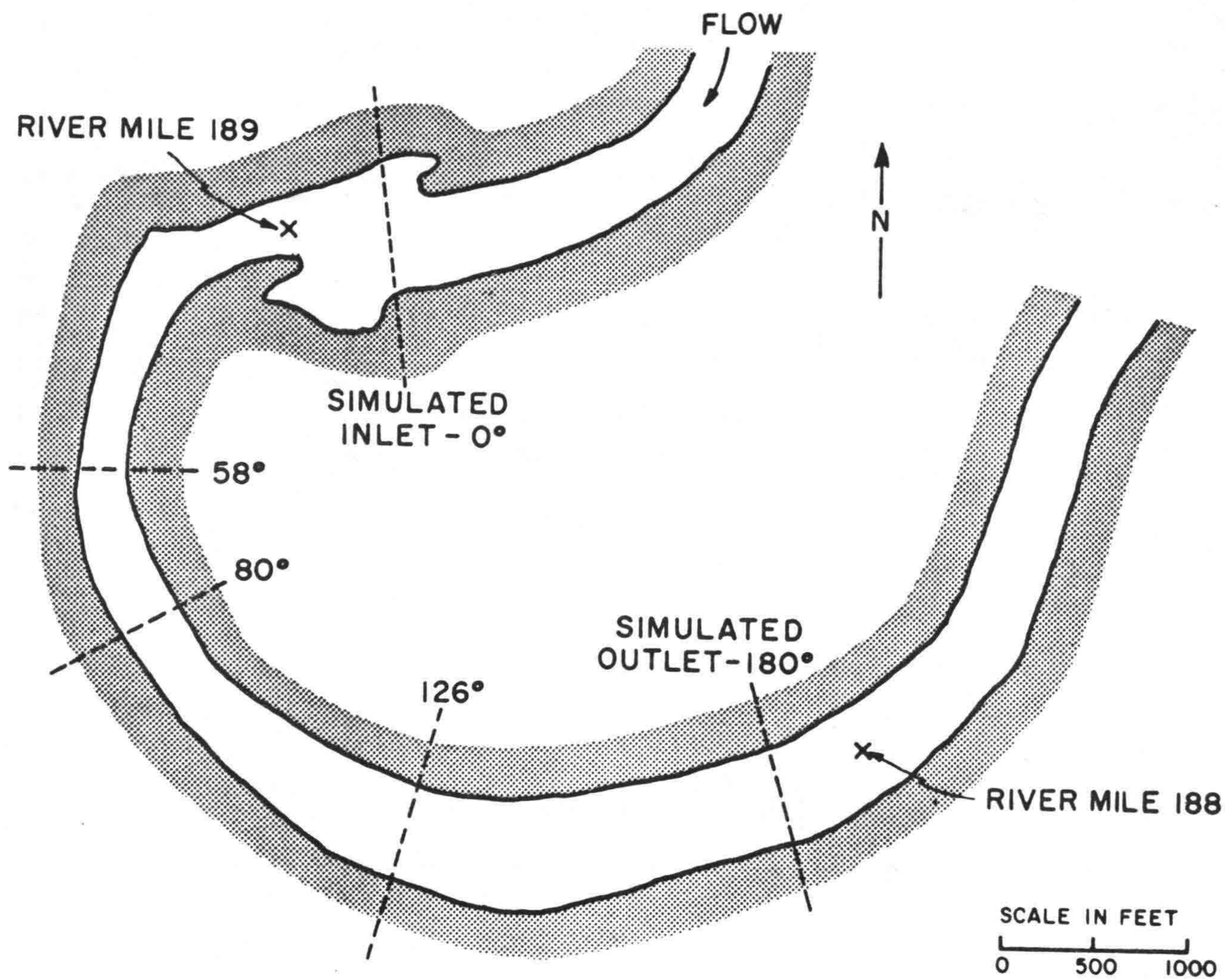

Figure 19 Map of the Sacramento River bend that was investigated

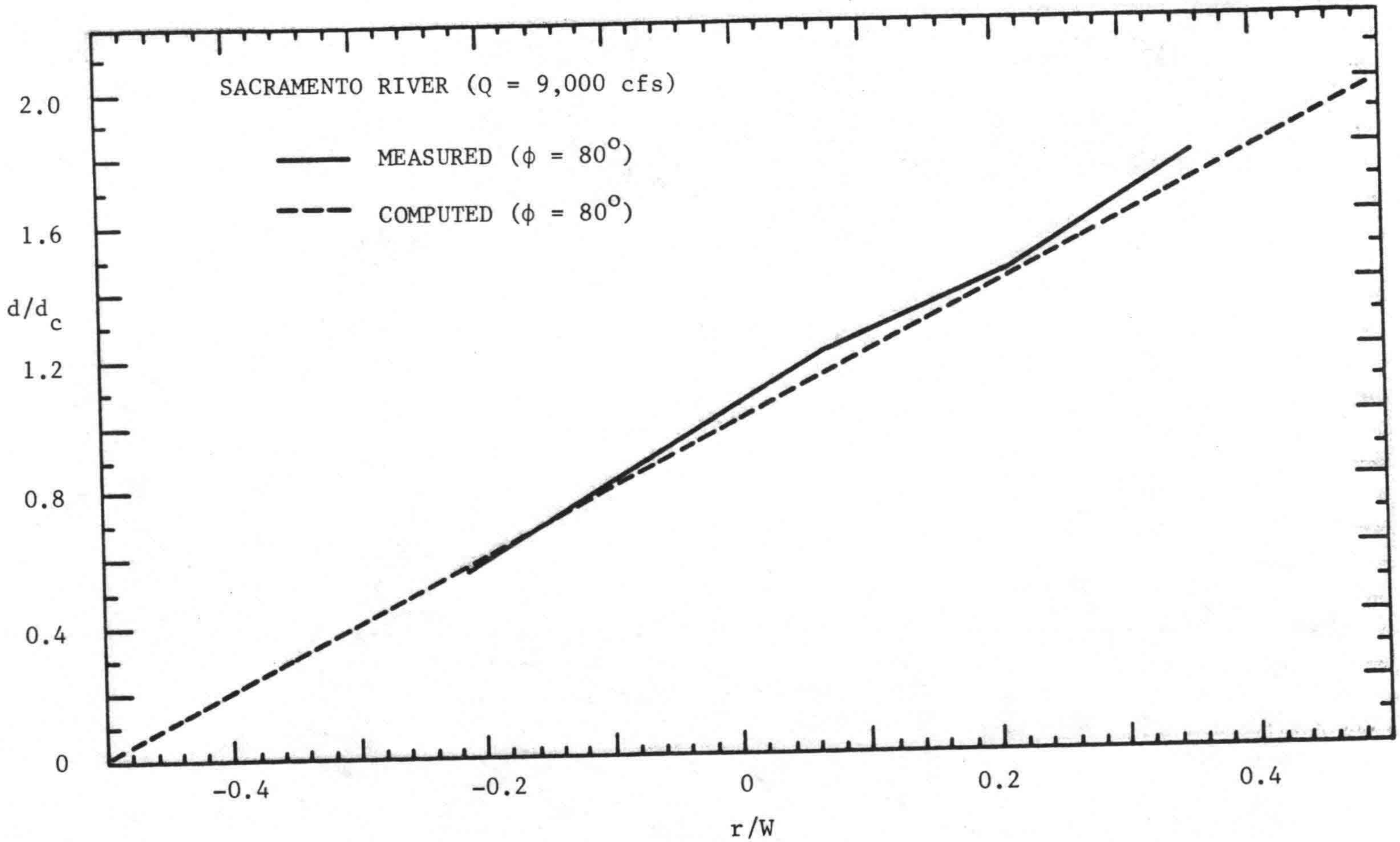

Figure 20 Transverse distributions of measured and computed d/d_c for the Sacramento River at low flow ($\phi = 80^o$)

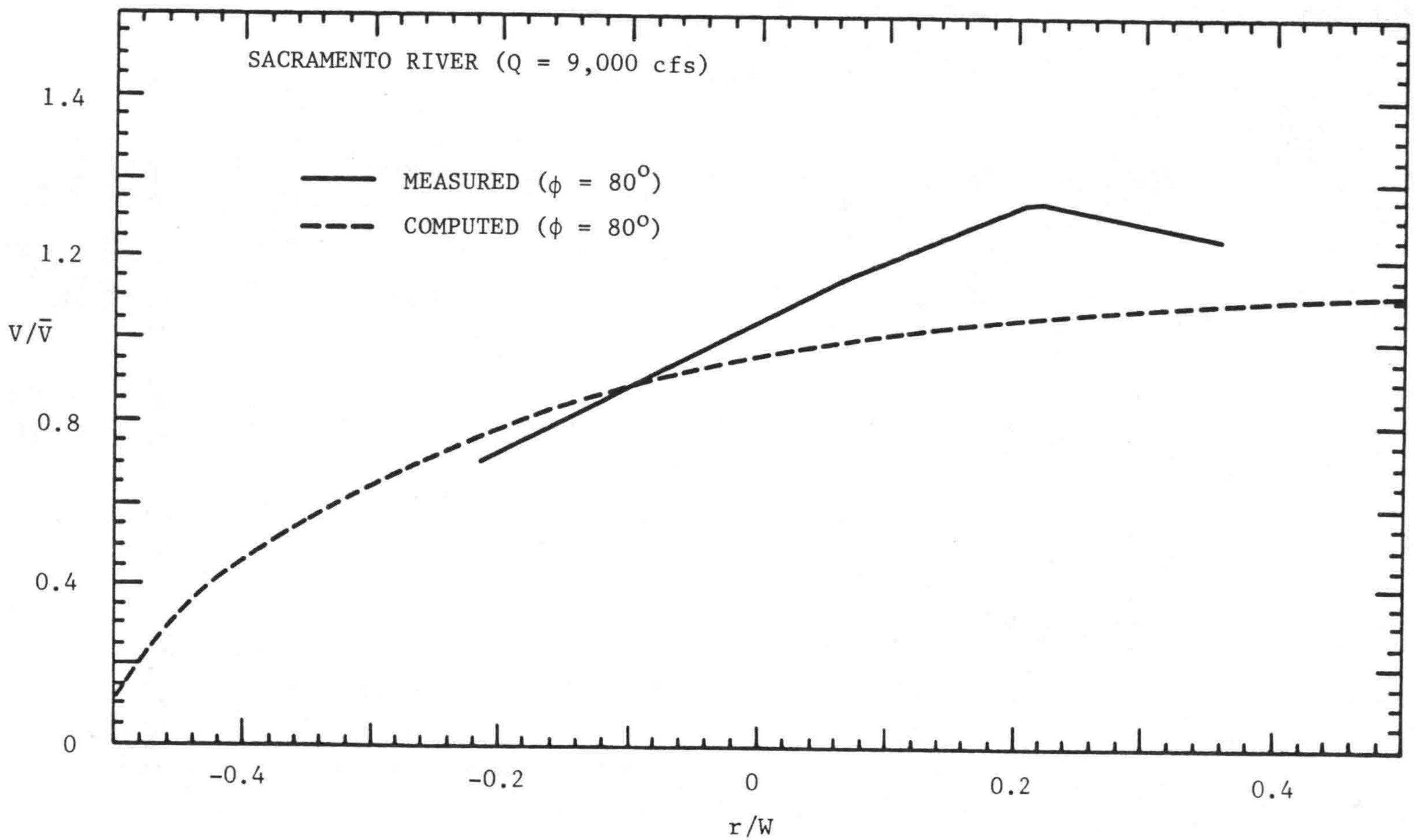

Figure 21 Transverse distributions of measured and computed $V/\bar{V}$ for the Sacramento River at low flow ($\phi = 80^o$)

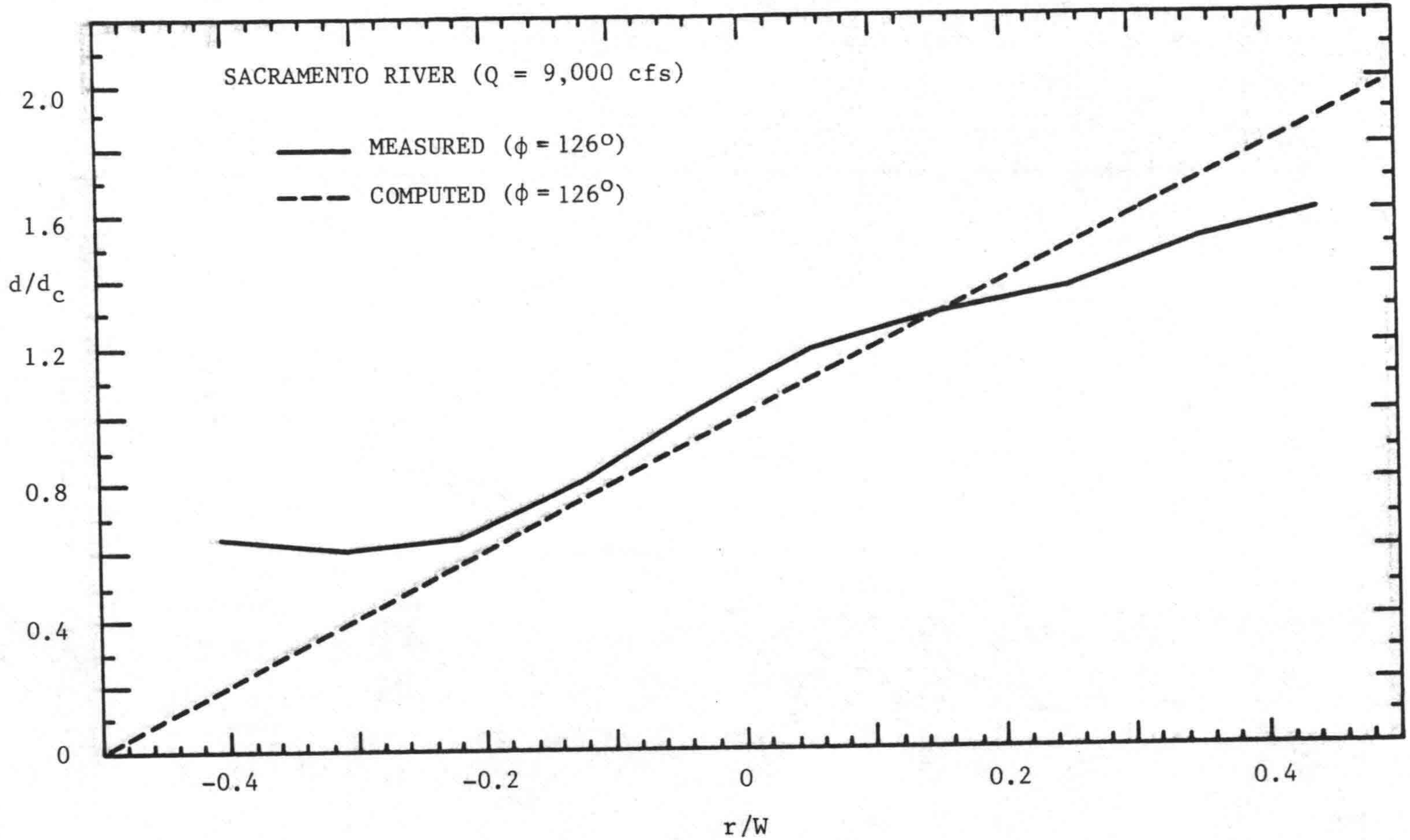

Figure 22 Transverse distributions of measured and computed d/d_c for the Sacramento River at low flow ($\phi = 126^{o}$)

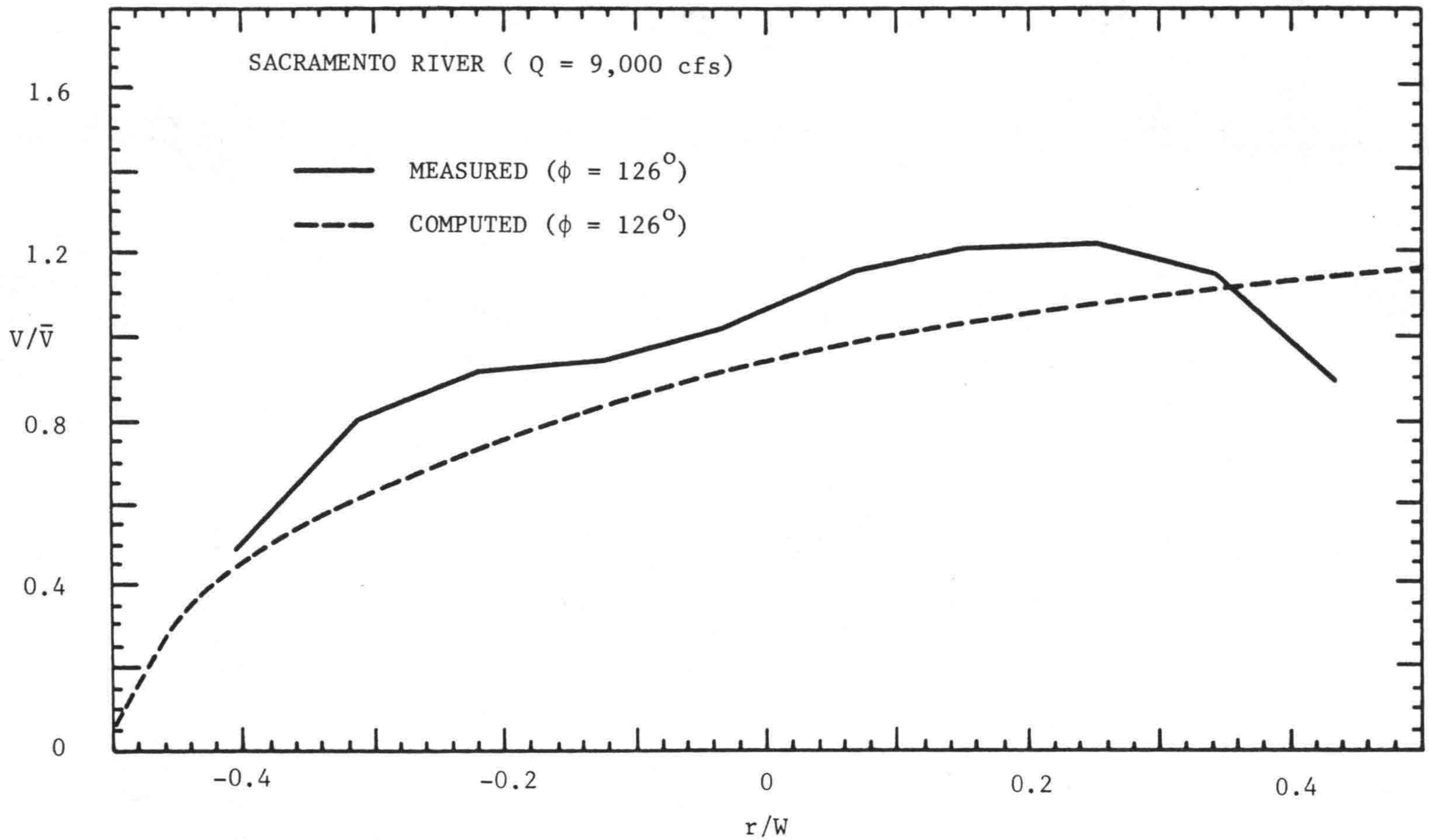

Figure 23 Transverse distributions of measured and computed $V/\bar{V}$ for the Sacramento River at low flow (ϕ = 126°)

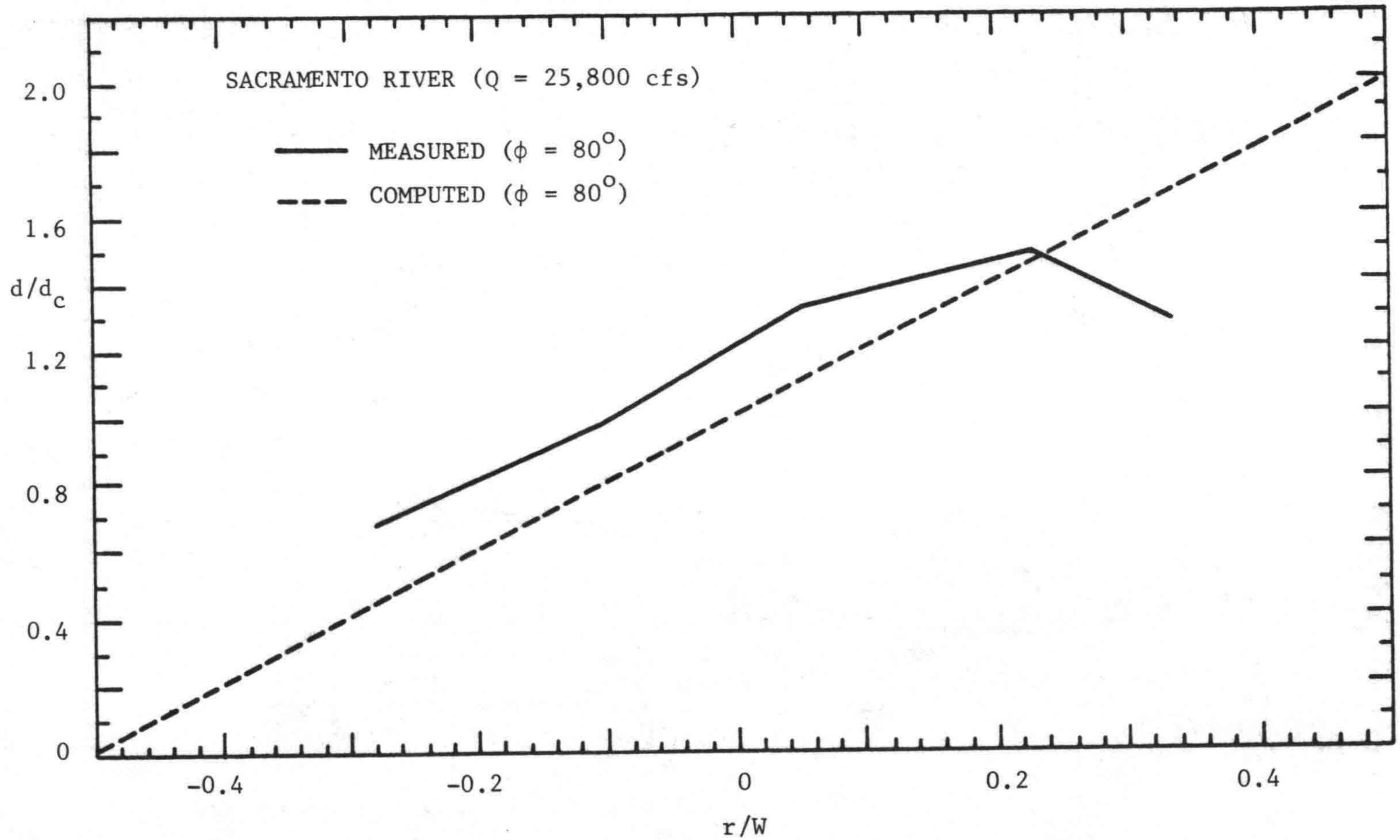

Figure 24 Transverse distributions of measured and computed d/d_c for the Sacramento River at high flow (ϕ = 80°)

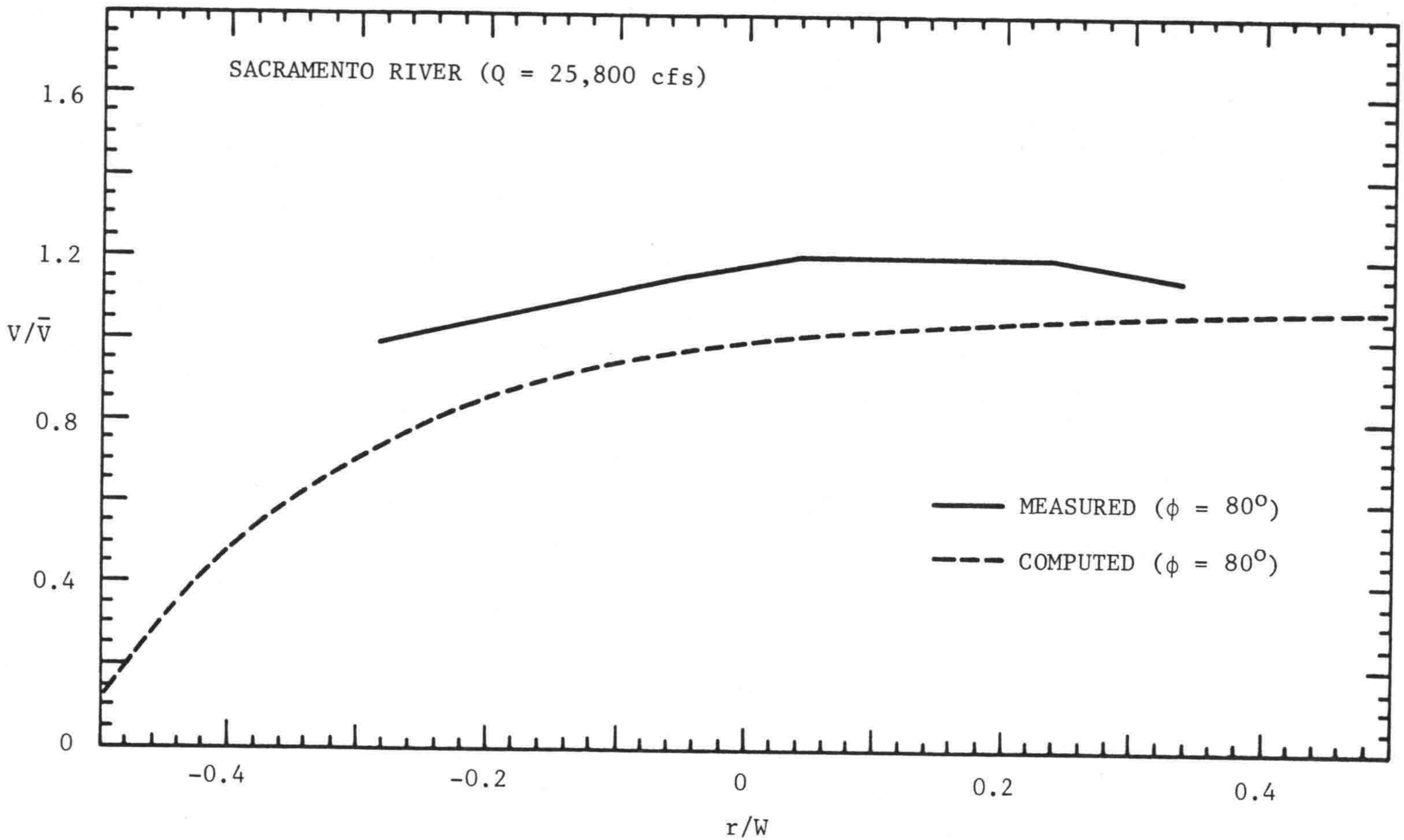

Figure 25 Transverse distributions of measured and computed $V/\bar{V}$ for the Sacramento River at high flow ($\phi = 80^{\circ}$)

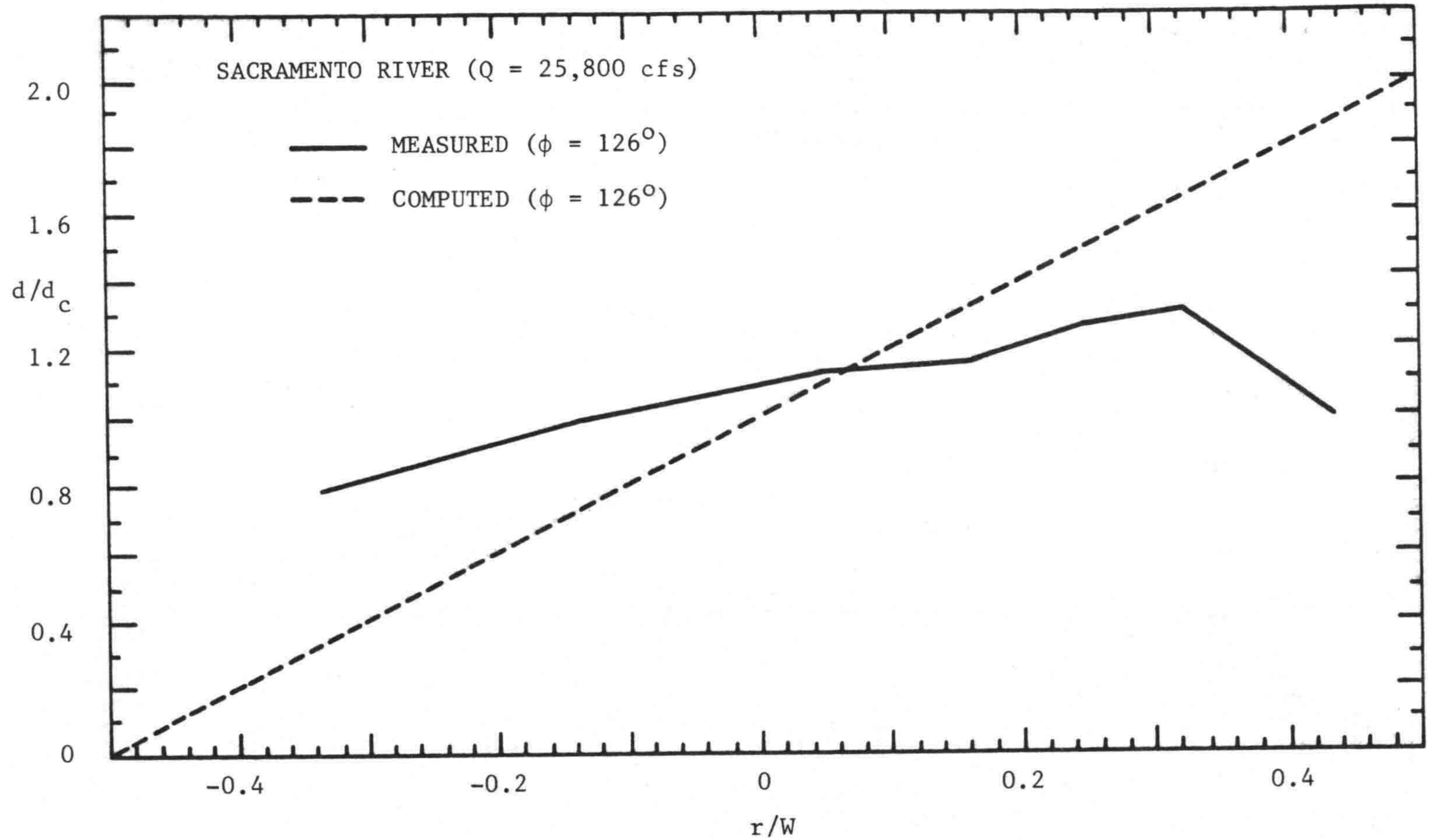

Figure 26 Transverse distributions of measured and computed d/d_c for the Sacramento River at high flow ($\phi = 126^\circ$)

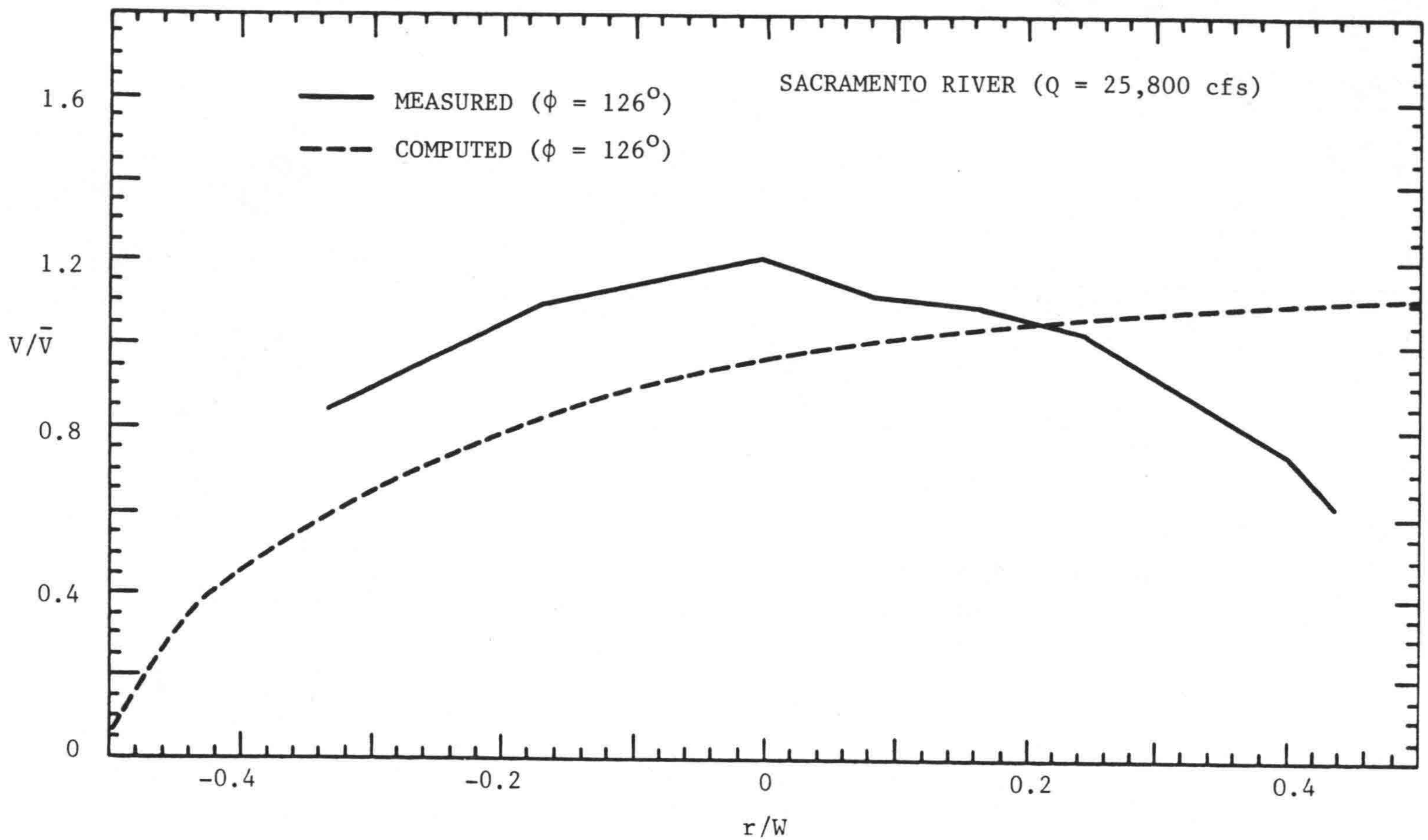

Figure 27 Transverse distributions of measured and computed $V/\bar{V}$ for the Sacramento River at high flow ($\phi = 126^{o}$)

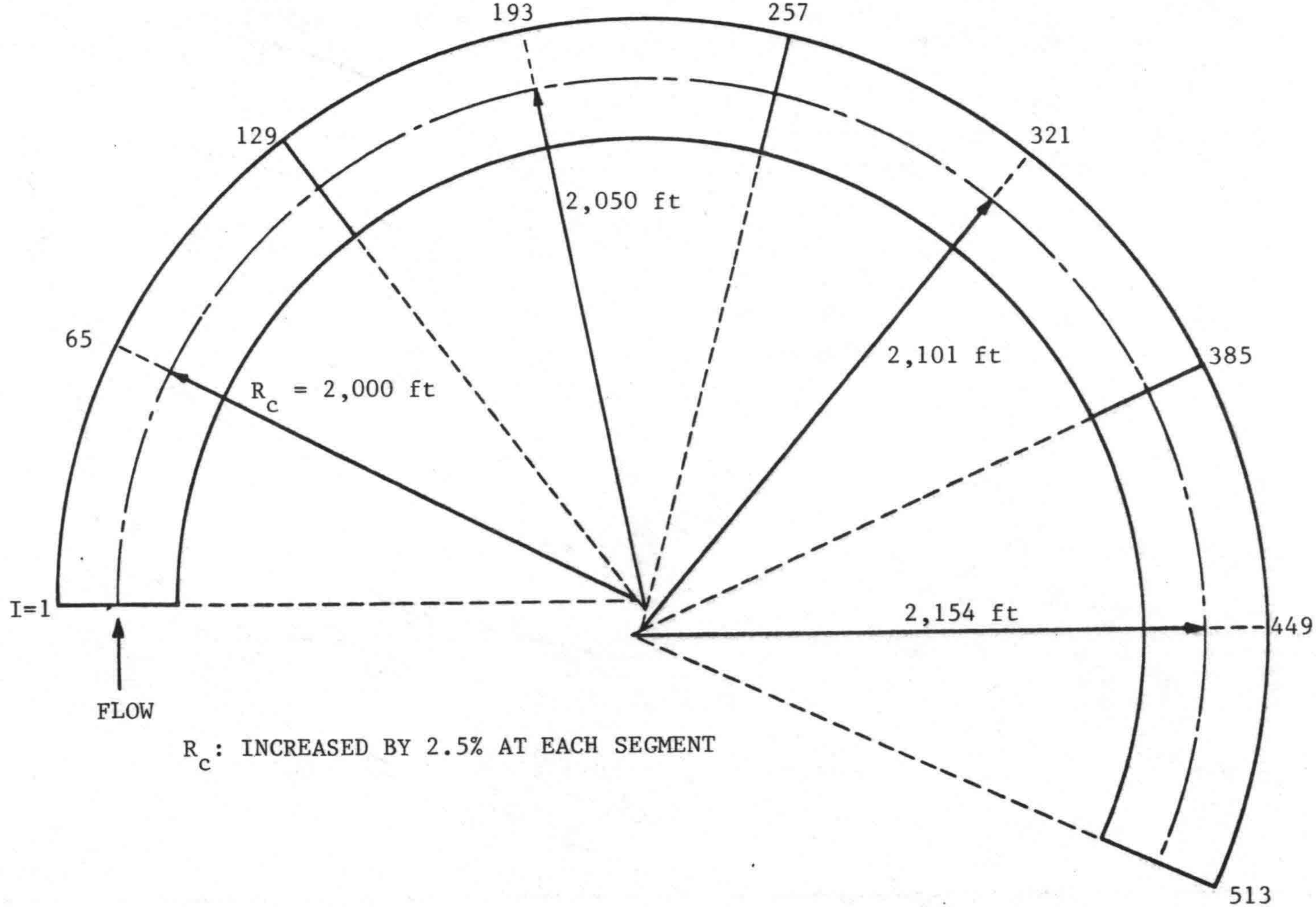

Figure 28 Idealized single bend with gradually increasing radius of centerline curvature

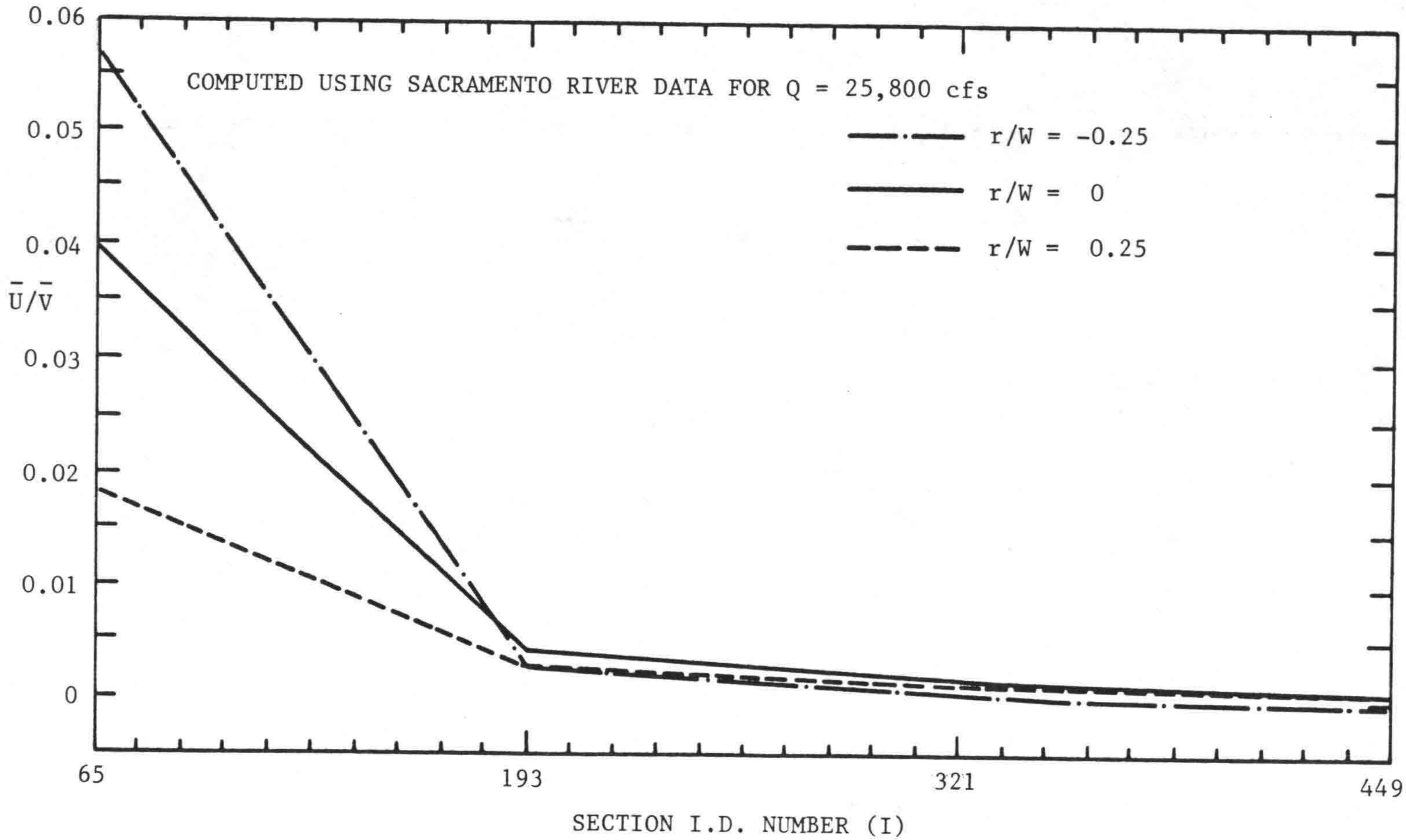

Figure 29 Longitudinal variations of $\bar{U}/\bar{V}$ for idealized single bend with gradually increasing radius of centerline curvature

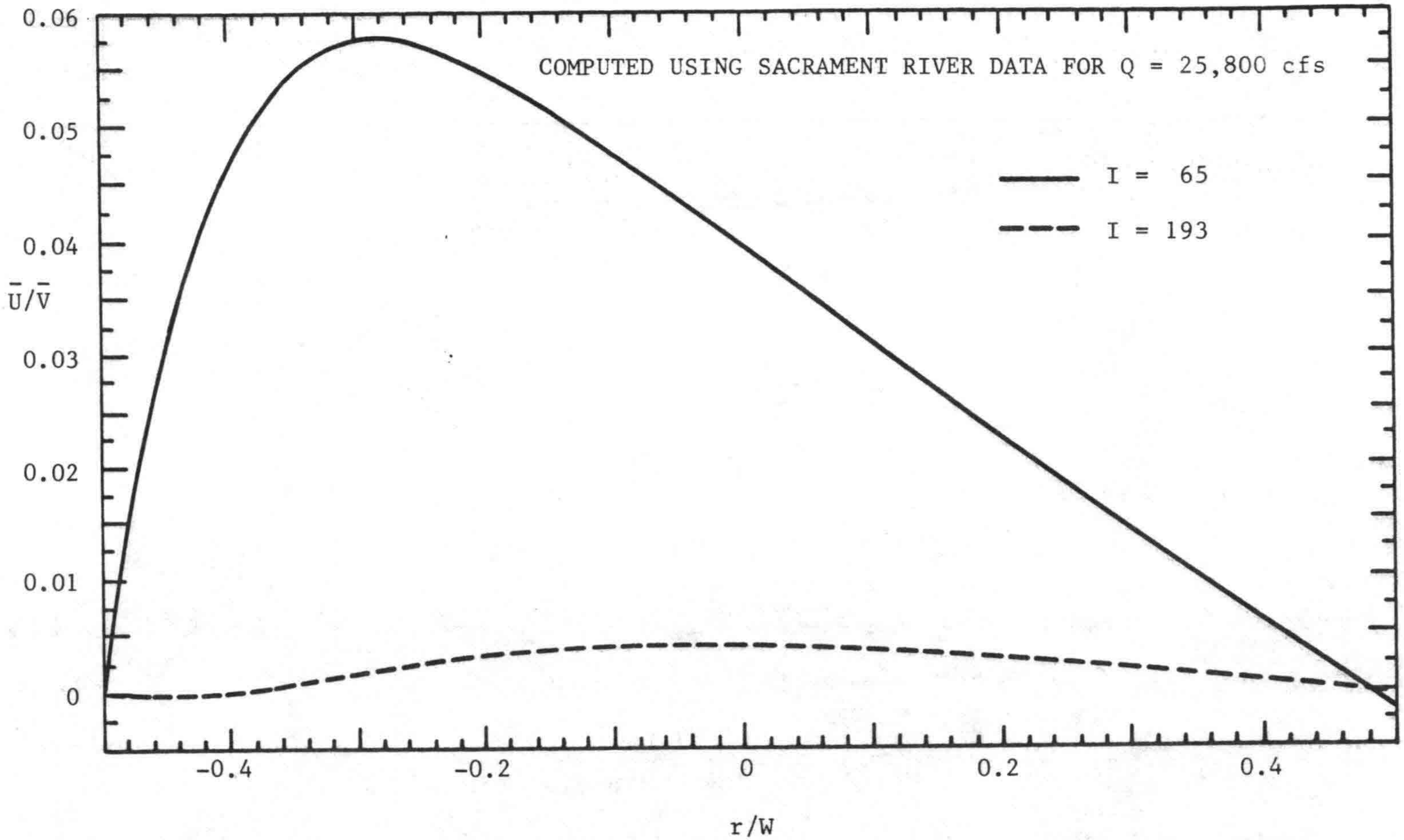

Figure 30 Transverse distributions of computed $\bar{U}/\bar{V}$ for idealized single bend with gradually increasing radius of centerline curvature

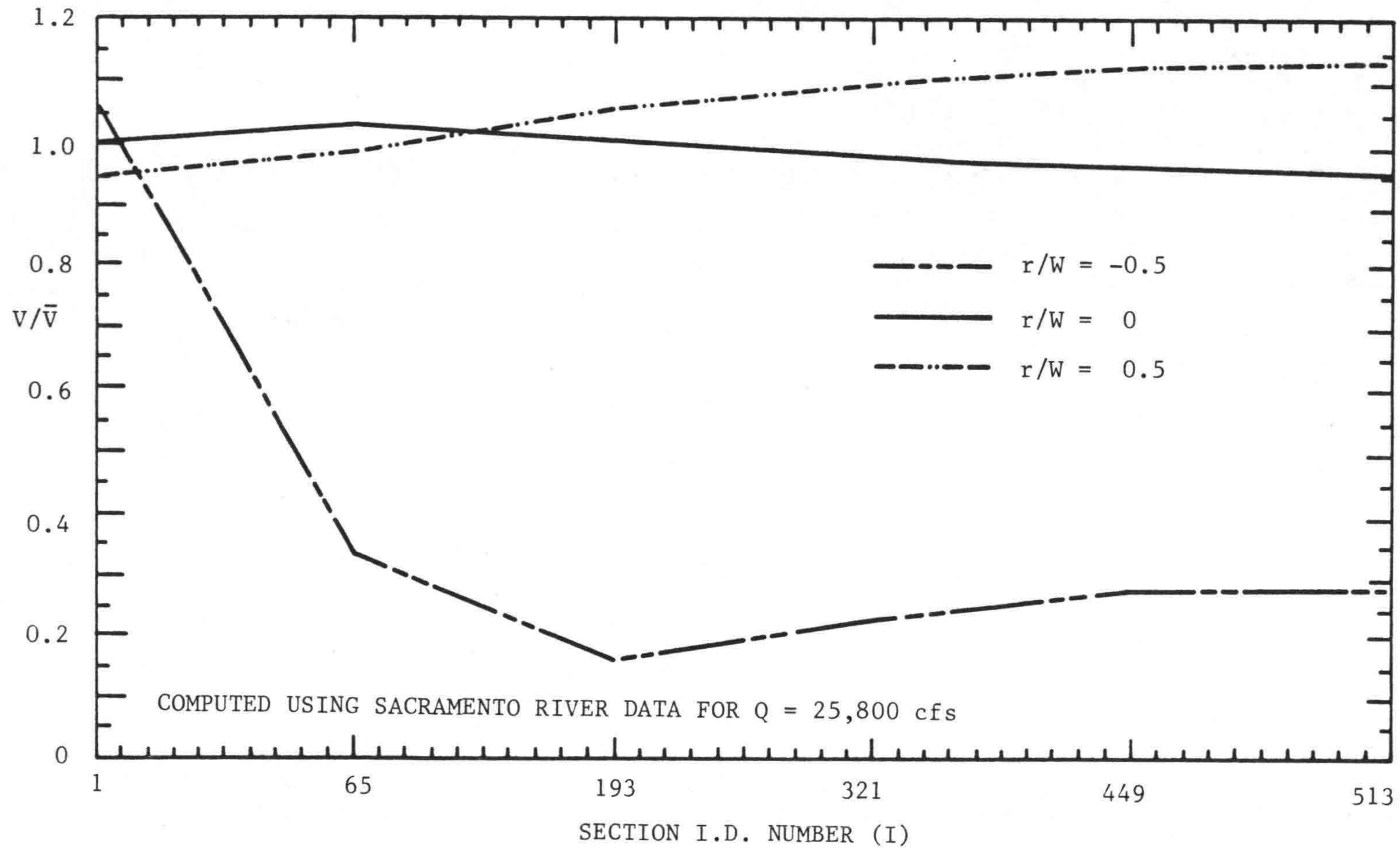

Figure 31 Longitudinal variations of computed $V/\bar{V}$ for idealized single bend with gradually increasing radius of centerline curvature

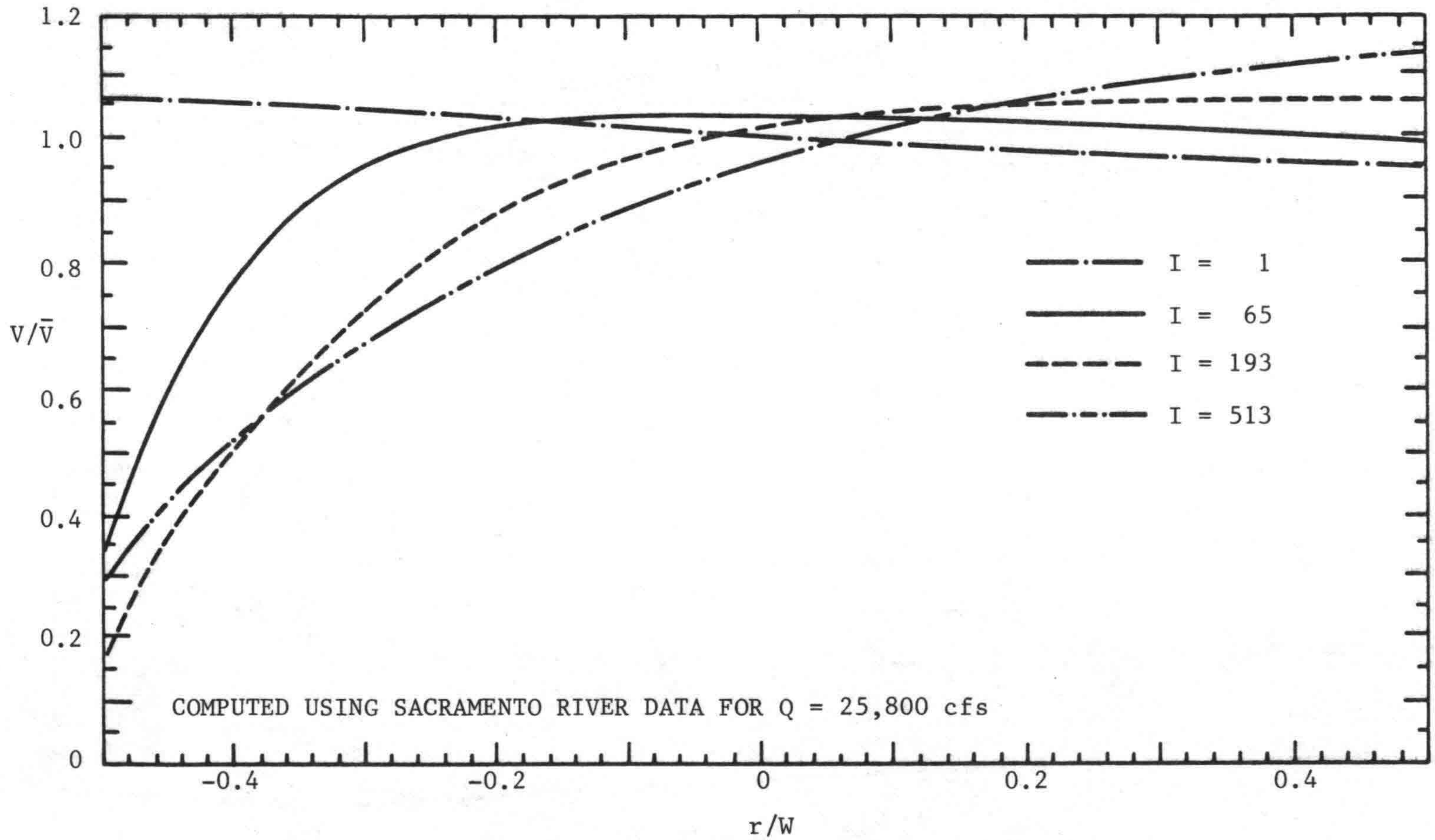

Figure 32 Transverse distributions of computed $V/\bar{V}$ for idealized single bend with gradually increasing radius of centerline curvature

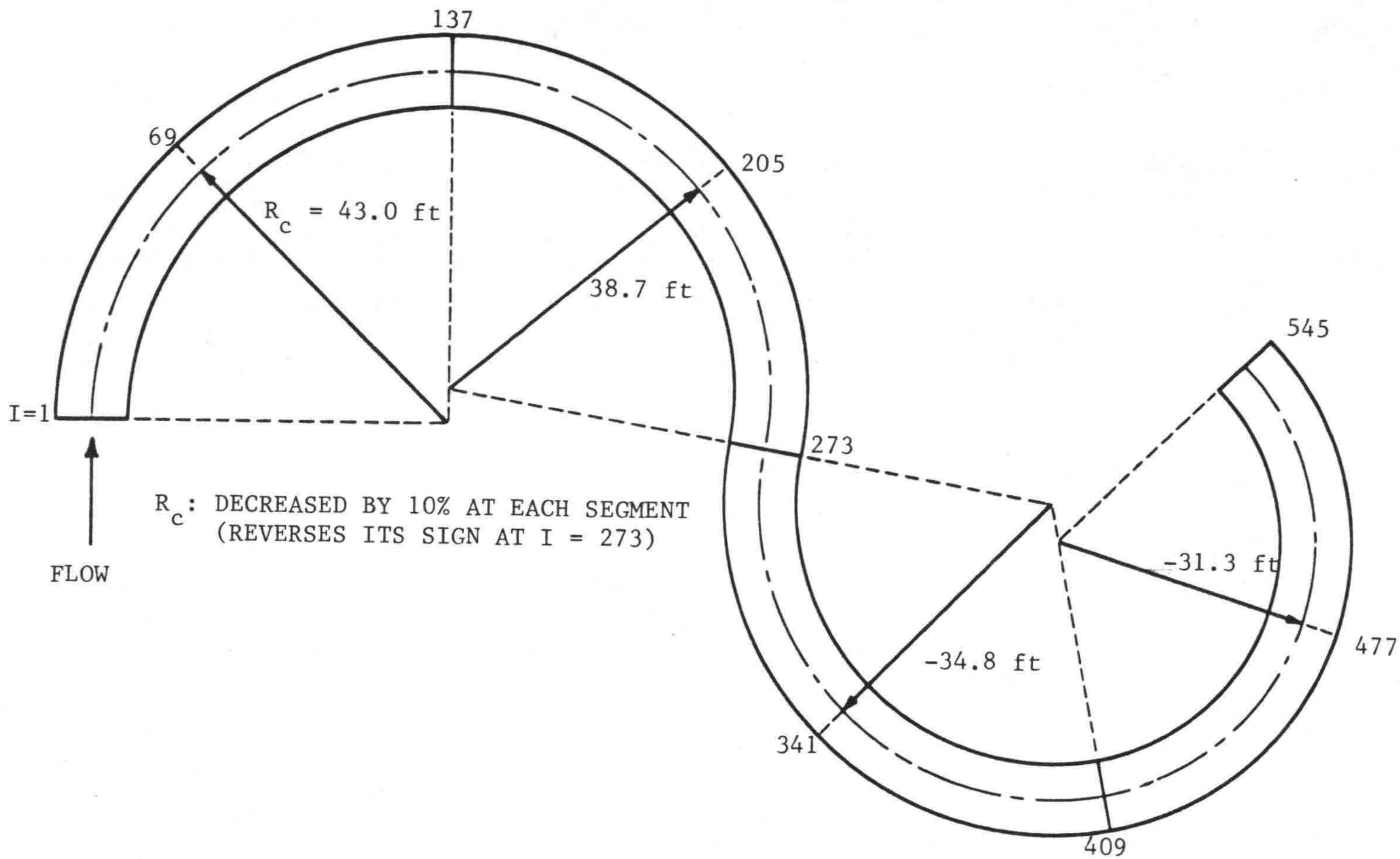

Figure 33 Idealized two-bend channel with gradually decreasing radius of centerline curvature

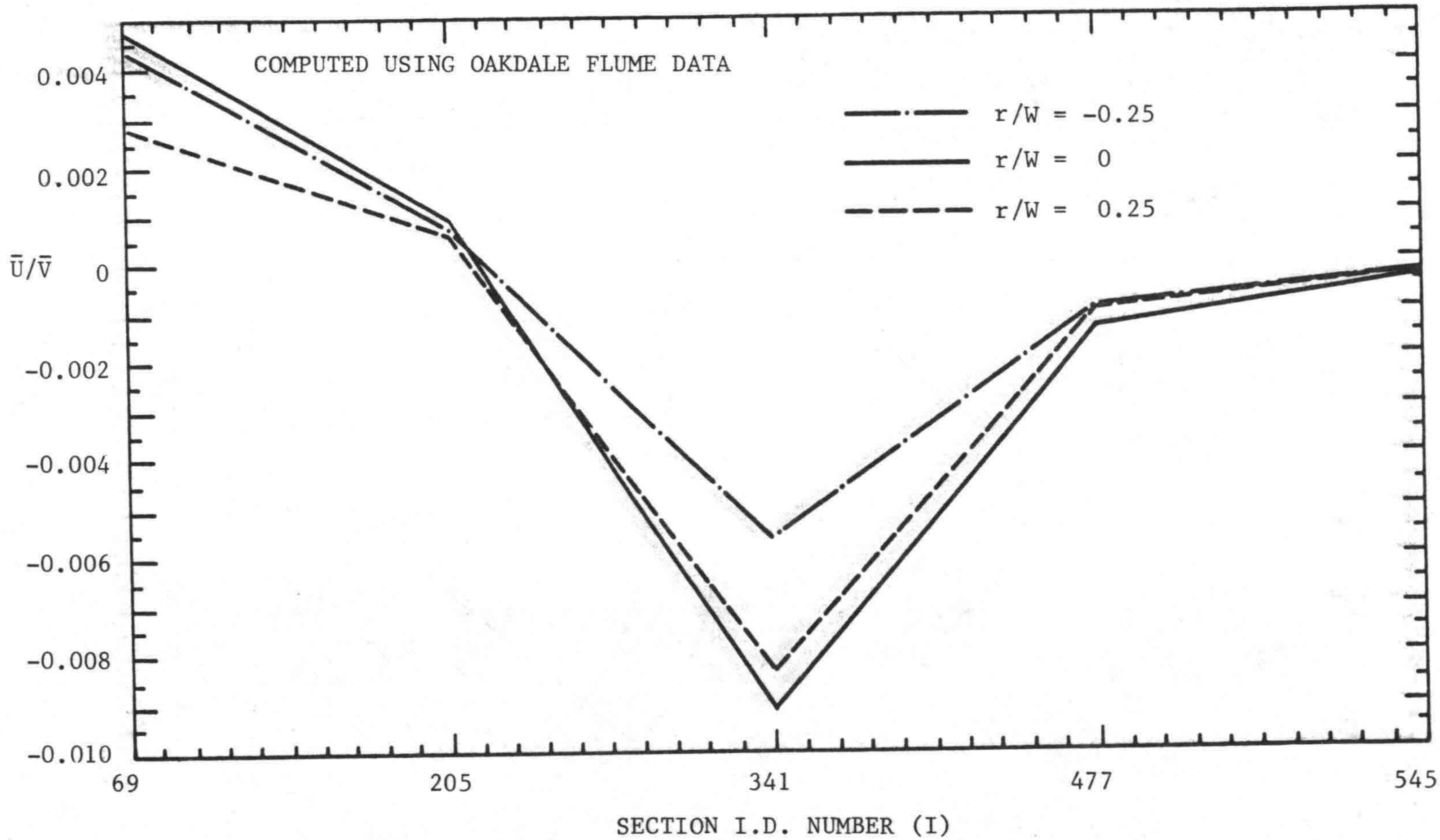

Figure 34 Longitudinal variations of computed $\bar{U}/\bar{V}$ for idealized two-bend channel with gradually decreasing radius of centerline curvature

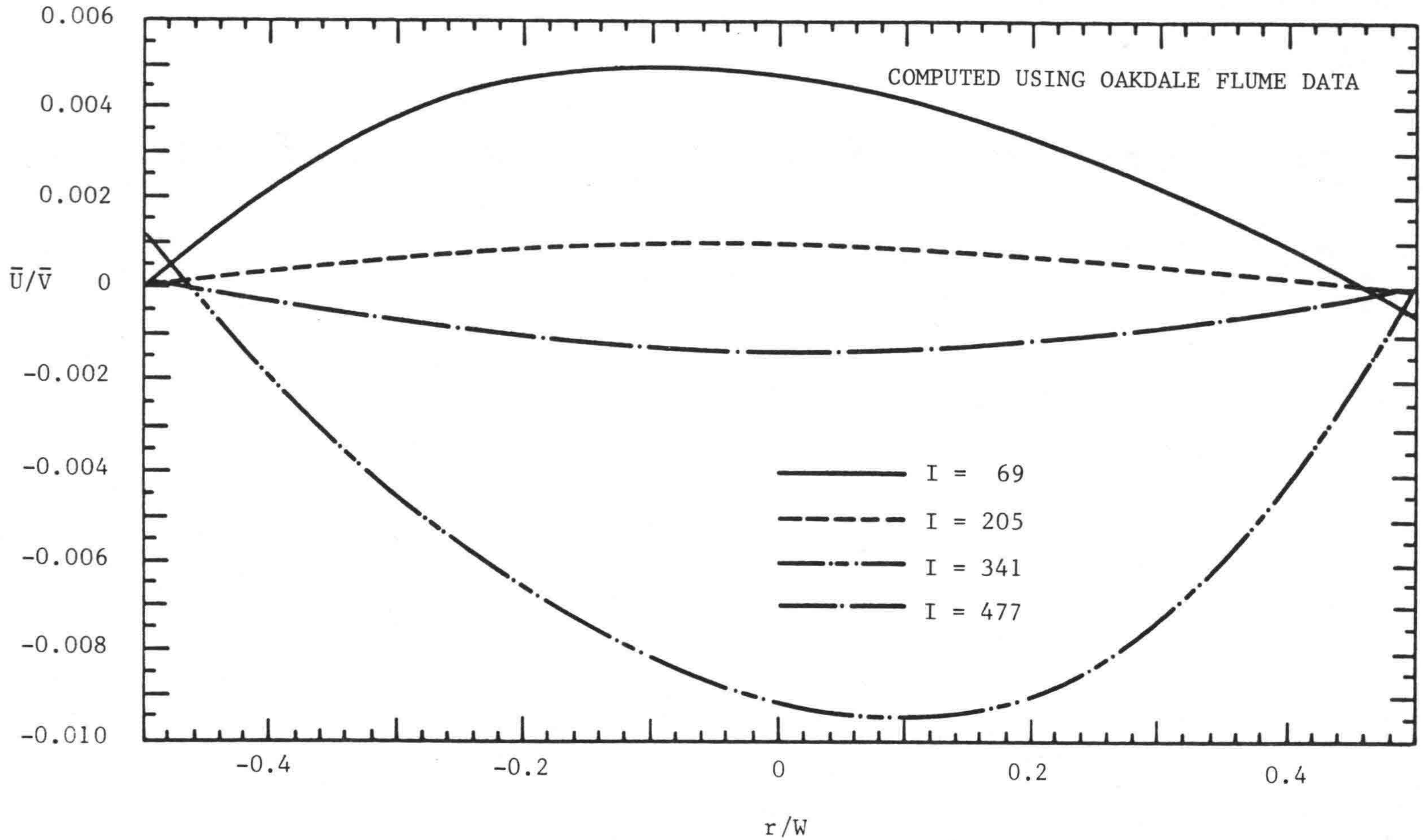

Figure 35 Transverse distributions of computed $\bar{U}/\bar{V}$ for idealized two-bend channel with gradually decreasing radius of centerline curvature

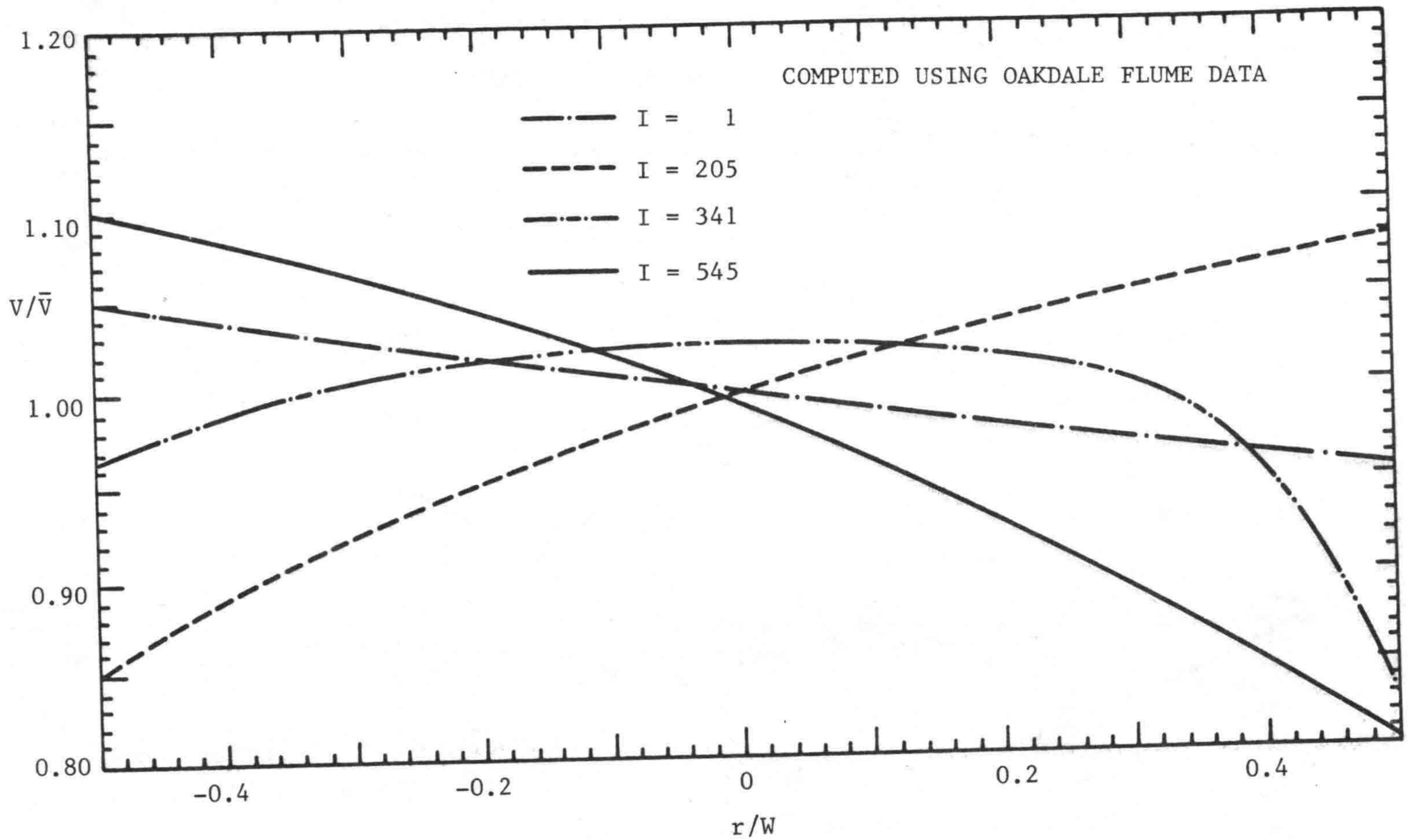

Figure 36 Transverse distributions of computed $V/\bar{V}$ for idealized two-bend channel with gradually decreasing radius of centerline curvature

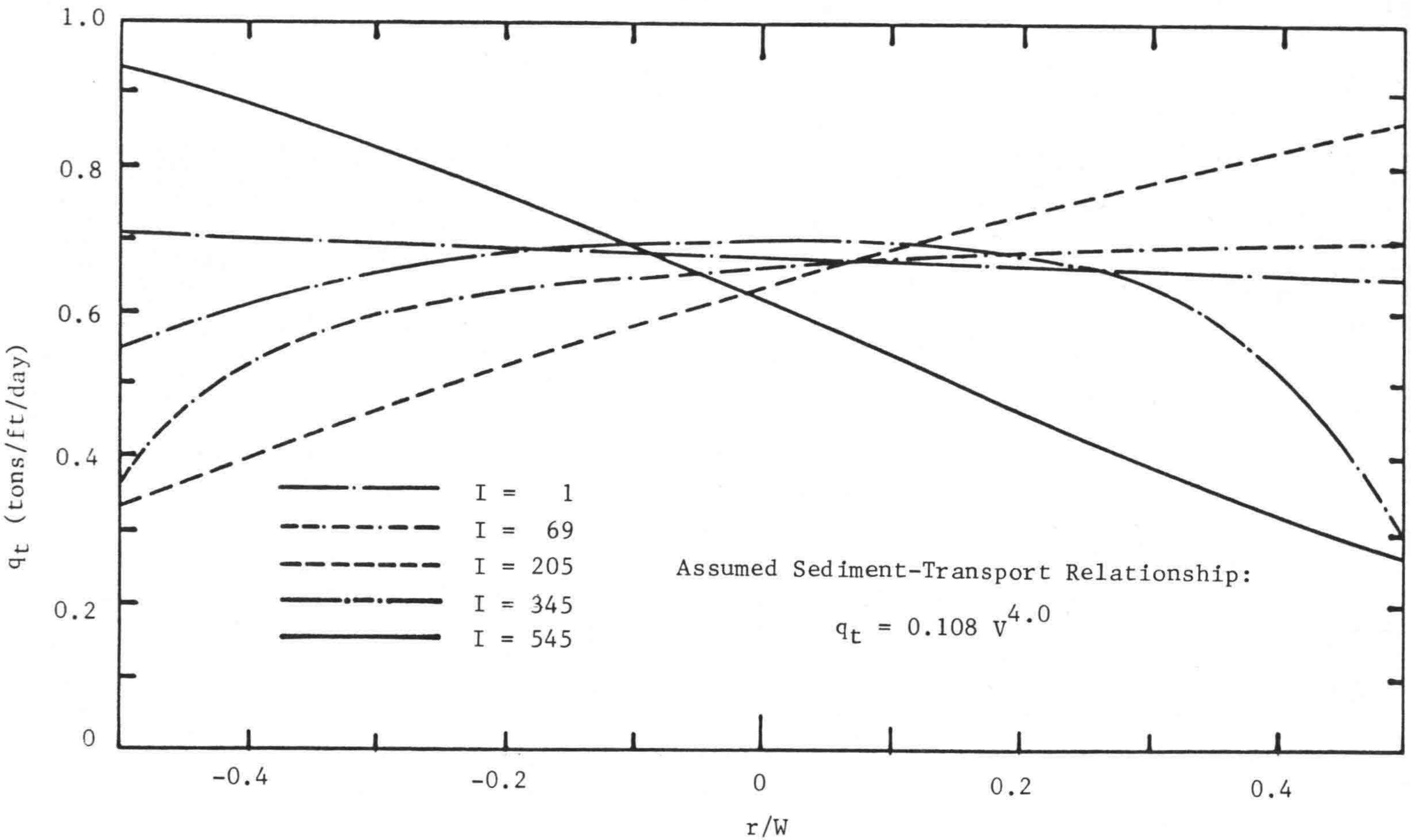

Figure 37 Transverse distributions of computed q_t for idealized two-bend channel with gradually decreasing radius of centerline curvature

APPENDIX A: FLOW IN ALLUVIAL-RIVER CURVES

by

Falcon, M., and Kennedy, J.F.

(Accepted for publication in the
Journal of Fluid Mechanics, Jan. 1983.)

FLOW IN ALLUVIAL-RIVER CURVES

by

Marco Falcon Ascanio[1]

and

John F. Kennedy[2]

I. INTRODUCTION

Even casual observers of Earth's geological features soon notice that natural alluvial streams are seldom straight along reaches of more than a few channel widths. Hydraulic engineers and other students of fluvial processes long have recognized meandering to be not only an intriguing geometrical and kinematical feature of rivers, but also one that has major effects on their sediment-transport and roughness characteristics. Fluid mechanicians appreciate further that the internal structure of flow in meandering rivers is as fascinating as their migrating, serpentine channel lineament. Especially engaging is the interaction between the vertical profile of the primary flow and the centrifugal forces resulting from the flow's curvature. The principal result is the well known spiraling or secondary flow in planes normal to the channel axis. Because the bed-surface sediment of a stream actively transporting its bed material is in a quasi-fluidized state, even the relatively small radial component of the bed shear stress and small near-bed

[1]Professor and Director, Instituto de Mecanica de Fluidos, Facultad de Ingeniereia, Universidad Central, Caracas, Venezuela. Formerly, Benedict Fellow, The University of Iowa, Iowa City, USA.

[2]Carver Professor and Director, Institute of Hydraulic Research, The University of Iowa, Iowa City, USA.

velocities produced by the secondary flow transport sediment toward the inner (convex) banks until the bed becomes inclined such that the gravity and shear forces exerted radially along the bed on the moving bed-load particles are in balance. The resulting greater depth near the outer banks increases the primary-flow velocities there, which in turn intensifies the erosive attack on the banks and also undermines them. Both of these effects aggravate bank erosion and thereby promote further growth of the meanders.

Although the seemingly disproportionate effects of channel meandering on river flow have been appreciated for several decades, attempts to develop a mathematical model for the secondary flow and its interactions with the primary flow and sediment motion have met with only limited success. The principal stumbling block encountered arises from the radial shear-stress force exerted on an elemental control volume at any elevation (the vertical distribution of which is the principal determinant of the radial-plane velocity profile) being the small difference between two much larger quantities: the centrifugal body force and the radial pressure force resulting from superelevation of the water surface. It is important to bear in mind that even though the integrals of these two forces over the depth are very nearly equal, locally they are grossly out of balance. The radial gradient of pressure resulting from the transverse inclination of the free surface is very nearly constant over the depth, while the centrifugal force varies from zero at bed level to a maximum near the free surface. In fact, it is precisely the difference between the distributions of these two nearly equal forces that is responsible for the secondary flow. Moreover, the secondary flow (or, viewed differently, the vertical gradient of the primary velocity) causes the radial water-surface slope to be greater than it would be for a flow with vertically uniform primary velocity (which would not produce a secondary current). This is because the secondary flow produces an inward radial shear force on the bed; the corresponding radially outward force on the flow must be balanced by part of the radial pressure-gradient force. Thus, just in determining the distributions of the three principal radial forces--pressure, shear, and centrifugal--exerted on the flow, one is faced with the problem of having two of them--shear and pressure--unknown, even if the velocity distribution of the primary flow and hence also the centrifugal-force distribution are known. Clearly to proceed with the calculation of these forces, another relation, in addition to the equation expressing the balance of radial forces, is needed. Further physical considerations or assumptions must be introduced to calculate the distribution of the radial velocity.

In the analytical model developed herein for vertical distributions of radial shear stress and velocity, and radial distributions of depth and streamwise velocity, an expression for the conservation of moment-of-momentum is the additional relation utilized to close the formulation of the radial forces. This aspect of the analysis is similar, for example, to use of equations expressing balances of forces and moments to calculate the supporting forces on a loaded, simply supported beam. One of the two unknown forces does not appear in the formulation of moments about one of the supports, and therefore the other can be calculated directly. A roughly parallel approach is followed in the present analysis. Formulation of the flux of moment-of-momentum about the longitudinal axis at the bed surface yields an expression for the radial pressure gradient. The radial momentum equation then is used to obtain the vertical distribution of radial shear stress. The transverse bed profile is determined from consideration of the force balance for the moving bed-load particles. The radial-velocity profile is calculated by introducing into the radial momentum equation a linear primary-shear-stress distribution and the eddy-viscosity distribution obtained from the power-law distribution utilized for the primary velocity. Finally, the radial distribution of local depth corresponding to the bed profile is used in the calculation of the transverse distribution of depth-averaged streamwise velocity. The analysis is limited to a channel of constant centerline radius, which is a good approximation to extended reaches of bows of many strongly meandering natural channels. Extension of the analytical model to weakly meandering channels is developed in Falcon's thesis (1979).

Some of the background literature on this problem is cited in connection with development of the present model. For a more complete review, reference is made to the surveys by Callander (1968, 1978), to Falcon's (1979) thesis, and to Odgaard's (1981) paper on river-bend topography.

II. ANALYSIS

General. The idealized channel treated here has infinite length, constant width, an erodible sediment bed, and banks with a common center of curvature. The central, longitudinal channel axis at the level of the bed has constant mean slope S_c, and describes a helix in space which traces a circle of radius r_c when projected onto a horizontal plane. The flow is conveniently described in cylindrical coordinates: the vertical z axis passes through the curvature center of the channel and is positive in the direction opposite to gravity; in planes perpendicular to the z axis, locations are specified by radial distance from the z axis, r, and polar angle, θ, as shown in figure 1. In order for the radial slopes of the bed and water surface to be constant along the channel, the local streamwise slope, S(r), of both must be

$$S = S_c \frac{r_c}{r}. \tag{1}$$

The flow is treated as uniform in the sense that its properties are invariant along any helix with constant radius r and slope S. The analysis will be restricted further to a central region of the channel, delineated in figure 1, throughout which the vertical velocity is much smaller than the characteristic velocities in the r and θ directions. The channel slope S_c will be limited to small values, so that forces and velocities parallel to the underlying bed-surface helices may be taken to be equal to those along the θ coordinate. Finally, the restriction $d/r \ll 1$ will be imposed, for reasons that become apparent in the next section.

Vertical distribution of radial shear stress. Calculation of the radial shear stress at any elevation requires, first, that the radial water-surface slope and associated pressure gradient be determined, for use in calculation of the vertical distribution of radial shear stress from the radial momentum equation. The radial water-surface slope will be calculated from a simplified, by means of an ordering analysis, formulation of the conservation of flux of moment-of-momentum for the control volume shown in figure 1, which extends over the whole flow depth and has base dimensions Δr and $\Delta s = r\,\Delta\theta$. For this control volume equation of moment-of-momentum about an axis r = constant at the bed surface is

$$\begin{aligned} d\int_0^1 \frac{\partial p}{\partial r}\eta\, d\eta - d\int_0^1 \rho\frac{v^2}{r}\eta\, d\eta + \int_0^1 \tau_{rz}\, d\eta + \frac{1}{d}\frac{\partial}{\partial s}\left[d^2\int_0^1 \rho uv\eta\, d\eta\right] \\ + \frac{1}{rd}\frac{\partial}{\partial r}\left[rd^2\int_0^1 \rho u^2\eta\, d\eta\right] - \int_0^1 \rho uw\, d\eta = 0 \end{aligned} \tag{2}$$

where, in addition to the quantities defined in figure 1, p = pressure; $\eta = \frac{z-h}{d}$; ρ = fluid density; $u(r,\eta)$, $v(r,\eta)$, and $w(r,\eta)$ = velocities in r, θ, and z directions, respectively; and $\tau_{rz}(r,\eta) = \tau_{zr}(r,\eta)$ = shear stress acting on surfaces normal to r and z axes, respectively. The fourth term in (2) is zero for uniform flow. The remaining terms will be ordered by taking $v = O(V)$, where $V(r)$ = depth-averaged flow velocity; $u = O(u(r,1) \equiv U_m)$; and the z-direction velocity $w = O(w_{max} \equiv W_m)$. Relative to the second term, the fifth and sixth terms are of order $O(\frac{U_m^2}{V^2})$ and $O(\frac{r}{d}\frac{U_m}{V}\frac{W_m}{V})$, respectively. Yen (1965) concluded from his measurements of flow in curved channels that $\frac{U_m}{V} = O(\frac{d}{r})$. This result is suggested also by the analysis of Zimmermann and Kennedy (1978, Eq. 7), which shows the ratio of radial to streamwise components of bed shear stress to be $O(\frac{d}{r})$. If $z = O(d)$, the continuity equation,

$$\frac{u}{r} + \frac{\partial u}{\partial r} + \frac{\partial v}{\partial s} + \frac{\partial w}{\partial z} = 0 \qquad (3)$$

in which $\frac{\partial v}{\partial s}$ is zero for the uniform flow being considered, requires that $\frac{W_m}{U} = O(\frac{d}{r})$. Because $\frac{U_m}{V} = O(\frac{d}{r})$, it follows that $\frac{W_m}{V} = O(\frac{d}{r})^2$. It is concluded then that the fifth and sixth terms of (2) are both $O(\frac{d}{r})$ relative to the centrifugal-force (second) term, and can be dropped.

The shear-stress (third) term of (2) may be ordered by utilizing the equality of shear stresses and the Boussinesq shear-stress relation for turbulent flow, and treating the eddy viscosity, ε_0, as constant over the depth:

$$\int_0^1 \tau_{rz}\, d\eta = \int_0^1 \tau_{zr}\, d\eta = \rho \frac{\varepsilon_o}{d} \int_0^1 \frac{\partial u}{\partial n}\, d\eta = \rho \frac{\varepsilon_o U_m}{d} \tag{4}$$

The eddy viscosity may be expressed as a product of the shear velocity, u_*, and depth; therefore,

$$\int_0^1 \tau_{rz}\, d\eta = O(\alpha \rho u_* U) \tag{5}$$

where $\alpha = \varepsilon_o / u_* d$ ($\alpha \simeq 0.079$, according to Hinze (1975)). From (5) it follows that

$$\frac{\int_0^1 \tau_{rz}\, d\eta}{d \int_0^1 \rho \frac{v^2}{r} \eta\, d\eta} = O\left(\alpha \frac{r}{d} \frac{u_*}{V} \frac{U}{V}\right) = O(\alpha \sqrt{f/8}) \tag{6}$$

in which f = Darcy-Weisbach friction factor. Both α and $\sqrt{f/8}$ are $O(10^{-1})$, and therefore the third term of (2) is two orders of magnitude smaller than the second and may be disregarded. Because $p = O(\rho V^2)$, the first and second terms are of the same order. Incorporation of the simplifications resulting from the foregoing ordering analysis reduces (2) to

$$\int_0^1 \frac{\partial p}{\partial r} \eta\, d\eta = \rho \int_0^1 \frac{v^2}{r} \eta\, d\eta \tag{7}$$

In the central region, where $\frac{U_m}{V} \ll 1$ and $\frac{W_m}{V} \ll 1$, it is reasonable to assume that the vertical distribution of p is hydrostatic:

$$\frac{\partial p}{\partial r} = \rho g \frac{\partial H}{\partial r} \equiv \rho g H' \tag{8}$$

where g = gravitational acceleration and H is defined in figure 1. It has been demonstrated by Yen (1965) that the deviation of the pressure from the hydrostatic distribution is $0(\frac{d}{r})$ or smaller in even moderately curved open-channel flow. The primary-flow velocity, $v(r,\eta)$, will be expressed by the power law,

$$\frac{v}{V} = \frac{n+1}{n} \eta^{1/n} \tag{9}$$

where 1/n = exponent, which is related to the Darcy-Weisbach friction factor by

$$\frac{1}{n} = \frac{1}{\kappa} \sqrt{f/8} \tag{10}$$

where κ = Karman's constant. The background of this relation is reviewed by Zimmermann and Kennedy (1978). Karim (1981) examined (10) critically, verified it with laboratory data, and formulated the dependence of κ on sediment concentration; this refinement will not be included in the present analysis. Substitution of (8) and (9) into (7) yields

$$H'(r) = \frac{n+1}{n} \frac{V^2}{rg} \tag{11}$$

By means of an ordering analysis similar to the one developed above and guided in some measure by his experimental results, Yen (1965) simplified the radial momentum equation for curved open-channel flow to

$$gH' - \frac{v^2}{r} - \frac{1}{\rho d} \frac{\partial \tau_{zr}}{\partial \eta} = 0 \tag{12}$$

It is noteworthy that τ_{zr} makes a first-order contribution to the radial-momentum relation, but the corresponding vertical shear stress, τ_{rz}, makes only a higher-order contribution to the moment-of-momentum equation if the moment axis is taken at bed level to avoid inclusion of the bed shear stress. This is, in fact, the motivation for utilizing the moment relation: it avoids specification of τ_{rz} at the bed in the determination of H'. Substitution of (9) into (12), integration of the resulting expression from arbitrary η to η = 1, and application of the boundary condition $\tau_{rz}(1) = 0$ yields

$$\tau_{zr}(r,\eta) = \rho g d \left[H'(\eta-1) - \frac{V^2}{rg} \frac{(n+1)^2}{n(n+2)} \left(\eta^{\frac{2+n}{n}} - 1\right)\right] \tag{13}$$

<u>Traverse bed profile and depth distribution</u>. Equilibrium of the transverse bed profile, $h(r,\theta)$ in figure 1, and of the depth, $d(r)$, are attained when the radial-plane forces acting on the moving, bed-load particles sum to zero. Bed-load movement will be treated as occurring in a layer of thickness y_b, as shown in figure 1. The shear forces exerted on this agitated, somewhat dilated, moving layer are in reality diffuse, "seepage" forces caused by the flow within the layer's intersticies, and any net force, however small, in the radial direction will produce transverse motion of the bed-load particles. Therefore, radial equilibrium will be reached when the local bed inclination, $\beta(r)$, is such that

$$\tau_{or} = \tau_{zr}(0) = y_b(1-p)\,\Delta\rho\, g \sin\beta \tag{14}$$

where p = porosity of the bed-layer; $\Delta\rho = \rho_s - \rho$; and ρ_s = density of bed particles. In the development of his detailed, computer-simulation model of sediment transport in streams, Karim (1981) concluded from inferential evidence that

$$y_b = D_{50} \frac{u_*}{u_{*c}} \qquad (15)$$

where D_{50} = median bed-material size, $u_*(r)$ = local shear velocity = $V\sqrt{f/8}$; and u_{*c} = critical shear velocity for incipient particle motion. In terms of the Shields parameter, θ, u_{*c} may be expressed

$$u_{*c} = \sqrt{g \frac{\Delta\rho}{\rho} D_{50}\, \theta} \qquad (16)$$

which defines θ. Substitution of (13), (11), (15) and (16) into (14), and incorporation of the simplification of (10) to Nunner's (1956) relation (Hinze 1975),

$$n = 1/\sqrt{f} \qquad (17)$$

which corresponds to $\kappa = 0.354$, yields

$$S_T \equiv \sin\beta = \frac{d}{r} F_D \frac{\sqrt{8\theta}}{(1-p)} \frac{1 + \sqrt{f}}{1 + 2\sqrt{f}} \qquad (18)$$

where $F_D = V/\sqrt{g \frac{\Delta\rho}{\rho} D_{50}}$.

The traverse bed profile may be calculated by neglecting the effect of H' on d(r); then

$$\sin \beta = \frac{dd}{dr} \tag{19}$$

The velocity V to be used in (18) is obtained by incorporating (1) into the local expression of the Darcy-Weisbach friction factor,

$$V(r) = \sqrt{8\frac{\tau_{0\theta}}{\rho f}} = \sqrt{8\frac{\delta S\rho g d(r)}{\rho f}} = \sqrt{8 S_c \frac{r_c}{r} \frac{g\delta d(r)}{f}} \tag{20}$$

where $\tau_{0\theta}$ = longitudinal shear stress acting on the bed; and $\delta(r)$ = bed-shear-stress reduction factor defined by

$$\tau_{0\theta}(r) = \delta S\rho g d(r) \tag{21}$$

which takes into account the transport of primary-flow momentum out of the central region to the vicinity of the outer bank, where it is balanced by bank shear. An analysis of δ is developed below. Substitution of (19), (20), and (1) into (18) and integration of the resulting expression for $\frac{dd}{dr}$ yields

$$\frac{1}{\sqrt{d}} - \frac{1}{\sqrt{d_c}} = \left[\frac{1}{\sqrt{r}} - \frac{1}{\sqrt{r_c}}\right] \frac{\sqrt{8\theta}}{(1-p)} \frac{1+\sqrt{f}}{1+2\sqrt{f}} \sqrt{\frac{8\, S_c r_c g\delta}{f\, g \frac{\Delta\rho}{\rho} D_{50}}} \tag{22}$$

where the subscript c denotes the centerline values used in setting the integration constant. Elimination of δS_c from (22) by means of (20) and replacing V by its section averaged value for the whole flow, $\overline{V}$, to facilitate verification, leads to

$$\sqrt{\frac{d}{d_c}} = 1 - (1 - \sqrt{\frac{r}{r_c}})\, \frac{\sqrt{8\theta}}{(1-p)}\, \frac{1 + \sqrt{f}}{1 + 2\sqrt{f}}\, \overline{F}_D \tag{23}$$

where $\overline{F}_D = \overline{V}/\sqrt{g \frac{\Delta\rho}{\rho} D_{50}}$

Utilization of the mean velocity for the whole cross section in the calculation of d(r) from (23), or in calculating an average value of S_T from (18), by replacing F_D with $\overline{F}_D$ neglects the effects of the variation of V across the channel, but nevertheless yields satisfactory results, as is demonstrated in Section III.

Equations 20 and 23 give the radial distribution of mean velocity for uniform flow. In practical applications, it generally suffices to take $\delta = 1$.

Vertical distribution of transverse velocity. Calculation of the radial-plane velocity will incorporate the following assumptions:

1. The primary-flow shear stress, $\tau_{z\theta}$, is linearly distributed and $\frac{\partial \tau_{r\theta}}{\partial r}$ makes a negligible contribution to the streamwise force balance:

$$\tau_{z\theta}(r,\eta) = \tau_{o\theta}(1-\eta) = \delta\rho g d S(1-\eta) \tag{24}$$

2. The eddy viscosity is isotropic and is given by

$$\varepsilon(r,\eta) = \frac{d}{\rho} \frac{\tau_{z\theta}}{\frac{\partial v}{\partial \eta}} \tag{25}$$

3. Because of the isotropy of ε, the radial velocity and shear stress are related by

$$\tau_{zr}(r,\eta) = \frac{\rho\varepsilon}{d}\frac{\partial u}{\partial \eta} \tag{26}$$

Substitution of (9) and (24) into (25) yields

$$\varepsilon = \frac{\delta g d^2 S_c r_c}{rV} \frac{n^2}{n+1} (1-\eta)\, \eta^{\frac{n-1}{n}} \tag{27}$$

which, when substituted along with (13) into (26), leads to

$$\frac{u}{V} = \frac{1}{\delta S_c} \frac{r}{r_c} \frac{n+1}{n^2} \int_0^{\eta} \left[-H'\eta^{\frac{1-n}{n}} - \frac{V^2}{rg} \frac{(n+1)^2}{n(n+2)} \frac{\eta^{\frac{3}{n}} - \eta^{\frac{1-n}{n}}}{1-\eta}\, d\eta\right] \tag{28}$$

For steady, uniform flow, u must satisfy

$$\int_0^1 u(\eta)\, d\eta = 0 \tag{29}$$

There is no assurance that (28) will satisfy this requirement if H' given by (11) is utilized, because of errors inherent in the Boussinesq eddy-viscosity model and other assumptions that have been made in the derivation of the relation for u. Therefore, the integral of (29) will be evaluated for arbitrary H', denoted by H'_u and expressed as

$$H'_u(r) \equiv T \frac{n+1}{n} \frac{V^2}{rg} \tag{30}$$

where $T = H'_u/H'$ and H' is given by (11). Substituion of (28) and (30) into (29), utilization of the expansion

$$\frac{1}{1-\eta} = \sum_{j=0}^{\infty} \eta^{j}; \; \eta < 1 \tag{31}$$

and term-by-term integration of the resulting series yields

$$\frac{u}{V} = \frac{1}{\delta S_c}\,\frac{V^2}{g r_c}\left(\frac{n+1}{n}\right)^3 \left[-\,T\eta^{\frac{1}{n}} - \frac{1}{n+2}\sum_{j=0}^{\infty}\left(\frac{\eta^{\frac{3}{n}+1+j}}{\frac{3}{n}+1+j} - \frac{\eta^{\frac{1}{n}+j}}{\frac{1}{n}+j}\right)\right] \tag{32}$$

Equation 29 is satisfied if T is given by

$$T(n) = -\,\frac{(n+1)}{n^2(n+2)}\sum_{j=0}^{\infty}\left[\frac{1}{(\frac{3}{n}+2+j)(\frac{3}{n}+1+j)} - \frac{1}{(\frac{1}{n}+1+j)(\frac{1}{n}+j)}\right] \tag{33}$$

Incorporation of (17), (20), and (33) into (32) gives

$$\frac{u}{V}\,\frac{r}{d} = 8\sum_{j=0}^{\infty}\left\{\frac{(n+1)^4}{n^2(n+2)}\left[\frac{1}{(\frac{3}{n}+2+j)(\frac{3}{n}+1+j)} - \frac{1}{(\frac{1}{n}+1+j)(\frac{1}{n}+j)}\right]\eta^{\frac{1}{n}}\right.$$

$$\left. -\,\frac{(n+1)^3}{n(n+2)}\left[\frac{\eta^{\frac{3}{n}+1+j}}{(\frac{3}{n}+1+j)} - \frac{\eta^{\frac{1}{n}+j}}{(\frac{1}{n}+j)}\right]\right\} \equiv G(\eta, n) \tag{34}$$

Equation 34 is portrayed in figure 2 for four values of n which span the range from very rough ($n = 2.5$; $f = 0.16$) to relatively smooth ($n = 10$, $f = 0.01$) channels. It is noteworthy that for all but very low values of n, the velocity profiles are nearly linear except near the bed, with $u = 0$ at about mid-depth.

A remark on H' and H'_u. In the foregoing analysis, two expressions were derived for the transverse slope of the water surface: (11), and (30) and (33). Corresponding to each of these is a different value of $\tau_{zr}(0)$, the radial component of the bed shear stress. Their ratio $T = H'_u/H'$ given by

(33) has a nearly constant value of 0.9 for $2 < n < 8$. In view of the near equality of H'_u and H', why was it necessary to utilize different values in the formulations of τ_{zr} and of $u(\eta)$? The problem is one of sensitivity, as will now be demonstrated. Equation 13 gives

$$\tau_{or}(r) = \tau_{zr}(r,0) = \rho gd \left[\frac{V^2}{rg}\frac{(n+1)^2}{n(n+2)} - H'\right] \tag{35}$$

which together with (11) for H' shows that τ_{or} is the difference between two small quantities multiplied by a large one, (ρgd). Therefore, small errors in the expression for the transverse water slope produce large errors in τ_{or}. For example, the ratio of τ_{or} given by (35) with H' replaced by H'_u obtained from (30) and (33), to τ_{or} yielded by (35) and (11) varies widely with n, from about 0.6 for $n = 2$ to nearly 0.2 for $n = 8$. Because the radial bed slope and thus also the bed profile depend directly on τ_{or}, as is shown by (14), it is important in their derivation to have an accurate estimate of τ_{or} --one whose calculation avoids use of such artifices as the Boussinesq relation, and instead directly utilizes a mechanics principle such as conservation of moment of momentum. The effect of the radial water-surface slope on $u(\eta)$ calculated from the Boussinesq relation may be examined by substituting (26) into (12) and treating ε as constant, say ε_o, which results in

$$\frac{\partial^2 u}{\partial \eta^2} = \frac{gd^2}{\varepsilon_o}\left(\frac{v^2}{gr} - H'\right) \tag{36}$$

Equation 36 shows that $\frac{\partial^2 u}{\partial \eta^2}$, and hence $u(\eta)$, also is very sensitive to the small difference between two nearly equal quantities multiplied by a large one. Accordingly, only a very small adjustment in the radial water-surface slope is required to compensate for the effects on u of the assumptions made in its calculation, and thereby to permit u to satisfy the continuity requirement, (29). But this small adjustment in H'--amounting to only about 10 percent, as just noted--has a major effect on τ_{or}, as (35) demonstrates.

Secondary-flow effects on $\tau_{z\theta}$ and v. In a laterally nonuniform curved flow, the secondary current produces a net radial transport of streamwise (θ-direction) momentum out of the central region, which in turn reduces $\tau_{z\theta}$ and in so doing modifies $v(r,\eta)$(or η). It was anticipation of this effect which prompted incorporation of the factor $\delta(r)$ into the shear-stress expressions, (20) and (21). Calculation of δ and the secondary-flow effect on $v(\eta)$ proceeds from the θ -direction momentum equation with $\tau_{r\theta}$ neglected,

$$u \frac{\partial v}{\partial r} + v \frac{\partial v}{\partial s} + w \frac{\partial v}{\partial z} + \frac{uv}{r} = - g \frac{\partial H}{\partial s} + \frac{1}{\rho} \frac{\partial \tau_{z\theta}}{\partial z}. \qquad (37)$$

Multiplication of (3) by v, addition of the result to (37), integration of the new relation from η to 1, and imposition of the boundary condition $\tau_{z\theta}(r,1,\theta) = 0$ gives

$$\tau_{z\theta} = \rho d \{- \int_{\eta}^{1} \frac{\partial (uv)}{\partial r} d\eta - \frac{2}{r} \int_{\eta}^{1} uv \, d\eta - \int_{\eta}^{1} \frac{\partial v^2}{\partial s} d\eta - \frac{1}{d} [(wv)_{\eta=1} - wv] + g S(1-\eta)\}. \qquad (38)$$

where $S = - \frac{\partial H}{\partial s}$. The z velocity, w, is evaluated from the continuity equation, (3), the relation for u, (32), and the identities,

$$\frac{\partial \eta}{\partial r} = - \frac{-d \frac{\partial h}{\partial r} - (z-h) \frac{\partial d}{\partial r}}{d^2} = \frac{-d \frac{\partial (H-d)}{\partial r} - \eta d \frac{\partial d}{\partial r}}{d^2} = \frac{(1-\eta) \frac{dd}{dr} - \frac{\partial H}{\partial r}}{d}, \qquad (39)$$

and, similarly,

$$\frac{\partial \eta}{\partial s} = \frac{S}{d}. \tag{40}$$

The result is

$$w(r,\eta) = -\left[\frac{d}{r} + \frac{dd}{dr} + d\left(\frac{3}{V}\ \frac{dV}{dr} - \frac{1}{\delta}\frac{d\delta}{dr}\right)\right] \int_0^{\eta} u\, d\eta$$
$$+ \left[\frac{\partial H}{\partial r} - \frac{dd}{dr}(1-\eta)\right] u - Sv. \tag{41}$$

Substitution of (9), (34), and (41) for v, u, and w along with

$$\frac{\partial v^2}{\partial s} = \frac{S}{d}\frac{\partial v^2}{\partial \eta} \tag{42}$$

into (38) yields

$$\frac{\tau_{z\theta}}{\rho g S d} = (1-\eta) - 64\delta \frac{d}{r} n(n+1)\left\{\left[\frac{dd}{dr} + 2\frac{d}{r} + 4\frac{d}{V}\frac{dV}{dr} - \frac{d}{\delta}\frac{d\delta}{dr}\right] \int_{\eta}^{1} G(n,\eta)\, \eta^{\frac{1}{n}}\, d\eta\right.$$
$$\left. + \left[\frac{dd}{dr} + \frac{d}{r} + 3\frac{d}{V}\frac{dV}{dr} - \frac{d}{\delta}\frac{d\delta}{dr}\right] \eta^{\frac{1}{n}} \int_0^{\eta} G(n,\eta)\, d\eta\right\} \tag{43}$$

where G is defined by (34).

The first terms on the right-hand side of (43) is the linear shear-stress distribution, and the second term expresses the shear-stress reduction due to the transverse gradient of lateral flux of streamwise momentum. In the calculation of $\tau_{z\theta}$ it is assumed that the $\frac{\partial \delta}{\partial r}$ term is negligible in comparison to the other derivative terms in brackets. Substitution of (18) for $\frac{dd}{dr}$ and of

(20) for V then permits calculation of the shear stress at any location. The bed-shear-stress reduction factor, δ, introduced in (20) and (21), is obtained by letting $\eta = 0$ in (43). To gain some idea of its magnitude, a representative constant value of δ for the whole central region, say $\overline{\delta}$, will be determined. For this calculation it is appropriate to replace V and d by their section-averaged values, $\overline{V}$ and $\overline{d}$, after carrying out the substitutions and taking the derivatives in (43); and to take $r = r_c$. The result is

$$\overline{\delta} = \frac{\tau_{o\theta}}{\rho gSd} = \left[1 + 192\,\frac{\overline{d}}{r_c}\; n\,(n+1)\,\overline{S}_T \int_0^1 G(n,\eta)\,\eta^{1/n}\,d\eta\right]^{-1} \tag{44}$$

where $\overline{S}_T$ is obtained from (18) by replacing d and V by $\overline{d}$ and $\overline{V}$. The integral of (44) was evaluated numerically, with the result shown in figure 3. Values of $\overline{\delta}$ for some field and laboratory flows are presented in the next section.

The effect of the secondary flow on the primary-flow velocity distribution may be estimated by substituting (17) into (20) and replacing δ by $\overline{\delta}$. If V is considered to be constant, n is increased, as $1/\sqrt{\overline{\delta}}$, which corresponds to the velocity becoming blunter. This is the observed effect of secondary flow on $v(\eta)$ (Falcon 1978).

III. VERIFICATION

Data utilized in the verifications reported here are summarized in table 1. Falcon (1978) presents additional comparisons of measured and computed quantities.

Bed topography. Zimmermann (1974) and Zimmermann and Kennedy (1978) reported the results of experiments conducted in three, concentric, 60-cm wide, circular-plan-form flumes with a central angle that approached 2π. Two different sediments, with median diameters of 0.21 mm and 0.55 mm, were used. Longitudinal bed profiles were measured at 11 different radii, and the transverse bed profiles obtained from them for numerous cross-sections in the reaches of fully developed flow were plotted and averaged. The transverse profiles were found to be slightly convex upward, as illustrated in figure 4. Mean transverse bed slopes, averaged across numerous sections for each run, were then computed. Figure 5 shows the transverse slopes, $\overline{S}_T$, so determined plotted in the format of (18) based on cross-section-averaged properties. Excellent agreement between measured and computed values is obtained if $\frac{\sqrt{8\theta}}{(1-p)} = 1.3$. If the limiting value (for fully turbulent boundary layers) of the Shields parameter, $\theta = 0.06$, is adopted, the resulting porosity is $p = 0.47$, a not unreasonable value for the agitated, dilated, moving bed-load particles. The computed profile for Zimmermann's (1974) Run No. RII-13 shown in figure 4 was obtained from (23), using these values of θ and p. The centerline depth, $d_c = 9.66$ cm utilized in computing the profile was obtained by equating the reported mean depth, 10.1 cm, to the mean depth $\overline{d}$ calculated by integration of d given by (23) across the channel width:

$$\frac{\overline{d}}{d_c} = 1 - 2\phi + 2\phi^2 + \frac{4}{3}\,\frac{(\phi-\phi^2)(r_o^{3/2} - r_i^{3/2})}{\sqrt{r_c}\,(r_o - r_i)} \tag{45}$$

where $\phi = \overline{F}_D \frac{\sqrt{8\theta}}{(1-p)} \frac{1 + \sqrt{f}}{1 + 2\sqrt{f}}$, and r_i and r_o = radii of the inner and outer banks, respectively. Calculation of the relation between $\overline{d}$ and d_c in this way is consistent with the measurement procedure that was used. Falcon (1978) describes calculation of $\overline{d}$ in a way that is consistent with conservation of bed-material volume in a curved channel. The friction factor utilized, f = 0.165 for this flow, is the value for the bed section obtained from the sidewall-correction procedure (Vanoni 1976, p. 152). The measured and computed profiles are in excellent agreement. The bed-shear-stress reduction factor obtained from (44) for this flow is $\bar{\delta} = 0.43$, which shows that in this relatively narrow channel the secondary current produced a major reduction in the bed shear.

Figure 6 compares measured and computed transverse bed profiles for a Missouri River section (Falcon 1978). In computing the profile, $\bar{d}$ was taken to be equal to d_c, because of the difficulty of determining r_c for a wide natural stream, and of the insensitivity of d_c to r_c (see (45)). Included in figure 6 is the mean bed profile given by (18), which also is seen to give quite good results. Equation 44 gives $\bar{\delta} = 0.97$ for this relatively wide, shallow flow, demonstrating the bed shear stress at any r in the central region of this natural channel is nearly equal the local value of ρgdS. Other comparisons of measured and computed bed profiles yielded conformities as good as those demonstrated in figures 4 and 6. In evaluating data from natural streams, in which the flow is seldom steady for appreciable periods, there is always uncertainty about the equilibrium of the bed topography. Moreover, the bed-material size often varies widely across a section, often by a factor of five or more. In view of these difficulties, it is suggested that in the calculation of bed topography by means of (18) and (23), averaged (across channel sections, and along subreaches that are sufficiently short that r_c is practically constant) values of $\bar{d}$ and $\bar{V}$ be used, and that the median diameter of the material that can be moved by the flow be utilized for D_{50}. Furthermore, for most natural-stream situations, the refinement given by (23) is probably not justified; a straight-line profile with slope S_T given by (18) and passing through $d = \bar{d}$ at $r = r_c$ is generally as accurate as the field data warrant, and perhaps within the reproducibility of bed topography of natural streams with their vagaries of discharge and bed-sediment characteristics.

Velocity distributions. It is very difficult to obtain reliable data on $u(n,r)$ in erodible-bed channels, because of the small values of the secondary-flow velocities, and of the problems posed by the moving sediment and the continuous bed changes attendant to migration of bed forms. Therefore, the two measured profiles obtained by Kikkawa, Ikeda, and Kitagawa (1976) from uniform flow in a circular-plan-form, rigid channel were utilized in the verification of (34), with the results shown in figure 7. Kikkawa et al (1976) developed an analytic model for $u(n)$, which can be seen in their paper also to yield generally satisfactory results except near the bed, where it does not satisfy the no-slip condition. Comparisons presented by Falcon (1979) of (34) with the rigid, sinuous-channel data on transverse-velocities reported by Yen (1965) also demonstrate very satisfactory agreement.

The transverse distributions of V, the depth-averaged streamwise velocity, in erodible-bed channels are somewhat easier to measure than the radial-velocity distributions. Velocity data obtained by Onishi (1972) at the apex cross sections in two of his rigid-bank, erodible-bed, meandering-channel flows were used to validate the distribution of V obtained from (20) and (23). The average friction factors, $\overline{f}$, used in the computations were obtained from the reported mean values of velocity, depth and slope for the flows, and the Darcy-Weisbach relation in the form

$$\overline{f} = \frac{8g\overline{d}S}{\overline{V}^2} \tag{46}$$

Note that computation of $\overline{f}$ from (46), which assumes $\delta = 1$, and of the corresponding n from (17), computation of $\overline{\delta}$ from (44) for this n, and use of $\overline{\delta}$ and $\overline{f}$ in (20) to determine $V(r)$ is slightly inconsistent. Falcon recommends iteration between (20) with $V = \overline{V}$, (44), and (17) to obtain consistent values of n, f, and $\overline{\delta}$. However, the convergence is quite rapid and the effect on the computed $V(r)$ or $u(\eta)$ is not great. The computed and measured distributions of $V(r)$ shown in figure 8 agree quite well except near the banks, where V must tend to zero.

IV. CONCLUDING REMARKS

It must be borne in mind that the model developed here is strictly valid only for uniform, curved-channel flows. However, the available experimental data on flows in strongly curved channels (Zimmermann 1974, Zimmermann and Kennedy 1978, Odgaard and Kennedy 1982) indicate that they are characterized by relatively small phase shifts or lag distances between local secondary-flow properties or bed topography and local channel curvature. Therefore, application of the present model utilizing local channel and flow characteristics in nonuniform flows, as was done in the foregoing comparison with Onishi's (1972) data, will generally yield satisfactory results. However, in the case of flow in weakly meandering sinuous channels, as investigated by Gottlieb (1976) and Falcon (1979), the phase shift between local channel curvature and secondary-flow strength approaches $\pi/2$.

The analytical model developed here is valid only for the central regions of curved-channel flows, which generally extend to about one local depth from the bank. In the near-bank regions, the flow becomes strongly three-dimensional and heavily influenced by local bank characteristics (erodibility, slope, roughness, etc). Analysis of the flow and sediment transport in these regions is correspondingly more difficult than for the central region, and likely must await availability of better experimental data for its guidance.

ACKNOWLEDGEMENTS

The analysis presented here was largely developed in the course of the Ph.D. thesis research of the first author. Further work was done after his departure from The University of Iowa under the sponsorship of the U.S. Army Corps of Engineers Waterways Experiment Station (Contract No. DACW39-80-C-0129). The analysis was completed and the manuscript prepared under support provided by the National Science Foundation (Grant No. CEE-8023003).

REFERENCES

CALLANDER, R.A., "Instability and River Meanders," Ph.D. Thesis, Univ. of Auckland, New Zealand, 1968.

CALLANDER, R.A., "River Meandering," Ann. Rev. Fluid Mech., Vol. 10, pp. 129-158, 1978.

GOTTLIEB, L., "Three-Dimensional Flow Pattern and Bed Topography in Meandering Channels," Series Paper 11, Institute of Hydrodynamics and Hydraulic Engineering, Tech. Univ. of Denmark, Lyngby, February 1976.

HINZE, J.O., Turbulence, Second Edition, McGraw-Hill Book Company, New York, 1975.

KARIM, M.F., "Computer-Based Predictors for Sediment Discharge and Friction Factor of Alluvial Streams," Ph.D. Thesis, Dept. of Mech. and Hyd., Univ. of Iowa, 1981.

FALCON, M.A., "Analysis of Flow in Alluvial Channel Bends," Ph.D. Thesis, Dept. of Mech. and Hydr., Univ. of Iowa, 1979.

KIKKAWA, H., IKEDA, S., and KITAGAWA, A., "Flow and Bed Topography in Curved Open Channels," Proc. ASCE, Jour. Hyd. Div., HY9, Vol. 102, pp. 1327-42 September 1976.

NUNNER, W., Warmeubergang und druckabfall in rauhen Rohren", VDI-Forschungscheft 455, B, Band 2, 1956.

ODGAARD, A.J., "Transverse Bed Slope in Alluvial Channel Bends", Proc. ASCE, Jour. Hyd. Div., HY12, pp. 1677-94, December 1981.

ODGAARD, A.J. and KENNEDY, J.F., "Analysis of Sacramento River Bend Flows, and Development of a New Method for Bank Protection", IIHR Report No. 241, Iowa Institute of Hydraulic Research, Univ. of Iowa, May 1982.

ONISHI, Y., "Effect of Meandering on Sediment Discharges and Friction Fators of Alluvial Streams", Ph.D. Thesis, Dept. of Mech. and Hydr., Univ. of Iowa, 1972.

VANONI, V.A. (ed)., <u>Sedimentation Engineering</u>, Am. Soc. of Civ. Engrs., Manual No. 54, ASCE, New York, 1975.

YEN, B.C., "Characteristics of Subcritical Flow in a Meandering Channel", Ph.D. Thesis, Dept. of Mech. and Hydr., Univ. of Iowa, Iowa City, Iowa, 1965. (Also available as unnumbered report from the Iowa Institute of Hydraulic Research).

ZIMMERMANN, C., "Sohlausbildung, Reibungsfaktoren, und Sediment-Transport in Gleichformig Gekrummten und Geraden Gerinnen," Ph.D. thesis, Inst. of Hydromechanics, Univ. of Karlsruhe, Karlsruhe, Germany, 1974.

ZIMMERMANN, C., and KENNEDY, J.F., "Transverse Bed Slopes in Curved Alluvial Streams," Proc. ASCE, Jour. Hyd. Div., Vol. 104, HY1, pp. 33-48, January 1978.

FIGURE CAPTIONS

1. Definition sketch for flow in an alluvial-channel bend.

2. Distribution of radial-plane, secondary-flow velocity given by (34).

3. Result of the numerical evaluation of $\int_0^1 G(n,\eta)\eta^{\frac{1}{n}}\, d\eta$, where G is given by (34).

4. Transverse bed profiles measured in Zimmermann's (1974) Run RII-13, and computed from (23).

5. Comparison of (18) and Zimmermann and Kennedy's (1978) measured transverse bed slopes.

6. Transverse bed profile measured in Missouri River (Falcon 1978) and, those computed from (18) (----) and (23) (——) .

7. Secondary-flow velocity profiles measured by Kikkawa et al (1976) and computed from (34).

8. Comparison of Onishi's (1972) measured transverse distributions of depth-averaged velocity and those computed from (20) and (23).

Table 1

Summary of Data Used in Verification Calculations

Ref	Run No.	$\overline{V}$ cm/sec	$\overline{d}$ cm	D_{50} mm	S	$\overline{f}$	r_c m	r_o-r_i m	$\overline{\delta}$
Zimmermann (1974)	RII-13	36.7	10.5	0.21	0.0028	0.165	2.55	0.60	0.43
Falcon (1978)	Missouri River	156	354	0.23	0.00015	0.0171	2,975	~ 150	0.97
Kikkawa et al (1976)	F-1	40	5.0	-	0.002	0.049	4.50	0.90	-
	F-3	48	6.3	-	0.002	0.043	4.50	0.90	-
Onishi (1972)	C-13	54.2	13.1	0.25	0.0024	0.083	8.53	2.08	0.68
	CH-13	53.6	13.3	0.25	0.018	0.62	9.09	0.90	0.65

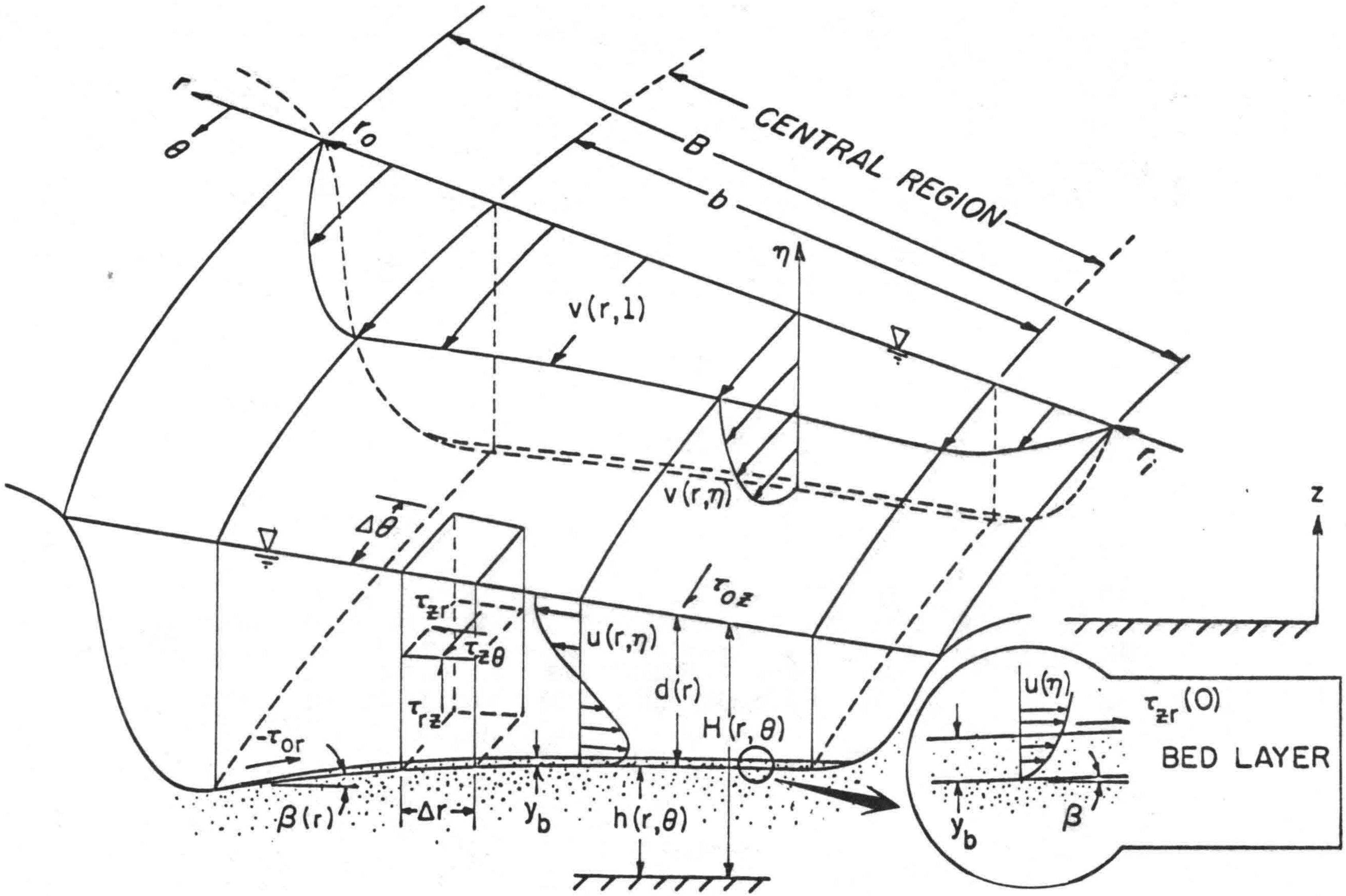

Figure 1. Definition sketch for flow in an alluvial-channel bend.

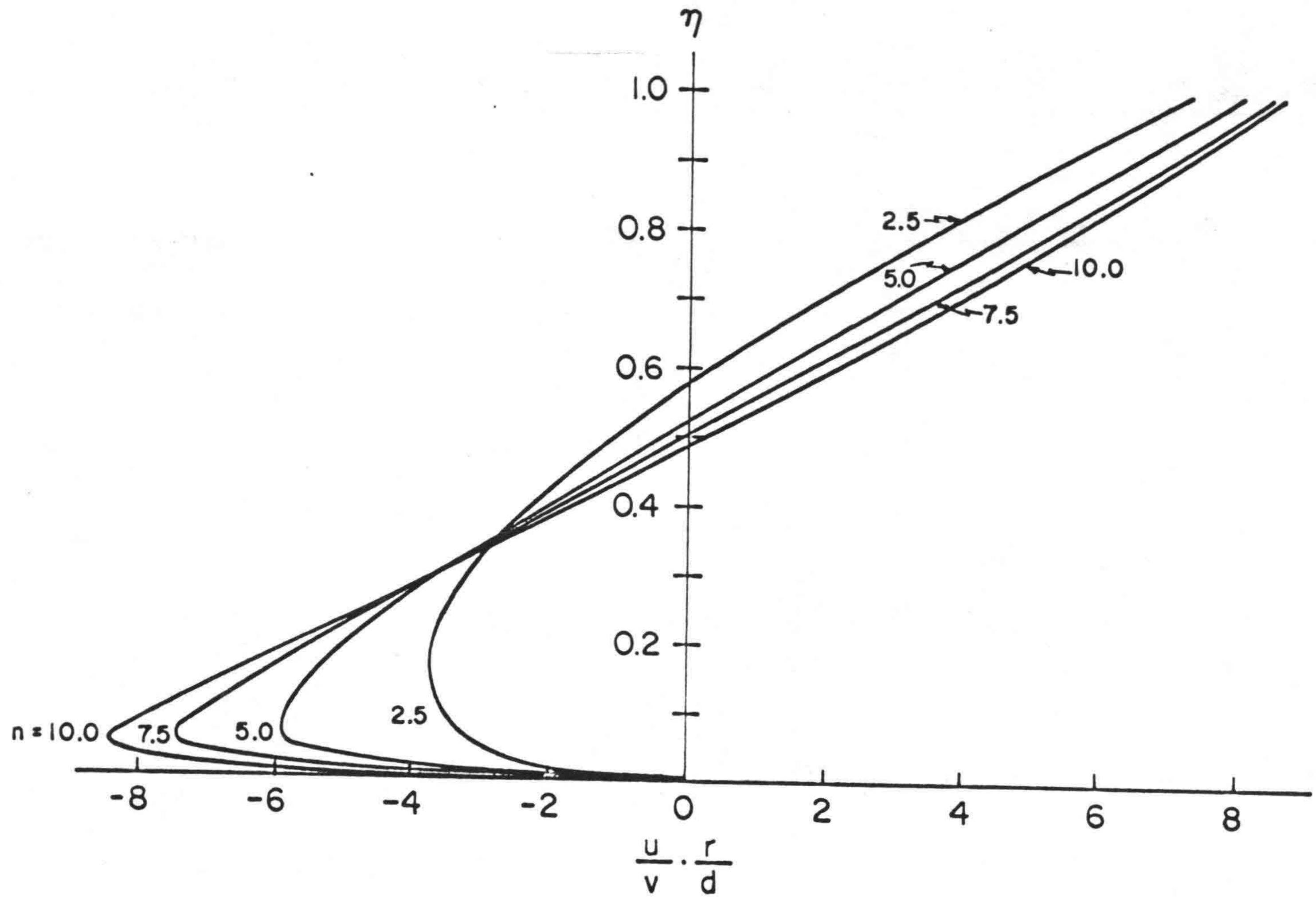

Figure 2. Distribution of radial-plane, secondary-flow velocity given by (34).

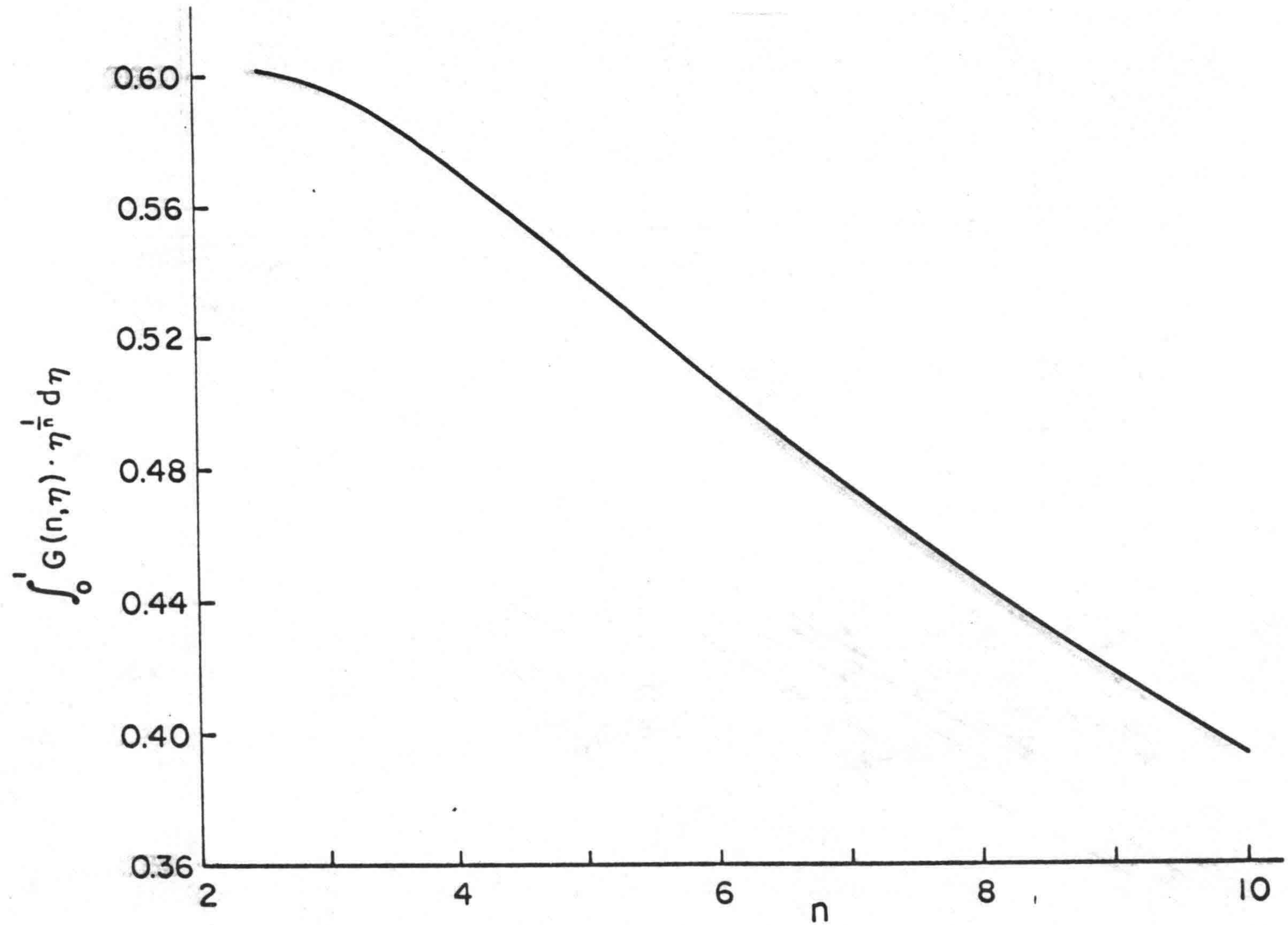

Figure 3. Result of the numerical evaluation of $\int_0^1 G(n,\eta)\eta^{\frac{1}{n}}\,d\eta$, where G is given by (34).

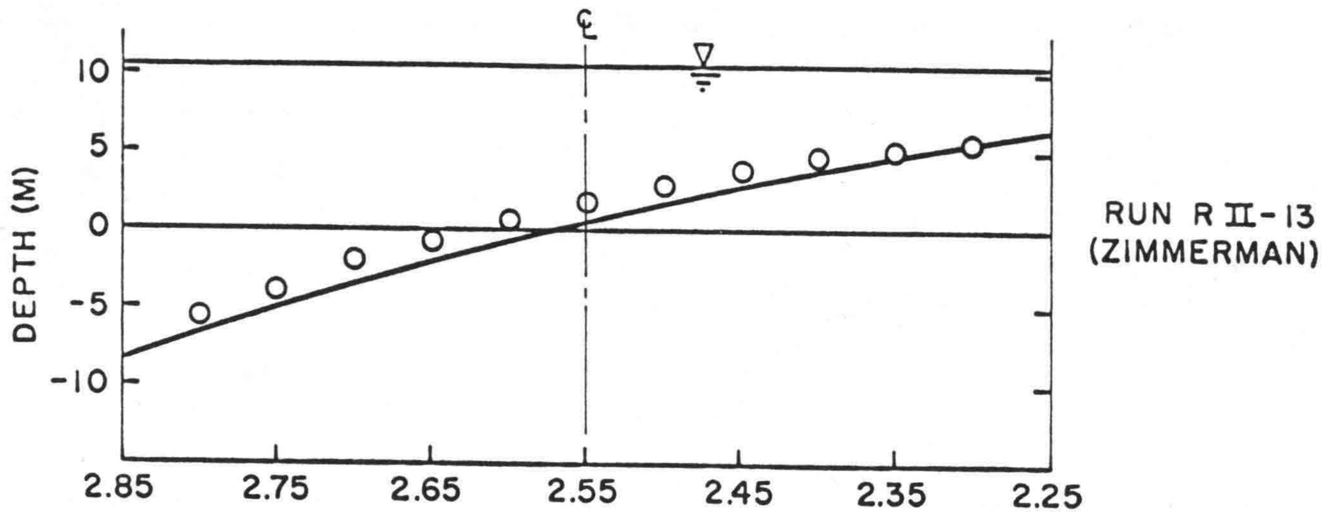

Figure 4. Transverse bed profiles measured in Zimmermann's (1974) Run RII-13, and computed from (23).

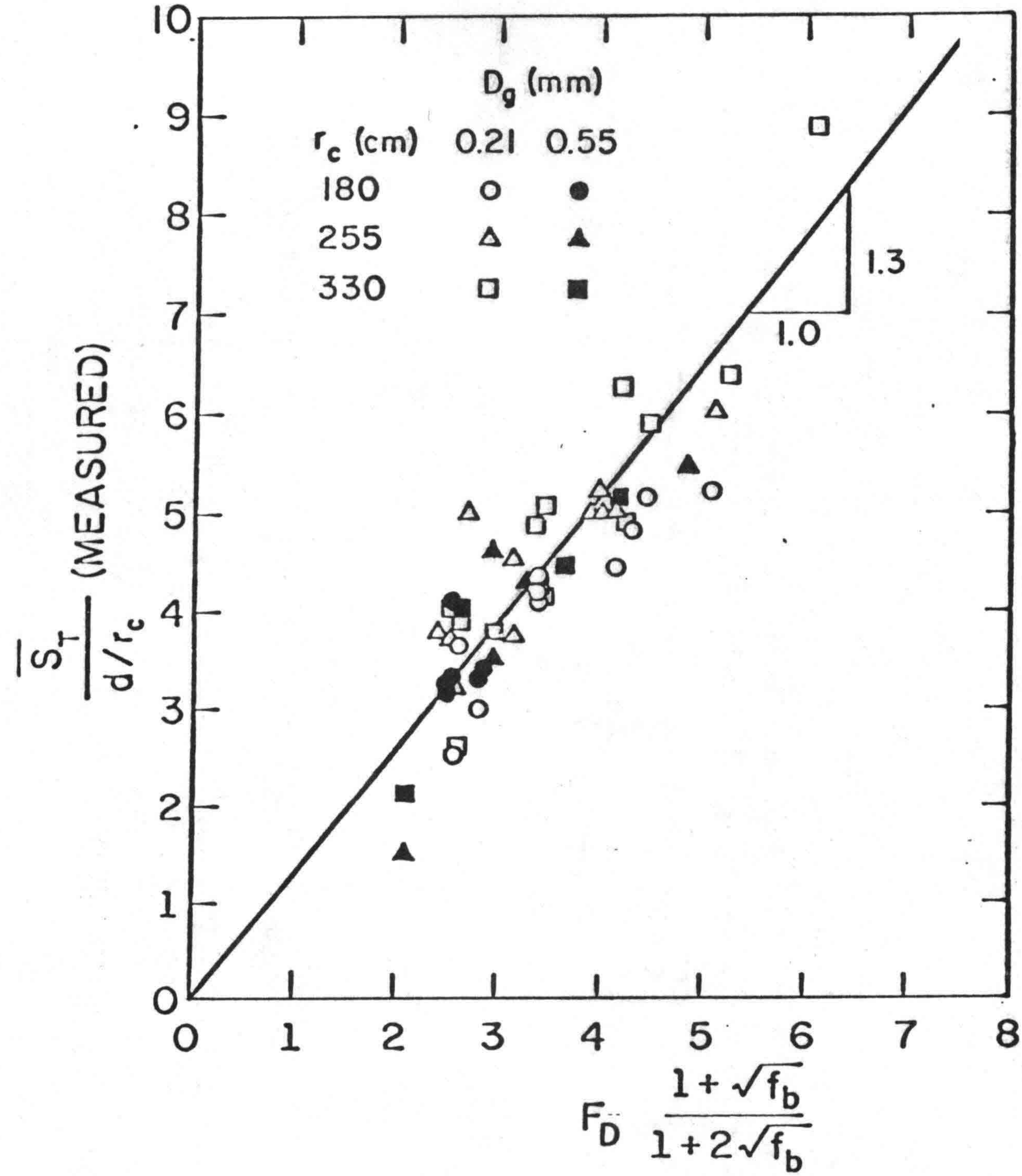

COMPARISON OF MEASURED AND COMPUTED TRANSVERSE BED SLOPES IN ALLUVIAL CHANNELS.
(DATA: ZIMMERMANN AND KENNEDY 1978)

Figure 5. Comparison of (18) and Zimmermann and Kennedy's (1978) measured transverse bed slopes.

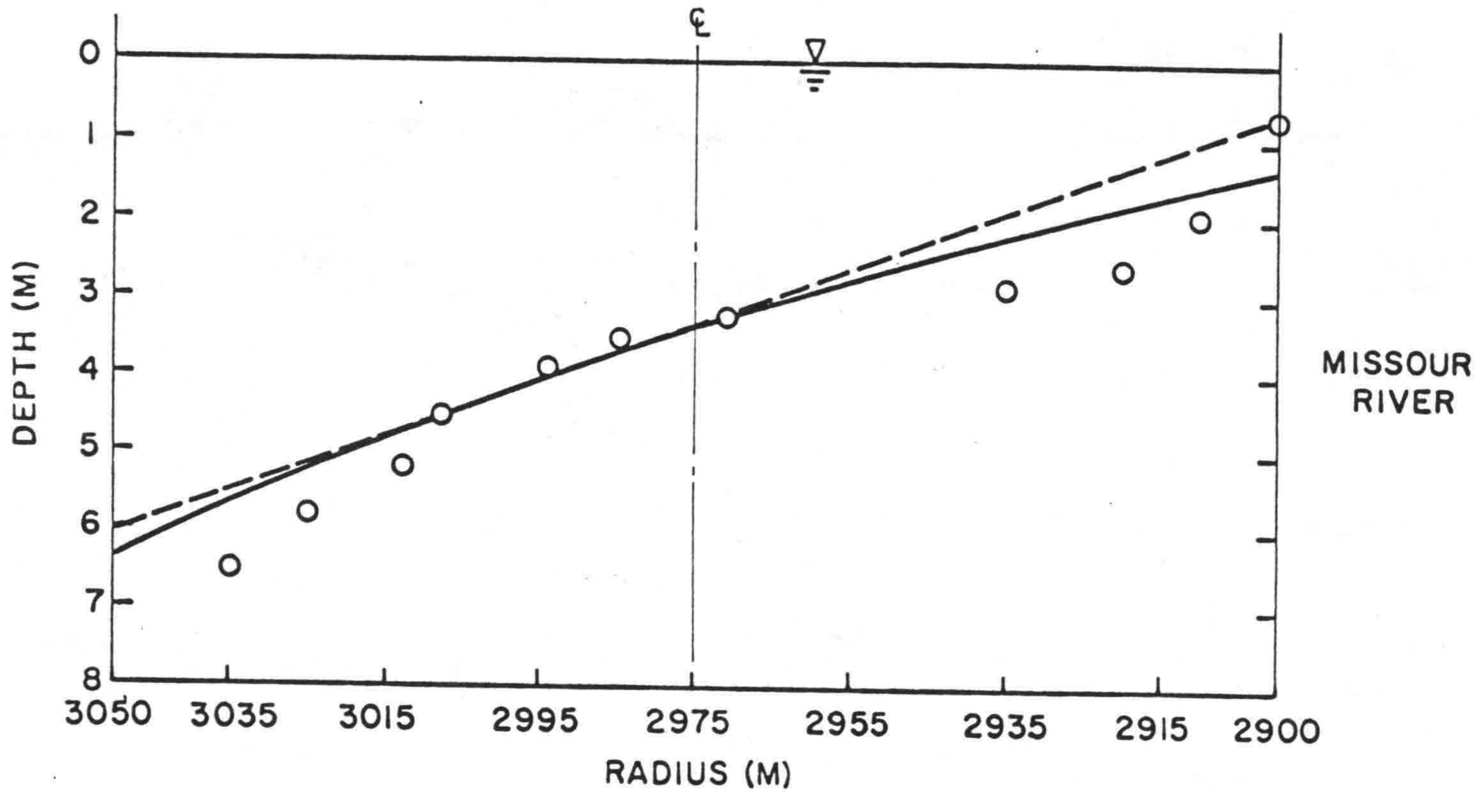

Figure 6. Transverse bed profile measured in Missouri River (Falcon 1978) and, those computed from (18) (----) and (23) (——).

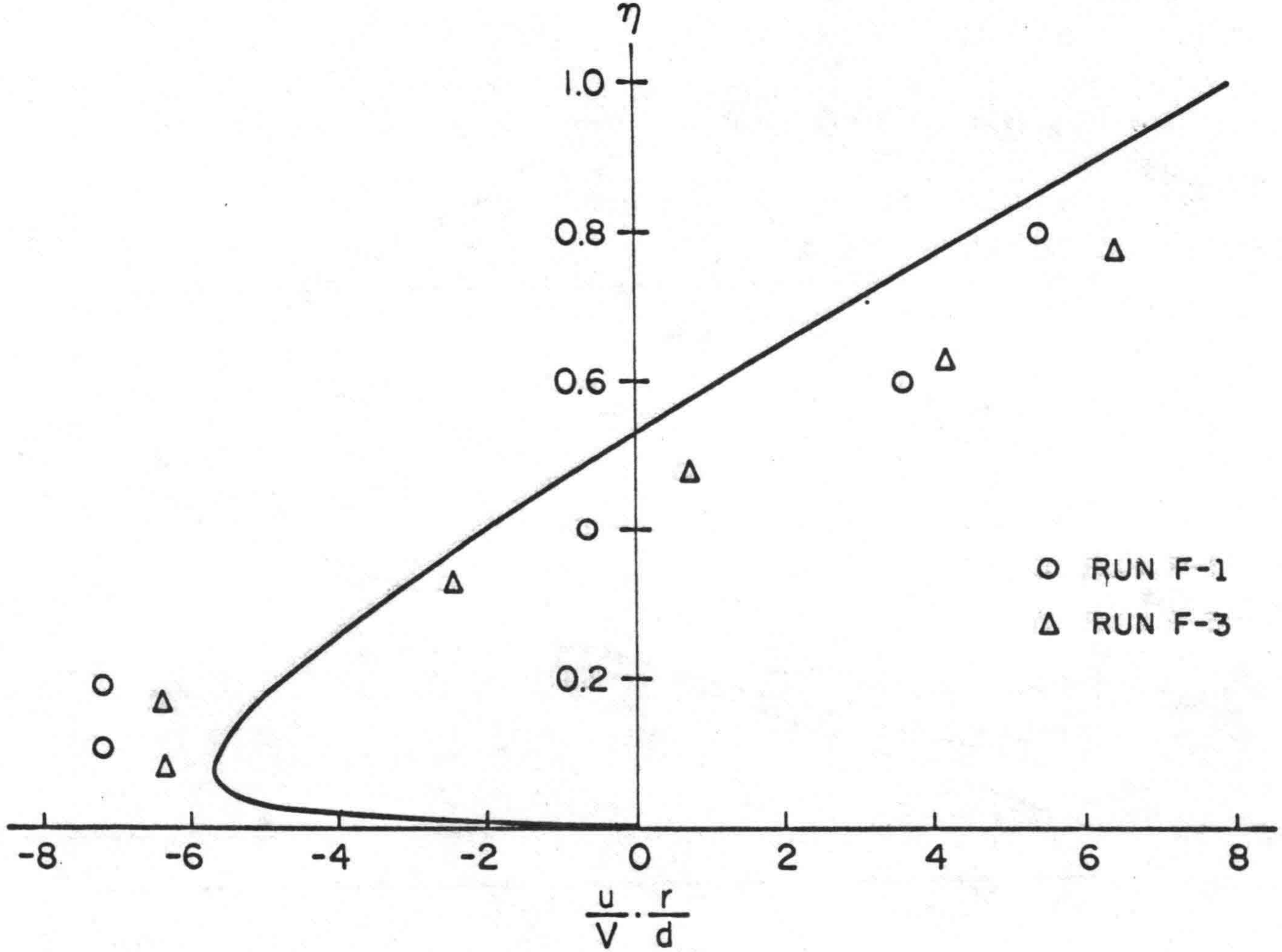

Figure 7. Secondary-flow velocity profiles measured by Kikkawa et al (1976) and computed from (34).

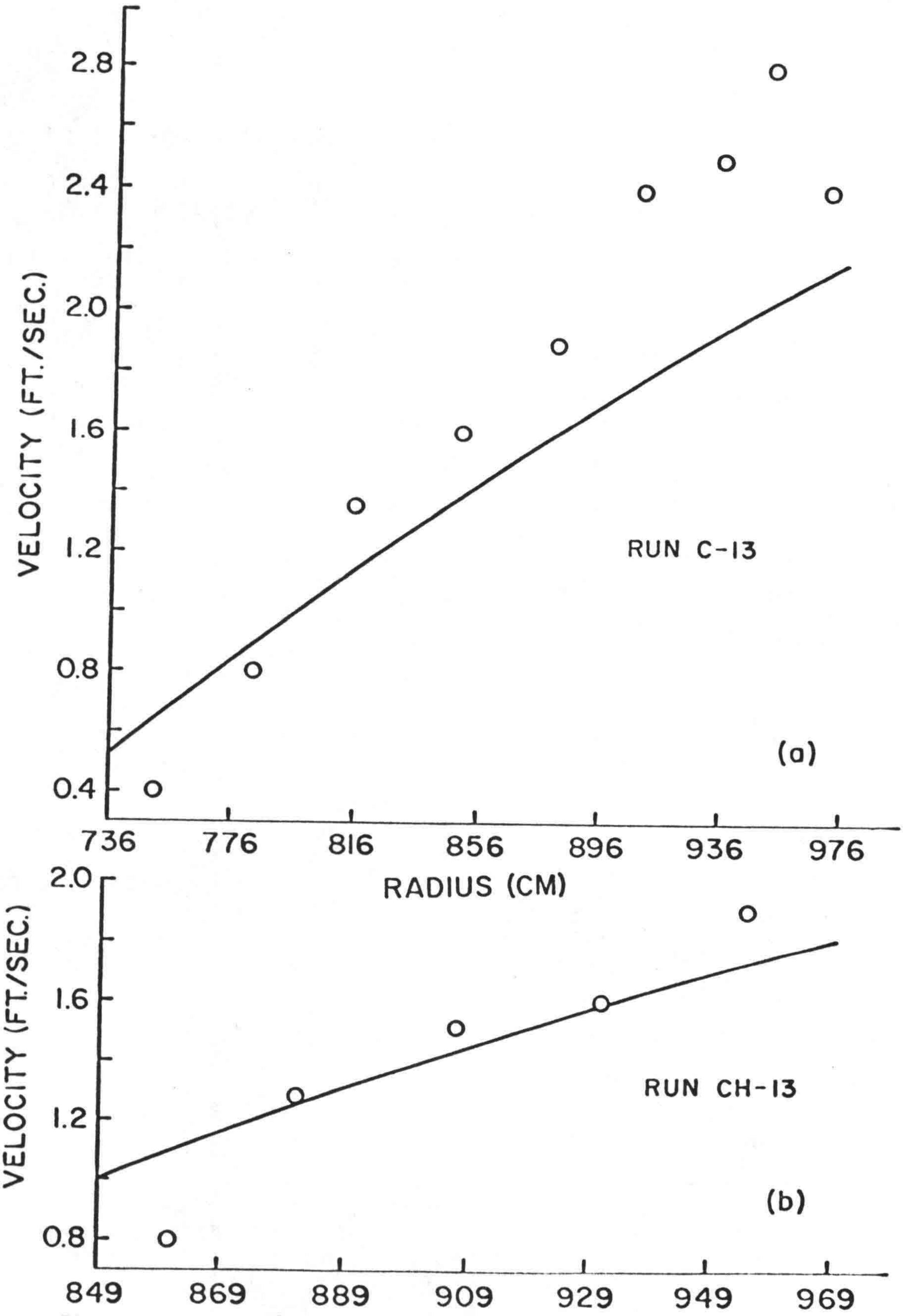

Figure 8. Comparison of Onishi's (1972) measured transverse distributions of depth-averaged velocity and those computed from (20) and (23).

APPENDIX B: LISTING OF COMPUTER PROGRAM PR-SEG6

AND INPUT-OUTPUT SAMPLES

MAIN PROGRAM PR-SEG6

```
C ****************** MAIN PROGRAM  PR-SEG6 *********************
C       THIS IS A GENERAL PROGRAM FOR A RIVER REACH COMPOSED *
C       OF SEVERAL SEGMENTED BENDS WITH POSITIVE OR NEGATIVE *
C       RADII  OF CURVATURE.  THIS PROGRAM SIMULTANEOUSLY    *
C       SOLVES THE CONTINUITY AND MOMENTUM EQUATIONS BY      *
C       ITERATING BETWEEN THEM. EACH NEW SEGMENT INPUT DATA  *
C       MUST BE READ AT THE FIRST SECTION OF EACH SEGMENT.   *
C * * * * * * * * * * * * * * * * * * * * * * * * * * * * * * *
C       SUBROUTINES:                                         *
C     FALL : DETERMINES THE F-PARAMETERS, WHICH DEPEND ON THE*
C            FOLLOWING:                                      *
C            F1 = ( ST, RC, R, H )                           *
C            F2 = ( ST, RC, R, G1, G2, G3, H )               *
C            F3 = ( ST, RC, V, R, G1, G2, G3, H, F, VBAR )   *
C            F4 = ( ST, R, H )                               *
C     GALL : DETERMINES THE G-PARAMETERS, WHICH DEPEND ON:   *
C            G = ( RHOS, BETA, ALPHA )                       *
C           G1 = ( F, BETA )                                 *
C           G2 = ( F )                                       *
C           G3 = ( VBAR, RHOS, D50, F, BETA, ALPHA, THETAC,  *
C                POR, G )                                    *
C   INTGRL : EVALUATES THE INTEGRAL:                         *
C            SUM = INT( R * SQRT( (A * R + B) / (R + D) ) )  *
C                  FROM R(J-1) TO R(J)                       *
C     CALQ : DETERMINES THE DISCHARGE OVER THE CROSS         *
C            SECTION GIVEN:                                  *
C            ( M, V, HL, R --- GETS VA, VQ, AT, QT )         *
C * * * * * * * * * * * * * * * * * * * * * * * * * * * * * * *
C       VARIABLES:                                           *
C      UBI = TRANSVERSE SHIFT VELOCITY (FT/SEC)              *
C    UBIM1 = VALUES FOR UBAR AT THE PREVIOUS SECTION.  USED  *
C            WHEN CHANGING ORIENTATION OR WHEN USED AS AN    *
C            APPROXIMATION TO THE CURRENT SECTION'S VALUES   *
C            (KOPT1=1)                                       *
C      TUB = TEMPORARY STORAGE OF UBAR WHEN CHANGING         *
C            ORIENTATION                                     *
C     UBNI = UPDATED TRANSVERSE SHIFT VELOCITY (FT/SEC)      *
C       VI = STREAMWISE VELOCITY (FT/SEC)                    *
C     VIM1 = PREVIOUS VALUE OF VI AT ( I - 1 )               *
C     TEMV = TEMPORARY STORAGE OF V WHEN CHANGING ORIENTATION*
C            OR VALUES OF ETA-MODIFIED V                     *
C      VNI = UPDATED STREAMWISE VELOCITY (FT/SEC)            *
C       UI = LOCAL SECONDARY FLOW VELOCITY--MODIFIED (FT/SEC)*
C     HLIV = LOCAL FLOW DEPTH AT SECTION I      (FT)         *
C            NONDIMENSIONALIZED BY THE VERTICAL LENGTH---H   *
C     HLIH = LOCAL FLOW DEPTH AT SECTION I      (FT)         *
C            NONDIMENSIONALIZED BY THE HORIZONTAL LENGTH---W *
C   HLIM1V = LOCAL FLOW DEPTH AT PREVIOUS SECTION (I-1) FT   *
C   HLIM1H =   "     "     "     "        "         "      " *
C     THLV = TEMPORARY STORAGE OF HLV WHEN CHANGING          *
C            ORIENTATION                                     *
C     THLH =   "           "        "  HLH  "       "        *
```

```
C         SI = LOCAL STREAMWISE POSITION AT SECTION I     (FT)   *
C       SIM1 = LOCAL STREAMWISE POSITION AT PREVIOUS SECTION     *
C              (I - 1) (FT)                                      *
C      TEMPS = TEMPORARY S STORAGE FOR REVERSING ORIENTATION     *
C         UC = CENTERLINE SECONDARY FLOW VELOCITY (FT/SEC)       *
C         U0 = INITIAL CONDITION FOR THE SECONDARY FLOW          *
C              INTEGRATION                                       *
C        STI = CUMULATIVE TRANSVERSE BED SLOPE                   *
C          R = RADIAL COORDINATE FROM THE CENTERLINE (FT)        *
C      TEMPR = TEMPORARY R STORAGE FOR REVERSING ORIENTATION     *
C         VA = LOCAL FLOW AREA (SQ FT)                           *
C         VQ = LOCAL FLOW DISCHARGE (CFS)                        *
C          V = STORAGE ARRAY FOR OUTPUT                          *
C         VB =     "      "     "    "                           *
C          U =     "      "     "    "                           *
C         HL =     "      "     "    "                           *
C       ILOC = ARRAY DENOTING THE SECTION NUMBER WHERE EACH NEW*
C              SEGMENT BEGINS                                    *
C        IST = ARRAY DENOTING THE SECTION NUMBER WHERE THE       *
C              VELOCITIES AND DEPTHS ARE KEPT UNTIL FINAL        *
C              TABULATION MAXIMUM OF 6 VALUES STORED-INLET,      *
C              4 OTHERS, OUTLET                                  *
C       ISEG = VARIABLE FOR THE ILOC ARRAY                       *
C       NIST = VARIABLE FOR THE IST ARRAY                        *
C       ISTD = LAST VALUE OF NIST IN IST-ARRAY : DIMENSION       *
C              OF IST                                            *
C      IKEEP = PARAMETER TO TELL WHETHER TO STORE FOR TABULATION
C              (IKEEP=1) OR PASS ON TO NEXT SECTION (IKEEP=0)    *
C * * * * * * * * * * * * * * * * * * * * * * * * * * * * * * * * *
C          H = MEAN FLOW DEPTH (FT)                              *
C         HV = H NONDIMENSIONALIZED BY H---THUS UNITY            *
C         HH = H         "               "   W                   *
C         RC = RADIUS OF CURVATURE (FT)                          *
C              RC IS POSITIVE IF THE ORIGIN IS LOCATED ON THE    *
C              RIGHT BANK SIDE                                   *
C              RC IS NEGATIVE IF THE ORIGIN IS LOCATED ON THE    *
C              LEFT BANK SIDE                                    *
C         R0 = PREVIOUS SECTION'S RC TO CHECK ORIENTATION        *
C     S1, S2 = STARTING, ENDING CENTERLINE COORDINATES OF EACH   *
C              BEND SEGMENT                                      *
C         SC = CUMULATIVE CENTERLINE STREAMWISE COORDINATE       *
C        SC0 = PREVIOUS SECTION'S CENTER LINE COORDINATE         *
C         DS = CENTER LINE DISTANCE BETWEEN SECTIONS             *
C          F = DARCY-WEISBACH FRICTION FACTOR                    *
C              NOTE THAT F IS USUALLY DETERMINED BY              *
C                       F = 8.0 * G * R * S / ( V**2 )           *
C              THUS, SPECIFYING 3 OF ( F, R, S, OR V )           *
C              DETERMINES THE FOURTH PARAMETER                   *
C       VBAR = MEAN STREAMWISE FLOW VELOCITY (FT/SEC)            *
C              REMAINS IN ORIGINAL UNITS BY THE NAME VACT        *
C        SCL = CENTERLINE WATER-SURFACE SLOPE                    *
C          W = RIVER WIDTH (FT)                                  *
```

```
C              REMAINS IN THE ORIGINAL UNITS BY THE NAME WACT    *
C          N = NUMBER OF STREAMWISE POSITIONS                     *
C          M = NUMBER OF RADIAL POSITIONS---TAKEN ODD FOR         *
C              CENTERLINE                                         *
C       NSEG = NUMBER OF CONSECUTIVE SEGMENTED BENDS              *
C     NSTEPS = NUMBER OF SECTIONS THAT INTERVAL ( S1, S2 ) IS     *
C              TO BE DIVIDED                                      *
C * * * * * * * * * * * * * * * * * * * * * * * * * * * * * * * * *
C      ALPHA = CONSTANT USED IN BED-LAYER RELATIONSHIP            *
C       BETA = CONSTANT USED IN SHEAR-STRESS RELATIONSHIP         *
C        POR = BED-LAYER POROSITY                                 *
C         SG = SPECIFIC GRAVITY OF SEDIMENT                       *
C        D50 = MEDIAN BED-MATERIAL PARTICLE SIZE (MM)             *
C        RMU = DYNAMIC VISCOSITY                                  *
C     THETAC = SHIELDS PARAMETER                                  *
C * * * * * * * * * * * * * * * * * * * * * * * * * * * * * * * * *
      DIMENSION VI(17), VIM1(17), VNI(17)
      DIMENSION UBI(17), UBIM1(17), UBNI(17), UI(17)
      DIMENSION SI(17), SIM1(17), HLIV(17), HLIM1V(17)
      DIMENSION HLIH(17), HLIM1H(17)
      DIMENSION R(17), VA(17), VQ(17)
      DIMENSION TUB(17), TEMV(17), THLV(17), THLH(17)
      DIMENSION TEMPR(17), TEMPS(17)
      DIMENSION ILOC(5), IST(6)
      DIMENSION V(6,17), UB(6,17), U(6,17), HL(6,17)
      DIMENSION UBPU(6,17), UTRAN(6,17), ANGLE(6,17)
      DIMENSION QQSS(6,17)
C
C       PRIMOS I/O COMMENT
C
      OPEN(5,FILE='SEGDAT')
      OPEN(6,FILE='OUTT')
      READ(5,10) VBAR,H,W,SCL,POR,SG,RMU,NSEG
      WRITE(6,5)
    5 FORMAT(//,20X,'MATHEMATICAL MODEL FOR THE PREDICTION OF '
     $ ,/,24X,'THE VELOCITY FIELD IN RIVER FLOW',//)
      WRITE(6,6)
    6 FORMAT(1X,78('*'))
   10 FORMAT(6F10.5,E15.5,I4)
      NSEGP1 = NSEG + 1
      READ(5,12) ( ILOC(I),I=1,NSEGP1 )
   12 FORMAT(7I10)
      WRITE(6,14)
   14 FORMAT(//,15X,'VALUES FOR VBAR, H, W, SCL, POR, SG, RMU,
     $  NSEG :')
      WRITE(6,15) VBAR, H, W, SCL, POR, SG, RMU, NSEG
   15 FORMAT(5X,3F10.3,E13.5,2F7.3,E11.3,I4,/)
      WRITE(6,16)
   16 FORMAT(14X,'SECTION NUMBERS WHERE NEW SEGMENTS BEGIN
     $  ARE :')
      WRITE(6,12) ( ILOC(I),I=1,NSEGP1 )
```

```
      WRITE(6,6)
C*********************************************************************
C         DEFINITIONS OF VARIOUS TERMS USED
C * * * * * * * * * * * * * * * * * * * * * * * * * * * * * * * * * *
C      MCL  = RADIAL CENTERLINE POSITION                              *
C      IM1  = DESIGNATED RADIAL POSITION TO BE PRINTED                *
C      IM2  =          "       "        "       "  "    "             *
C      IM3  =          "       "        "       "  "    "             *
C      IM4  =          "       "        "       "  "    "             *
C             NOTE: 5 POSITIONS PRINTED IN ALL:                       *
C                                        1 = NEGATIVE RIGHT BANK      *
C                                        2 = QUARTER POINT            *
C                                        3 = CENTER LINE              *
C                                        4 = 3-QUARTER POINT          *
C                                        5 = POSITIVE LEFT BANK       *
C       MP  = INCREMENT FOR RADIAL LOCATION OUTPUT                    *
C       NP  = INCREMENT FOR DOWNSTREAM SECTION OUTPUT                 *
C        I  = DOWNSTREAM SECTION INDEX                                *
C     IOUT  = D/S PRINTING OPTION PARAMETER FOR RESULTS               *
C             EVERY IOUT-TH SECTION IS PRINTED                        *
C     NOUT  = TEST PARAMETER/VARIABLE FOR IOUT-TH SECTION             *
C     EPSV  = EPSILON FOR ERROR IN V BETWEEN ITERATIONS               *
C     EPSU  =     "     "    "     " UBAR BETWEEN ITERATIONS          *
C    KOUNT  = ITERATION COUNTER OF UBAR                               *
C     KMAX  = MAXIMUM NUMBER OF ITERATIONS DESIRED FOR UBAR           *
C             CALCULATION                                             *
C     KTIM  = FREQUENCY OF OUTPUT DURING ITERATION PROCEDURE FOR*
C             UBAR                                                    *
C       KP  = PRINTING PARAMETER FOR KTIM-TH ITERATION OUTPUT         *
C    KOPT1  = OPTION PARAMETER FOR INITIAL APPROXIMATION FOR UBAR
C           = 1 FOR USING PREVIOUS SECTION'S VALUES                   *
C           = 2 FOR USING DISCRETIZED CONTINUITY EQUATION             *
C           = 3 FOR ANALYTIC SOLUTION OF THE CONTINUITY EQUATION*
C    KOPT2  = OPTION PARAMETER FOR SOLVING QUADRATIC FORMULA          *
C             FOR V                                                   *
C           = 1 FOR ORIGINAL DISCRETIZED MOMENTUM EQUATION            *
C           = 2 FOR MODIFIED DISCRETIZED MOMENTUM EQUATION WHICH*
C               INCLUDES THE CONTINUITY EQUATION                      *
C    KOPT3  = OPTION PARAMETER FOR RADIAL INTEGRATION DIRECTION *
C           = 1 FOR DIRECTION FROM THE POSITIVE LEFT  BANK ACROSS
C               TO THE NEGATIVE RIGHT BANK                            *
C           = 2 FOR DIRECTION FROM THE NEGATIVE RIGHT BANK ACROSS
C               TO THE POSITIVE LEFT BANK                             *
C * * * * * * * * * * * * * * * * * * * * * * * * * * * * * * * * * *
C        MORE DEFINITIONS                                             *
C       PI  = PI !!!   BOSTON CREME, APPLE, PUMPKIN, ETC.             *
C        G  = GRAVITATIONAL CONSTANT                                  *
C      AAA  = COEFFICIENT IN SEDIMENT RELATION                        *
C      BBB  = EXPONENT IN SEDIMENT RELATION                           *
C             SEDIMENT RELATION --- POWER LAW OF THE FORM             *
C                   QS = AAA * VBAR ** BBB                            *
```

```
C     FTMM = CONVERSION NUMBER OF MM IN ONE FOOT                       *
C     KUVM = MAX NUMBER OF ITERATIONS FOR U-V COMPATIBILITY            *
C     ISTD = SIZE OF IST-ARRAY --- PRINT 1, ISTD --- LAST VALUE*
C *********************************************************************
C        Q = WATER DISCHARGE                                           *
C       QS = SEDIMENT DISCHARGE                                        *
C    QSACT = SEDIMENT DISCHARGE---ACTUAL                               *
C    VSTAR = SHEAR VELOCITY                                            *
C   FROUDE = FROUDE NUMBER                                             *
C       RN = POWER LAW EXPONENT                                        *
C     DELR = RADIAL STEP SIZE                                          *
C   BL, BR = POSITIVE LEFT  AND  NEGATIVE RIGHT BANKS,                 *
C            RESPECTIVELY                                              *
C *********************************************************************
C GP1,GP2 = DIMENSIONLESS GRAVITATIONAL TERMS BY DEPTH H AND           *
C            WIDTH W                                                   *
C   RESTAR = BOUNDARY REYNOLDS NUMBER                                  *
C   VSTARC = CRITICAL SHEAR VELOCITY                                   *
C      FRD = DENSIMETRIC FROUDE NUMBER                                 *
C *********************************************************************
C          VARIABLES TO DEFINE EVERY RUN
      PI = 3.141592654
      G = 32.174
      FTMM = 304.8
      AAA = 0.108
      BBB = 4.0
      N = 545
      M = 17
      MCL = 9
      IM1 = 5
      IM2 = MCL
      IM3 = 13
      IM4 = M
      IOUT = 2
      MP = 1
      NP = 1
      EPSV = 0.001
      EPSU = 0.01
      KMAX = 20
      KTIM = 10
      KOPT1 = 3
      KOPT2 = 2
      KOPT3 = 2
      KUVM = 20
      ISTD = 6
      IST(1) = 1
      IST(2) = 69
      IST(3) = 205
      IST(4) = 341
      IST(5) = 477
      IST(ISTD) = N
```

```
      WRITE(6,20) N, M, MCL, IM1, IM2, IM3, IM4, IOUT, MP, NP
   20 FORMAT(5X,'DOWNSTREAM STEPS = ',I5,'  RADIAL STEPS = ',I5,
     $ '  CENTER AT M = ',I5,/,5X,'RADIAL POSITIONS STORED AT
     $ J = 1 ',4I5,/,5X,'RESULTS OUTPUT EVERY ',I5,
     $ '  SECTIONS',/,5X,D/S AND RADIAL OUTPUT FREQUENCY IS ',
     $ 2I5,'   STEPS',/)
      WRITE(6,22) EPSV, EPSU, KMAX, KTIM, KOPT1, KOPT2, KOPT3
   22 FORMAT(5X,'RELATIVE ERROR CRITERIA FOR V AND UBAR ARE ',
     $ 2F10.5,/,5X,'MAXIMUM ITERATIONS ',I5,'  PRINTED EACH ',I5,
     $ 'ITERATIONS', /,5X,'PROGRAM OPTIONS FOR UBAR, MOMENTUM
     $ FORM ,DIRECTION ARE ', 3I5,/)
      WRITE(6,24) NN, KUVM, ISTD, (IST(K),K=1,ISTD)
   24 FORMAT(5X,'INITIAL NUMBER OF SUBINTERVALS FOR SIMPSON
     $ RULE + ',I5, /,5X,'MAX NUMBER OF U-V ITERATIONS IS = ',
     $ I5,/,5X, 'DIMENSION OR NUMBER OF SECTIONS TO BE TABULATED
     $  IS = ',I5,/,5X, 'AND ARE AT SECTIONS: ',(/,5X,7I10))
      WRITE(6,25) AAA, BBB
   25 FORMAT(/,5X,'SEDIMENT POWER LAW OF THE FORM  QS = A *
     $ ( V )**B', /,5X,' WITH A, B = ',2F12.4,/)
      WRITE(6,6)
C ****************************************************************
C        COMPUTE QUANTITIES TO BE USED IN THE PROGRAM
      Q = VBAR * H * W
      QSACT = AAA * VBAR**BBB
      VSTAR = SQRT( G * H * SCL )
      FROUDE = VBAR / SQRT( G * H )
      F = 8.0 * G * H * SCL / ( VBAR**2)
      RN = 1.0 / SQRT( F )
      RN2 = ( RN + 1.0 )**2 / ( RN * ( RN + 2.0 ) )
      DELR = W / ( M - 1 )
      BL = W / 2.0
      BR = -W / 2.0
      WRITE(6,65) Q,F,RN,DELR,BL,BR,VSTAR,FROUDE,RN2,QSACT
   65 FORMAT(5X,'DISCHARGE = ',F13.4,' DARCY-WEISBACH F = ',
     $ E14.6,/,5X, 'POWER-LAW N = ',E16.8,' RADIAL STEP = ',
     $ E12.4,/,5X, 'LEFT & RIGHT BANK AT R = ',2E12.4,/,5X,
     $ 'SHEAR VELOCITY ',E14.6,'  FROUDE NO = ',E14.6,/,5X,
     $ 'N-TERM GIVEN BY ',E14.6,/,5X,'QS = ',E15.6,'
     $'ENG TONS/DAY',/)
      WRITE(6,6)
C ****************************************************************
C        DETERMINE THE NONDIMENSIONAL TERMS
      VACT = VBAR
      WACT = W
      GP1 = G * H / VBAR**2
      GP2 = G * W / VBAR**2
      HH = H / W
      BL = BL / W
      BR = BR / W
      DELR = DELR / W
      VBAR = 1.0
```

```
      Q = 1.0
      HV = 1.0
      W = 1.0
      WRITE(6,70)
   70 FORMAT(//,27X,'NONDIMENSIONAL QUANTITIES : ')
      WRITE(6,72) GP1, GP2, HH, BL, BR, DELR
   72 FORMAT(5X,'TWO GRAVITY TERMS FOR -VERT-, -HOR- ARE ',
     $ 2E14.6,/,5X, 'DEPTH = ',E14.6,' LEFT AND RIGHT BANKS AT ',
     $2E14.6,/,5X, 'RADIAL STEP ',E14.6)
      WRITE(6,6)
C ****************************************************************
C          DEFINE THE INITIAL ORIENTATION OF THE RADIAL POSITIONS
      IF( KOPT3 .EQ. 2 ) GO TO 75
C         RADIAL POSITIONS DEFINED FROM THE POSITIVE LEFT BANK
C         TO THE NEGATIVE RIGHT BANK
C ***************  KOPT3 = 1 OPTION   ****************************
      DO 74 J = 1, M
      R(J) = BL - ( J - 1 ) * DELR
   74 CONTINUE
      GO TO 79
   75 CONTINUE
C         RADIAL POSITIONS ARE DEFINED FROM THE NEGATIVE
C         RIGHT BANK TO THE POSITIVE LEFT BANK
C  **************  KOPT3 = 2 OPTION   ****************************
      DO 78 J = 1, M
      R(J) = BR + ( J - 1 ) * DELR
   78 CONTINUE
   79 CONTINUE
C ****************************************************************
      ISEG = 1
      I = 0
      NIST = 1
C  *********  NEW   SECTION    ***********************************
   80 CONTINUE
      I = I + 1
      IF( IST(NIST) .EQ. I ) GO TO 95
C     DO NOT WANT TO STORE THIS SECTION'S DEPTHS AND VELOCITIES
      IKEEP = 0
      GO TO 100
   95 CONTINUE
C     WANT TO STORE THIS SECTION'S DEPTHS AND VELOCITIES FOR LATER
C     TABULATION
      IKEEP = 1
      IK = NIST
      NIST = NIST + 1
  100 CONTINUE
      IF( I .EQ. 2 ) GO TO 220
      IJK = ILOC(ISEG) + 1
      IF( I .EQ. IJK ) GO TO 120
      IF( I .NE. 1 ) GO TO 220
  120 CONTINUE
```

```
C   ********  EITHER ONE SECTION DEEP INTO A NEW SEGMENT    *****
C                        OR AT THE INLET SECTION
      ISEG = ISEG + 1
      READ(5,125) RC, S1, S2, ALPHA, BETA, THETAC, D50, NSTEPS
  125 FORMAT(7F11.5,I3)
      WRITE(6,6)
      WRITE(6,127) I,RC,S1,S2,ALPHA,BETA,THETAC,D50,NSTEPS
  127 FORMAT(//,17X,'NEW SEGMENT-IMPORTANT PARAMETERS GIVEN AS '
     $ ,/, 5X,'FOR SECTION I = ',I5,'  RC = ',E14.6,/,5X,'SEGMENT
     $  LOCATION BETWEEN ',2E15.6,/,5X,'ALPHA, BETA = ',2F8.4,
     $ '  THETAC, D50 = ', 2F8.4,/,5X,'NUMBER OF SECTIONS BETWEEN
     $S1 & S2 IS ',I5,//)
C         COMPUTE OTHER VARIABLES
      RESTAR = VSTAR * D50 / ( RMU * FTMM )
      VSTARC = SQRT( (SG - 1.0) * G * D50 * THETAC / FTMM )
      RATIO = VSTAR / VSTARC
      FRD = VACT /  SQRT( (SG - 1.0) * G * D50 / FTMM )
      DS = ( S2 - S1 ) / NSTEPS
C         COMPUTE NONDIMENSIONAL QUANTITIES
      RC = RC / WACT
      S1 = S1 / WACT
      S2 = S2 / WACT
      DS = DS / WACT
      D50 = D50 / ( FTMM * H )
      CALL PG(F,VBAR,D50,THETAC,POR,ALPHA,BETA,SG,GP1,G1,G2,G3)
C        NOTE:  G1 = G1( N, F, BETA )
C               G2 = G2( N )
C               G3 = G3( BETA, ALPHA, POR, F, THETAC, VBAR,
C                    G, D50, DRHOS )
      WRITE(6,130)
  130 FORMAT(//,5X,'COMPUTED VARIABLES FOR THE NEW SEGMENT
     $ GIVEN BY',/)
      WRITE(6,132) RESTAR, VSTARC, RATIO, FRD, G1, G2, G3
  132 FORMAT(5X,'RESTAR, VSTARC, RATIO = ',3E15.6,/,5X,'DENSI-
     $METIC FROUDE = ',E14.6,/,5X,'G1, G2, G3 = ',3E15.7,/)
      WRITE(6,6)
      WRITE(6,135)
  135 FORMAT(5X,'NONDIMENSIONALIZED QUANTITIES GIVEN BY ',//)
      WRITE(6,137) RC, S1, S2, D50, DS
  137 FORMAT(5X,'RC, S1, S2 = ',3E14.6,' D50 ',E14.6,/,5X,
     $ 'INTERVAL BETWEEN SECTIONS DS = ',E15.7,/)
      WRITE(6,6)
C         TEST FOR INLET
C         TEST FOR REQUIRED NEW RADIAL ORIENTATION
      IF( I .EQ. 1 ) GO TO 145
      ORIEN = RC / R0
      R0 = RC
      IF( ORIEN .GE. 0.0 ) GO TO 220
  138 CONTINUE
      IF( KOPT3 .EQ. 1 ) GO TO 139
      KOPT3 = 1
```

```
      GO TO 140
  139 CONTINUE
      KOPT3 = 2
  140 CONTINUE
      DO 142 J = 1, M
      TEMPR(J) = R(J)
      TEMPS(J) = SIM1(J)
      TUB(J) = UBIM1(J)
      TEMV(J) = VIM1(J)
      THLV(J) = HLIM1V(J)
      THLH(J) = HLIM1H(J)
  142 CONTINUE
      DO 144 J = 1, M
      JJ = ( M + 1 ) - J
      R(J) = TEMPR(JJ)
      SIM1(J) = TEMPS(JJ)
      VIM1(J) = TEMV(JJ)
      UBIM1(J) = TUB(JJ)
      HLIM1V(J) = THLV(JJ)
      HLIM1H(J) = THLH(JJ)
  144 CONTINUE
      GO TO 220
  145 CONTINUE
C ************************  INLET SECTION   *******************
C              SET ARBITRARY CONDITIONS---CAN IMPOSE ANYTHING
      R0 = RC
      SC = 0.0
      U0 = 0.0
  160 CONTINUE
C         ESTIMATE INITIAL DOWNSTREAM V-VELOCITIES AT INLET
C         SECTION USING DARCY-WEISBACH APPROXIMATION---NOTE THAT
C         VALUES AT BANKS ARE NONZERO
      DO 170 J = 1, M
      HLIV(J) = HV
      HLIH(J) = HH
      SI(J) = 0.0
      UI(J) = 0.0
      VNI(J) = SQRT(8.0*GP1*HLIV(J)*SCL*RC/(F*(RC + R(J))))
  170 CONTINUE
      WRITE(6,174)
  174 FORMAT(/,5X,'INLET SECTION V = ',/)
      WRITE(6,176) (VNI(J),J=1,M,MP)
  176 FORMAT(/,(3X,5E15.7))
      WRITE(6,177)
  177 FORMAT(//)
C     CALCULATE THE FLOW DISCHARGE AND THEN ADJUST THE V-
C     VELOCITIES TO SATISFY THE MEAN FLOW CONTINUITY
      CALL PQN(M,R,VNI,HLIV,VA,VQ,AT,QT)
      ETA = 1.0
      ETA = Q / QT
      WRITE(6,178) Q, QT, ETA
```

```
  178 FORMAT(//,5X,'Q, QT, ETA = ',3E16.8,//)
      DO 180 J = 1, M
      VNI(J) = VNI(J) * ETA
  180 CONTINUE
      CALL PQN(M,R,VNI,HLIV,VA,VQ,AT,QT)
      WRITE(6,182)
  182 FORMAT(5X,'ETA-MODIFIED V-VELOCITIES WITH UNIT
     $ DISCHARGES')
      DO 190 J = 1, M, MP
      WRITE(6,185) J,VNI(J),VA(J),VQ(J)
  185 FORMAT(5X,'J =',I3,' V = ',E16.8,' VA =',E16.8,' VQ =',
     $ E16.8)
  190 CONTINUE
      WRITE(6,191) QT
  191 FORMAT(5X,'NEW VALUE OF QT WITH MODIFIED V = ',E16.8)
C         COMPUTE SEDIMENT DISCHARGE
      QS = 0.0
      DO 193 J = 1, M
      VVV = VNI(J) * VACT
      RATA = VA(J) / VA(MCL)
      QS = QS + RATA * VVV**BBB
  193 CONTINUE
      QS = QS * AAA / ( M - 1 )
      QSND = QS / QSACT
      WRITE(6,194) QS, QSND
  194 FORMAT(/,5X,'QS = ',E14.6,' ENG TONS/DAY   QS/QSACT = ',
     $ E15.6,/)
C * * * * * * * * * * * * * * * * * * * * * * * * * * * * * * *
C         FIND INITIAL VALUES FOR UBAR AT INLET SECTION
C         FROM THE ANALYTICAL SOLUTION OF THE SIMPLIFIED
C         CONTINUITY EQUATION USING A ZERO-VALUE BOUNDARY
C         CONTINUITY AT THE OUTSIDE BANK
C         USE CONTINUITY EQUATION WITH DARCY-WEISBACH FOR
C         D(V*HL)/DS AT INLET TO APPROXIMATE UBAR
      TEMP = 0.0
      UBNI(1) = 0.0
      IF(KOPT3 .EQ. 1) TJM1 = (-2.0+BL/RC) * SQRT(1.0+BL/RC)
      IF(KOPT3 .EQ. 2) TJM1 = (-2.0+BR/RC) * SQRT(1.0+BR/RC)
      C1 = 8.0 * GP2 * SCL  / ( F * HH )
      C1 = -1.0 * ETA * G2 * G3 * SQRT( C1 ) * RC**2
      DO 200 J = 2, M
      RADR =  RC + R(J)
      UAL = ( -2.0 + R(J) / RC ) * SQRT( 1.0 + R(J) / RC )
      UBNI(J) = ( TEMP + C1 * ( UAL - TJM1 ) ) / RADR
      TEMP = UBNI(J) * RADR
      TJM1 = UAL
  200 CONTINUE
      WRITE(6,210) I, (UBNI(J),J=1,M,MP)
  210 FORMAT(/,' I =',I3,' VALUES FOR UBAR = ',/,(4X,5E15.7))
      WRITE(6,212)
  212 FORMAT(//,5X,'END OF INLET SECTION',//)
```

```
      WRITE(6,6)
      GO TO 763
  220 CONTINUE
C  *******************   NEW   SECTION   **********************
C                  SAME   OR   NEW   SEGMENT
C        FOR THE NEW SECTION, DEFINE THE ANGULAR COORDINATE
C        AND THE STREAMWISE POSITIONS ACROSS THE TRANSVERSE,
C        SI. THEN, DETERMINE THE CENTERLINE SECONDARY FLOW
C        VELOCITY UCLI, AND THE TRANSVERSE BED SLOPE, STI,
C        USING THE CENTERLINE STREAMWISE DISTANCE.
C        FINALLY, CALCULATE THE LOCAL FLOW DEPTH AT EACH OF
C        THE RADIAL POSITIONS.
  221 CONTINUE
      SC0 = SC
      SC = SC + DS
      UU1 = U0 / EXP( G1 * ( SC - SC0 ) / HH )
      UU2 = G2 * VBAR / EXP( G1 * SC / HH )
      UU3 = HH * ( EXP(G1*SC/HH) - EXP(G1*SC0/HH) )/( G1 * RC )
      UC = UU1 + UU2 * UU3
      STI = UC * G3 / VBAR
      U0 = UC
      DO 225 J = 1, M
      HLIH(J) = HH + R(J) * STI
      HLIV(J) = HLIH(J) / HH
C        TEST FOR NON-POSITIVE DEPTH.  IF SO, MUST MODIFY
C        PROGRAM.
C        EXIT IF ENCOUNTERED.
      IF(HLIV(J) .LE. 0.0) WRITE(6,224) I, J, HLIV(J)
  224 FORMAT(//,5X,'NON-POSITIVE FLOW DEPTH OCCURS AT SECTION
     $ I = ',I5, /,5X,'RADIAL POSITION J = ',I5,5X,'FLOW
     $ DEPTH= ',E2.4,/,5X, 'EXIT FROM PROGRAM TO MODIFY')
      IF(HLIV(J) .LE. 0.0) GO TO 950
  225 CONTINUE
C        DETERMINE INITIAL VALUES FOR SECONDARY FLOW USING
C        FALCON'S RELATION AND THE PREVIOUS SECTION'S V-VALUES
      DO 226 J = 1, M
      FAC = HLIV(J)*VIM1(J)*RC / ( HH*VIM1(MCL)*(RC + R(J)) )
      UI(J) = UC * FAC
  226 CONTINUE
      DANGLE = ( SC - SC0 ) / RC
      DO 230 J = 1, M
      SI(J) = ( RC + R(J) ) * DANGLE + SIM1(J)
  230 CONTINUE
C        NOTE: FOR RC < 0, THE TWO NEGATIVE QUANTITIES WILL
C              STILL YIELD A POSITIVE STREAMWISE COORDINATE, S.
      IF(KOPT1 .NE. 1) GO TO 235
C * * * * * * * * * * * * * * * * * * * * * * * * * * * * * * * *
C* * * * * * * * * * * * * KOPT1 = 1 OPTION * * * * * * * * * * * * *
C        FOR A ROUGH APPROXIMATION, ASSUME THAT THE CURRENT
C        VALUES OF UBAR ARE THE SAME AS THE VALUES CALCULATED
C        AT THE PREVIOUS SECTION.
```

```
      DO 232 J = 2, M
      UBI(J) = UBIM1(J)
  232 CONTINUE
      GO TO 250
  235 CONTINUE
      IF(KOPT1 .NE. 2) GO TO 241
C * * * * * * * * * * * * * * KOPT1 = 2 OPTION * * * * * * * * * * * * *
C        AS A ANOTHER ROUGH APPROXIMATION, DISCRETIZE THE
C        CONTINUITY EQUATION TO APPROXIMATE THE VALUES FOR UBAR
C        IN THE FIRST ITERATION.
      TEMP = 0.0
      B1 = 2.0 * GP2 * SCL  / F
      B2 = -1.0 * G1 * SI(MCL) / HH
      B1 = -3.0 * G2 * G3 * SQRT( B1 ) * EXP( B2 )
      DO 240 J = 2, M
      DELR = R(J) - R(J-1)
      TJ = HLIH(J) * ( RC + R(J) )
      FACJ = R(J) / ( ( RC + R(J) ) * SQRT(TJ / RC) )
      UAL = B1 * DELR * FACJ
      UBI(J) = UAL + TEMP / TJ
      TEMP = UBI(J) * TJ
  240 CONTINUE
      GO TO 250
  241 CONTINUE
C * * * * * * * * * * * * * * * * * * * * * * * * * * * * * * * * * * *
C * * * * * * * * * * * * * * KOPT1 = 3 OPTION * * * * * * * * * * * **
C        ANALYTICAL SOLUTION OF THE CONTINUITY EQUATION TO BE
C        USED TO SOLVE FOR UBAR AS AN INITIAL APPROXIMATION WHEN
C        STARTING A NEW SECTION.
      Z1 = -3.0 * G2 * G3 * SQRT( 2.0 * GP2 * SCL  / F )
      Z1 = Z1 * EXP( -G1 * SI(MCL) / HH )
      TENT = 0.0
      DO 246 J = 2, M
      CALL EVAL(STI,HH,RC,R(J),R(J-1),RIA)
      BOTJ = HLIH(J) * ( RC + R(J) )
      UBI(J) = ( Z1 * RIA + TENT) / BOTJ
      TENT = UBI(J) * BOTJ
  246 CONTINUE
  250 CONTINUE
C * * * * * * * * * * * * * * * * * * * * * * * * * * * * * * * * * * *
  255 CONTINUE
C        FIND STREAMWISE VELOCITY V BY SOLVING MOMENTUM EQUATION
C        THAT HAS BEEN DISCRETIZED INTO A QUADRATIC FORM USING A
C        SIMPLE BACKWARD DIFFERENCING
C        READY TO BEGIN SOLUTION OF DISCRETIZED MOMENTUM EQUATION
C        ROF V,  BUT FIRST, NEED A BOUNDARY CONDITION FOR V. USE
C        DARCY-WEISBACH EQUATION AT BANK.
      IF(KOPT3 .EQ. 1) RJ = BL
      IF(KOPT3 .EQ. 2) RJ = BR
      VI(1) = SQRT(8.0*GP1*HLIV(1)*SCL*RC / (F*(RC + RJ)))
      VNI(1) = VI(1)
```

```
      TEMV(1) = VI(1)
      KOUNT = 0
      ETA = 1.0
      KUVT = 0
      KQT = 0
      KTT = 0
  312 CONTINUE
      KQ = 0
  316 CONTINUE
      KUV = 0
  320 CONTINUE
C***************  DISCRETIZED MOMENTUM EQUATION FOR V   *****
C    ------GENTER HERE FOR NEW ITERATION AT SAME SECTION ------
      ERRV = 0.0
      DO 500 J = 2, M
C        DETERMINE F-FUNCTIONS AT SPECIFIC POSITION (S,R)
      CALL PF(F,HH,RC,VBAR,G1,G2,G3,R(J),STI,UI(J),F1,F2,F3,F4)
      DELS = SI(J) - SIM1(J)
      STEPR = R(J) - R(J-1)
C        CALCULATE COEFFICIENTS FOR QUADRATIC FUNCTION IN U:
C        AA * U**2 + BB * V + CC = 0.0
      TR = HH * F4 / STEPR
      TS = HH * F4 / DELS
C * * * * * * * * * * * * * * * * * * * * * * * * * * * * * * * * *
      IF(KOPT2 .NE. 1) GO TO 340
C * * * * * * * * * * * * * * * * * KOPT2 = 1 * * * * * * * * * * * * * *
C    COEFFICIENTS FOR REGULAR DISCRETIZED STREAMWISE MOMENTUM EQ.
C    DEPEND ON: V(I-1,J),VNEW(I,J-1),U(I,J),UBAR(I,J),UBAR(I,J-1)
      AA = RN2 * ( F2 + TS ) + F / 8.0
      BB = (F1 + TR) * (UBI(J) + UI(J) / (2.0 * RN + 1) )
      CC = GP1 * HV * SCL * F4 * RC / (RC + R(J))
      CC = CC + RN2 * TS * VIM1(J)**2
      C4 = TR * ( UBI(J-1) + UI(J) / ( 2.0 * RN + 1.0 ) )
      CC = -1.0 * (CC + C4 * VNI(J-1))
      GO TO 360
C * * * * * * * * * * * * * * * * * * * * * * * * * * * * * * * * * *
  340 CONTINUE
C * * * * * * * * * * * * * * * * * KOPT2 = 2 * * * * * * * * * * * * *
C        COEFFICIENTS FOR MODIFIED DISCRETIZED STREAMWISE MOMENTUM
C        EQUATION WHICH INCLUDES THE CONTINUITY EQUATION
C        NOTE:  NO RADIAL DIFFERENTIATION IN UBAR !!!
C        DEPEND ON:  V(I-1,J), VNEW(I,J-1), U(I,J), UBAR(I,J)
      AA = F2 * ( RN2 - 1.0 ) + TS * ( RN2 - 0.5 ) + F/8.0
      BB = TR * ( UBI(J) + UI(J) / ( 2.0 * RN + 1.0 ) )
      BB = BB + UI(J) * F1 / ( 2.0 * RN + 1.0 )
      CC1 = GP1 * HV * SCL * F4 * RC / ( RC + R(J) )
      CC2 = TR*( UBI(J) + UI(J) / ( 2.0*RN + 1.0 ) )*VNI(J-1)
      CC3 = TS * ( RN2 - 0.5 ) * VIM1(J)**2
      CC = -1.0 * ( CC1 + CC2 + CC3 )
C * * * * * * * * * * * * * * * * * * * * * * * * * * * * * * * * * *
  360 CONTINUE
```

```
      CHECK = BB**2 - 4.0 * AA * CC
      IF(CHECK .LT. 0.0) GO TO 400
      VNI(J) = ( -BB + SQRT(CHECK) ) / ( 2.0 * AA )
C        SUM THE DIFFERENCES BETWEEN THE OLD AND NEW VALUES---
C        NOTE THAT THE BOUNDARY VALUE IS NOT INCLUDED IN
C        THE ERROR SINCE IT IS FIXED
      ERRV = ERRV + ABS( VNI(J) - VI(J) )
      IF( VNI(J) .GE. 0.0 ) GO TO 500
C  ************  NEGATIVE  STREAMWISE  VELOCITY  **************
      WRITE(6,390) I, J, VNI(J)
  390 FORMAT(/,5X,'NEGATIVE STREAMWISE VELOCITY',/,5X,
     $ 'SECTION I =', I5,' RADIAL STEP J = ',I5,' V = ',E15.7,/)
      GO TO 415
  400 CONTINUE
      WRITE(6,410) CHECK
  410 FORMAT(//,5X,'NEGATIVE RADICAL IN U-QUADRATIC---CHECK = ',
     $ E10.2,/)
  415 CONTINUE
C        EXIT FROM PROGRAM FOR A NEGATIVE RADICAL
      GO TO 950
  500 CONTINUE
C  ******** FIND NEW U-VALUES BASED ON V JUST CALCULATED  *****
      DO 505 J = 1, M
      FAC = HLIV(J)*VNI(J)*RC / (HV*VNI(MCL)*(RC + R(J)) )
      UI(J) = UC * FAC
  505 CONTINUE
      ERRV2 = ( ERRV / (M - 1) ) / VBAR
      KUVT = KUVT + 1
      IF( ERRV2 .LE. EPSV ) GO TO 510
C *****************************************************************
C        RESULT OF V CHANGING TOO MUCH --- TRY NEW U-VALUES IN
C        CALCULATION OF NEW V-VALUES UNTIL CHANGES ARE MINOR
      KUV = KUV + 1
C        REPLACE OLD VALUES WITH NEW VALUES AND SOLVE FOR V
C        AGAIN BUT NOW WITH THE NEWLY UPDATED V-VALUES.  NOTE
C        THAT U-BOUNDARY REMAINS UNCHANGED.
      DO 508 J = 2, M
      VI(J) = VNI(J)
      VNI(J) = 0.0
  508 CONTINUE
      IF(KUV .LT. KUVM) GO TO 320
      WRITE(6,509) I, KUV, ERRV
  509 FORMAT(/,5X,'MAXIMUM NUMBER OF ITERATIONS FOR U-V EXCEEDED'
     $ ,5X, /,5X,'SECTION I = ',I5,'   KUV = ',I5,'   ERRV = '
     $E15.8,/)
      GO TO 950
  510 CONTINUE
C  ******************  V - U  COMPATIBILITY  ****************
      CALL PQN(M,R,VNI,HLIV,VA,VQ,AT,QT)
      RATQ = ABS( Q - QT ) / Q
      KQT = KQT + 1
```

```
C*********************************************************************
      ETA0 = ETA
      ETA = Q / QT
      DO 535 J = 2, M
      TEMV(J) = VNI(J) * ETA
  535 CONTINUE
      CALL PQN(M,R,TEMV,HLIV,VA,VQ,AT,QT)
C   **********   FIND NEW UBAR FROM ACTUAL (V-H) VALUES   ******
      ERRU = 0.0
      TEMP = 0.0
      UBNI(1) = 0.0
      KOUNT = KOUNT + 1
      IF(KOPT3 .EQ. 1) T1 = ( RC + BL )**2
      IF(KOPT3 .EQ. 2) T1 = ( RC + BR )**2
C         USE CONTINUITY EQUATION WITH ACTUALLY CALCULATED
C         VALUES FOR D(V*HL)/DS AT THIS SAME SECTION
C         TO GET THE SECOND APPROXIMATION OF UBAR,
C         AGAIN WITH UBAR EQUALS ZERO AT THE BANK.
      DO 600 J = 2, M
      CAPX = -0.5 * ( TEMV(J) * HLIH(J) - VIM1(J) * HLIM1H(J) )
      CAPX = CAPX / ( SI(J) - SIM1(J) )
      T2 = ( RC + R(J) )**2
      BOTJ = HLIH(J) * ( RC + R(J) )
      UBNI(J) = ( CAPX * ( T2 - T1 ) + TEMP ) / BOTJ
      T1 = T2
      TEMP = UBNI(J) * BOTJ
      ERRU = ERRU + ABS( UBNI(J) - UBI(J) )
  600 CONTINUE
C * * * * * * * * * * * * * * * * * * * * * * * * * * * * * * * * * * *
C         CONVERGENCE CRITERIA FOR ERRORS:  ITERATE UNTIL THE AVERAGE
C         DIFFERENCE BETWEEN 2 CONSECUTIVE ITERATIONS FOR ALL THE
C         RADIAL STEPS ACROSS THE TRANSVERSE, DIVIDED BY THE MEAN
C         DOWNSTREAM FLOW VELOCITY, IS SMALLER THAN SOME PRESCRIBED
C         SMALL VALUE.
C * * * * * * * * * * * * * * * * * * * * * * * * * * * * * * * * * * *
      ERRU2 = ERRU / ( ( M - 1 ) * ABS( UBNI(MCL) ) )
      KTT = KTT + 1
      IF(ERRU2 .LE. EPSU) GO TO 750
      IF(KOUNT .GE. KMAX) GO TO 770
C*********************************************************************
C         REACHED AS A RESULT OF LARGE ERROR WITHOUT EXCEEDING
C         THE MAXIMUN ALLOWABLE NUMBER OF ITERATIONS.
C         NO CONVERGENCE YET, SO
C         ITERATE THE WHOLE PROCESS AGAIN FOR A NEW V AND UBAR.
      KP = KOUNT / KTIM
      KP = KP * KTIM
      IF(KP .NE. KOUNT) GO TO 748
      WRITE(6,700) I, KOUNT, ETA, ETA0, ERRV2, ERRU2
  700 FORMAT(/,5X,'FOR SECTION I = ',I5,' KOUNT = ',I5,/,5X,
     $ ' CURRENT AND PREVIOUS ETA ARE ',2E15.6,/,5X,
     $ 'RELATIVE ERRORS IN V AND UBAR ARE ',2E15.6,/)
```

```
C      WRITE(6,705)
  705 FORMAT(5X,'PREVIOUS VALUES FOR V GIVEN BY ',/)
C      WRITE(6,710)  (VI(J),J=1,M)
  710 FORMAT(5X,6E12.4)
      WRITE(6,712)
  712 FORMAT(5X,'UN-ETA-MODIFIED MOMENTUM VALUES FOR
     $  V GIVEN BY ',/)
      WRITE(6,710)  (VNI(J),J=1,M)
C      WRITE(6,714)
  714 FORMAT(5X,'OLD VALUES FOR UBAR GIVEN BY ',/)
C      WRITE(6,710) (UBI(J),J=1,M)
      WRITE(6,716)
  716 FORMAT(5X,'NEW VALUES FOR UBAR GIVEN BY ',/)
      WRITE(6,710) (UBNI(J),J=1,M)
C      WRITE(6,718)
  718 FORMAT(5X,'LATEST VALUES FOR U ARE ',/)
C      WRITE(6,710) (UI(J),J=1,M)
  748 CONTINUE
C         RESET NEW VALUES  BEFORE REPEATING THE ITERATION
      DO 749 J = 2, M
      VI(J) = VNI(J)
      UBI(J) = UBNI(J)
      VNI(J) = 0.0
      UBNI(J) = 0.0
  749 CONTINUE
      GO TO 312
  750 CONTINUE
C*****************************************************************
C         REACHED AS A RESULT OF A SATISFACTORY SMALL ERROR
C         IN UBAR OR V THIS IS WANT WE WANT.
C         DETERMINE FINAL ETA-MODIFIED V-VALUE
      DO 752 J = 2, M
      VNI(J) = TEMV(J)
  752 CONTINUE
C ****************  DETERMINE SEDIMENT DISCHARGE  ********
      QS = 0.0
      DO 753 J = 1, M
      VVV = VNI(J) * VACT
      RATA = VA(J) / VA(MCL)
      QS = QS + RATA * VVV**BBB
  753 CONTINUE
      QS = AAA * QS / ( M - 1 )
      QSND = QS / QSACT
C **************************************************
      III = I - 1
      NOUT = III / IOUT
      NOUT = NOUT * IOUT
      IF(NOUT .NE. III) GO TO 763
      WRITE(6,755) I, STI, UC, ERRV2, ERRU2, KOUNT, RATQ
  755 FORMAT(/,5X,'FOR SECTION I = ',I4,' ST = ',E14.6,
     $ 'UCL = ',E14.6, /,5X,'SATISFACTORY ITERATION',
```

```
     $  5X,'ERRV2 = ',E14.6,' ERRU2 = ',E14.6,/,5X,
     $  'NUMBER OF ITERATIONS KOUNT = ',I4,/,5X,
     $ 'RELATIVE DIFFERENCE OF QT TO Q IS ',E15.7,/)
      WRITE(6,757) SC, RC, QT, ETA, QS, QSND
  757 FORMAT(5X,'CENTERLINE POSITION S = ',E14.6,' WITH RC = ',E1
     $4.6, /,5X,'NEWEST Q = ',E16.8,'  WITH ETA = ',E15.7,/,5X,
     $ 'SEDIMENT DISCHARGE = ',E14.5,'  QS/QSACT = ',E14.5,/)
      WRITE(6,760) KTT, KQT, KUVT
  760 FORMAT(5X,' NUMBER OF ITERATIONS FOR UB, Q, UV ARE ',3I6)
      WRITE(6,716)
      WRITE(6,710) (UBNI(J),J=1,M,MP)
      WRITE(6,761)
  761 FORMAT(5X,'ETA-MODIFIED MOMENTUM VALUES FOR V GIVEN BY')
      WRITE(6,710) (VNI(J),J=1,M,MP)
C     WRITE(6,718)
C     WRITE(6,710) (VI(J),J=1,M,MP)
      WRITE(6,762)
  762 FORMAT(/)
  763 CONTINUE
C        STORE VALUES FOR V, UBAR, AND U FOR LATER TABULATION
      IF( IKEEP .NE. 1 ) GO TO 767
      IF( KOPT3 .EQ. 1) GO TO 765
      DO 764 J = 1, M
      V(IK,J) = VNI(J)
      UB(IK,J) = UBNI(J)
      U(IK,J) = UI(J)
      HL(IK,J) = HLIV(J)
      QQSS(IK,J)=AAA*(VNI(J)*VACT)**BBB
      UBPU(IK,J)=UI(J)+UBNI(J)
      USQRT=UBPU(IK,J)**2+VNI(J)**2
      UTRAN(IK,J)=SQRT(USQRT)
      UCRII=VNI(J)
      IF(UCRII.EQ.0.) GO TO 1
      ANGUU=UBPU(IK,J)/VNI(J)
      ANGLE(IK,J)=57.29578*ATAN(ANGUU)
      GO TO 764
    1 ANGLE(IK,J)=90.0
  764 CONTINUE
      GO TO 767
  765 CONTINUE
      DO 766 J = 1, M
      JJ = ( M + 1 ) - J
      V(IK,JJ) = VNI(J)
      UB(IK,JJ) = UBNI(J)
      U(IK,JJ) = UI(J)
      HL(IK,JJ) = HLIV(J)
      QQSS(IK,JJ)=AAA*(VNI(J)*VACT)**BBB
      UBPU(IK,JJ)=UI(J)+UBNI(J)
      USQRT=UBPU(IK,JJ)**2+VNI(J)**2
      UTRAN(IK,JJ)=SQRT(USQRT)
      UCRII=VNI(J)
```

```
      IF(UCRII.EQ.0.0) GO TO 3
      ANGUU=UBPU(IK,JJ)/VNI(J)
      ANGLE(IK,JJ)=57.29578*ATAN(ANGUU)
      GO TO 766
    3 ANGLE(IK,JJ)=90.0
  766 CONTINUE
  767 CONTINUE
      DO 768 J = 1, M
      HLIM1V(J) = HLIV(J)
      HLIM1H(J) = HLIH(J)
      SIM1(J) = SI(J)
      VIM1(J) = VNI(J)
      UBIM1(J) = UBNI(J)
  768 CONTINUE
      DO 769 J = 1, M
      VI(J) = 0.0
      VNI(J) = 0.0
      TEMV(J) = 0.0
      UBNI(J) = 0.0
      UI(J) = 0.0
      UBI(J) = 0.0
      HLIV(J) = 0.0
      HLIH(J) = 0.0
      SI(J) = 0.0
  769 CONTINUE
      ETA = 1.0
      IF( I .GE. N ) GO TO 800
C *****************  TRIAL  STOPS   ****************************
C     IF( I .GE. 3 ) GO TO 950
C  ***********************************************************
      GO TO 80
  770 CONTINUE
C************************************************************
C         REACHED AS A RESULT OF EXCEEDING THE ALLOWABLE NUMBER
C         OF ITERATIONS
      WRITE(6,780) I, KOUNT, STI, SC, ERRV2, ERRU2
  780 FORMAT(/,5X,'FOR SECTION I = ',I5,' KOUNT = ',I5,' STI = '
     $,E15.6, /,5X,'CENTERLINE POSITION = ',
     $ E14.6,/,5X,'RELATIVE ERRORS IN V AND UBAR ARE ',2E15.6)
      WRITE(6,716)
      WRITE(6,710) (UBNI(J),J=1,M)
      WRITE(6,712)
      WRITE(6,710) (VNI(J),J=1,M)
      WRITE(6,718)
      WRITE(6,710) (UI(J),J=1,M)
      GO TO 950
  800 CONTINUE
C ***********************************************************
C   ----------- PRINT FINAL RESULTS OBTAINED -----------------
C        RESULTS ARE TABULATED FROM THE NEGATIVE RIGHT BANK TO
C                     THE POSITIVE RIGHT BANK---KOPT3 = 2
```

```
      IF( KOPT3 .EQ. 2 ) GO TO 808
      DO 802 J = 1, M
      TEMPR(J) = R(J)
  802 CONTINUE
      DO 804 J = 1, M
      JJ = ( M + 1 ) - J
      R(J) = TEMPR(JJ)
  804 CONTINUE
  808 CONTINUE
C**********************************************************************
C          RESULTS FOR TRANSVERSE SHIFT VELOCITY UBAR
      WRITE(6,810)
  810 FORMAT(//,32X,'VALUES FOR UBAR',//)
      WRITE(6,820)
  820 FORMAT(3X,'R',43X,'  I  ',/)
      WRITE(6,830) (IST(I),I=1,ISTD)
  830 FORMAT(4X,6I12)
      DO 850 J = 1, M
      WRITE(6,840) R(J), (UB(I,J),I=1,ISTD)
  840 FORMAT(F7.3,6E12.4)
  850 CONTINUE
      WRITE(6,852)
  852 FORMAT(//,3X,'  I  ',32X,'R')
      WRITE(6,854) R(1),R(IM1),R(IM2),R(IM3),R(IM4)
  854 FORMAT(6X,5F12.4)
      DO 858 I = 1, ISTD
      WRITE(6,8) I,UB(I,1),UB(I,IM1),UB(I,IM2),UB(I,IM3)
     $  ,UB(I,IM4)
    8 FORMAT(I5,5X,5E12.4)
  858 CONTINUE
C          RESULTS FOR SECONDARY FLOW VELOCITY U
      WRITE(6,860)
  860 FORMAT(//,32X,'VALUES FOR U',//)
      WRITE(6,820)
      WRITE(6,830) (IST(I),I=1,ISTD)
      DO 880 J = 1, M
      WRITE(6,840) R(J), (U(I,J),I=1,ISTD)
  880 CONTINUE
C          RESULTS FOR STREAMWISE VELOCITY V
      WRITE(6,890)
  890 FORMAT(//,32X,'VALUES FOR V',//)
      WRITE(6,820)
      WRITE(6,830) (IST(I),I=1,ISTD)
      DO 900 J = 1, M
      WRITE(6,840) R(J), (V(I,J),I=1,ISTD)
  900 CONTINUE
      WRITE(6,852)
      WRITE(6,854) R(1), R(IM1), R(IM2), R(IM3), R(IM4)
      DO 908 I = 1, ISTD
      WRITE(6,8) I,V(I,1),V(I,IM1),V(I,IM2),V(I,IM3),V(I,IM4)
  908 CONTINUE
```

```
C         RESULTS FOR LOCAL FLOW DEPTH
      WRITE(6,910)
  910 FORMAT(//,32X,'VALUES FOR HL',//)
      WRITE(6,820)
      WRITE(6,830) (IST(I),I=1,ISTD)
      DO 920 J = 1, M
      WRITE(6,840) R(J), (HL(I,J),I=1,ISTD)
  920 CONTINUE
      WRITE(6,921)
  921 FORMAT(//,25X,'VALUES FOR UBAR + U',//)
      WRITE(6,820)
      WRITE(6,830) (IST(I),I=1,ISTD)
      DO 930 J=1, M
      WRITE(6,840) R(J), (UBPU(I,J), I=1,ISTD)
  930 CONTINUE
      WRITE(6,931)
  931 FORMAT(//,25X,'VALUES FOR SQRT((UBAR+U)**2+V**2)',//)
      WRITE(6,820)
      WRITE(6,830) (IST(I),I=1,ISTD)
      DO 940 J=1, M
      WRITE(6,840) R(J), (UTRAN(I,J), I=1,ISTD)
  940 CONTINUE
      WRITE(6,941)
  941 FORMAT(//,25X,'VALUES FOR VELOCITY VECTOR ANGLES',//)
      WRITE(6,820)
      WRITE(6,830) (IST(I),I=1,ISTD)
      DO 945 J=1, M
      WRITE(6,840) R(J), (ANGLE(I,J), I=1,ISTD)
  945 CONTINUE
      WRITE(6,946)
  946 FORMAT(//,20X,'VALUES FOR UNIT SEDIMENT DISCHARGES',//)
      WRITE(6,820)
      WRITE(6,830) (IST(I),I=1,ISTD)
      DO 947 J=1, M
      WRITE(6,840) R(J), (QQSS(I,J), I=1,ISTD)
  947 CONTINUE
  950 CONTINUE
C
C       PRIMOS I/O COMMENT
C
      CLOSE(5)
      CLOSE(6)
      STOP
      END
C * * * * * * * * * * * * * * * * * * * * * * * * * * * * * * * * *
      SUBROUTINE PQN(M,R,V,HL,VA,VQ,AT,QT)
C         THIS SUBROUTINE DETERMINES THE FLOW DISCHARGE FOR A      *
C         GIVEN RECTANGULAR CROSS SECTION OF CONSTANT              *
C         BOTTOM SLOPE WITH KNOWN VELOCITIES AND DEPTHS            *
C * * * * * * * * * * * * * * * * * * * * * * * * * * * * * * * * *
C         VARIABLES:
                                                                   *
```

```
C     M = NUMBER OF INCREMENTS OR VERTICALS IN THE CROSS SECTION
C     R = LOCAL RADIAL POSITION ARRAY (FT)                      *
C     V = LOCAL FLOW VELOCITY ARRAY (FT/SEC)                    *
C    HL = LOCAL FLOW DEPTH ARRAY (FT)                           *
C    VA = UNIT FLOW AREA ARRAY (SQ FT)                          *
C    VQ = UNIT FLOW DISCHARGE (CFS)                             *
C    AT = TOTAL FLOW AREA (CUBIC FT)                            *
C    QT = TOTAL FLOW DISCHARGE (CFS)                            *
C * * * * * * * * * * * * * * * * * * * * * * * * * * * * * * * *
      DIMENSION R(17), V(17), HL(17), VA(17), VQ(17)
      AT = 0.0
      QT = 0.0
      DO 10 I = 1,M
      VA(I) = 0.0
      VQ(I) = 0.0
   10 CONTINUE
      DO 200 J = 1,M
      IF(J .EQ. M) GO TO 100
      IF(HL(J+1) .LT. 0.0) GO TO 120
      IF(J .GT. 1) GO TO 50
      W2 = 0.5 * ABS( R(J+1) - R(J) )
      H2 = ( HL(J) + HL(J+1) ) / 2.0
      VA(J) = W2 * ( HL(J) + H2 ) / 2.0
      VQ(J) = VA(J) * V(J)
      GO TO 110
   50 CONTINUE
      W1 = W2
      H1 = H2
      W2 = 0.5 * ABS( R(J+1) - R(J) )
      H2 = ( HL(J) + HL(J+1) ) / 2.0
      A1 = W1 * ( H1 + HL(J) ) / 2.0
      A2 = W2 * ( HL(J) + H2 ) / 2.0
      VA(J) = A1 + A2
      VQ(J) = VA(J) * V(J)
      GO TO 110
  100 CONTINUE
      W1 = W2
      H1 = H2
      VA(J) = W1 * ( H1 + HL(J) ) / 2.0
      VQ(J) = VA(J) * V(J)
  110 CONTINUE
      AT = AT + VA(J)
      QT = QT + VQ(J)
      GO TO 200
  120 CONTINUE
      W1 = W2
      H1 = H2
      W2 = 0.5 * ABS( R(J+1) - R(J) )
      H2 = ( HL(J) + HL(J+1) ) / 2.0
      FAC = H1 / ( H1 - HL(J+1) )
      W0 = FAC * ABS( R(J+1) - ( R(J) + R(J-1) ) / 2.0 )
```

```
      IF( H2 .LT. 0.0 ) GO TO 150
      DELW = ABS( WO - ( W1 + W2 ) )
      VA(J+1) = 0.5 * H2 * DELW
      VQ(J+1) = VA(J+1) * V(J)
      A1 = W1 * ( H1 + HL(J) ) / 2.0
      A2 = W2 * ( HL(J) + H2 ) / 2.0
      VA(J) = A1 + A2
      VQ(J) = VA(J) * V(J)
      AT = AT + VA(J) + VA(J+1)
      QT = QT + VQ(J) + VQ(J+1)
      GO TO 220
  150 CONTINUE
      VA(J) = 0.5 * WO * H1
      VQ(J) = VA(J) * V(J)
      AT = AT + VA(J)
      QT = QT + VQ(J)
      GO TO 220
  200 CONTINUE
  220 CONTINUE
      RETURN
      END
C * * * * * * * * * * * * * * * * * * * * * * * * * * * * * * * * *
      SUBROUTINE PG(F,VBAR,D50,THETAC,POR,A,B,RHOS,G,G1,G2,G3)
C          THIS SUBROUTINE DETERMINES DIMENSIONLESS PARAMETERS   *
C          G1, G2, AND G3 FOR THE DEFINED AND INPUT QUANTITIES   *
C * * * * * * * * * * * * * * * * * * * * * * * * * * * * * * * * *
C          DEFINED:                                              *
C  RHOS = SPECIFIC GRAVITY OF THE SEDIMENT PARTICLES             *
C     B = PARAMETER IN THE VELOCITY-SHEAR RATIO RELATION         *
C     A = PARAMETER IN THE SHEAR-BED LAYER RATIO RELATION        *
C          INPUT VARIABLES:                                      *
C     F = DARCY-WEISBACH FRICTION FACTOR                         *
C  VBAR = MEAN STREAMWISE FLOW VELOCITY (FT/SEC)                 *
C   D50 = MEDIAN BED MATERIAL PARTICLE SIZE (MM)                 *
C THETAC= SHIELDS CRITICAL SHEAR PARAMETER                       *
C   POR = BED LAYER POROSITY                                     *
C     G = GRAVITATIONAL CONSTANT                                 *
C * * * * * * * * * * * * * * * * * * * * * * * * * * * * * * * * *
      CALL PG1(F,B,G1)
      CALL PG2(F,G2)
      CALL PG3(VBAR,RHOS,D50,F,B,A,THETAC,POR,G,G3)
      RETURN
      END
C * * * * * * * * * * * * * * * * * * * * * * * * * * * * * * * * *
      SUBROUTINE PG1(F,B,G1)
      RN = 1.0 / SQRT(F)
      T = (3.0*RN + 1.0)*(2.0*RN + 1.0)/(2.0*RN**2 + RN + 1.0)
      G1 = T * B * F / 8.0
      RETURN
      END
C * * * * * * * * * * * * * * * * * * * * * * * * * * * * * * * * *
```

```
      SUBROUTINE PG2(F,G2)
      RN = 1.0 / SQRT(F)
      T1 = (3.0 * RN + 1.0) * (2.0 * RN + 1.0) * (RN + 1.0)
      T2 = (2.0 * RN**2 + RN + 1.0) * (RN + 2.0) * RN
      G2 = T1 / T2
      RETURN
      END
C * * * * * * * * * * * * * * * * * * * * * * * * * * * * * * * * * *
      SUBROUTINE PG3(VBAR,RHOS,D50,F,B,A,THETAC,POR,G,G3)
      T1 = F * THETAC
      T2 = 8.0 * G * D50 * (RHOS - 1.0)
      T3 = SQRT(T1 / T2)
      T4 = B * VBAR / (A * (1.0 - POR))
      G3 = T4 * T3
      RETURN
      END
C * * * * * * * * * * * * * * * * * * * * * * * * * * * * * * * * * *
      SUBROUTINE PF(F,H,RC,VBAR,G1,G2,G3,R,ST,U,F1,F2,F3,F4)
C        THIS SUBROUTINE DETERMINES ALL FOUR OF THE                    *
C        DIMENSIONLESS FUNCTIONS F1, F2, F3, AND F4 FOR THE            *
C        INPUT QUANTITIES GIVEN                                        *
C * * * * * * * * * * * * * * * * * * * * * * * * * * * * * * * * * *
C        INPUT VARIABLES:                                              *
C              F = DARCY-WEISBACH FRICTION FACTOR                      *
C              H = MEAN DEPTH OF FLOW OVER CROSS SECTICN (FT)          *
C             RC = RADIUS OF CURVATURE OF CHANNEL CENTERLINE (FT)
C           VBAR = MEAN STREAMWISE FLOW VELOCITY (FT/SEC)              *
C       G1,G2,G3 = DIMENSIONLESS PARAMETERS                            *
C              R = RADIAL POSITION FROM CHANNEL CENTERLINE (FT) *
C             ST = TRANSVERSE BED SLOPE                                *
C              U = MAXIMUM SECONDARY FLOW VELOCITY (FT/SEC)            *
C    F1,F2,F3,F4 = DIMENSIONLESS FUNCTIONS TO BE EVALUATED             *
C * * * * * * * * * * * * * * * * * * * * * * * * * * * * * * * * * *
      CALL PF1(ST,RC,R,H,F1)
      CALL PF2(ST,RC,R,G1,G2,G3,H,F2)
      CALL PF3(ST,RC,U,R,G1,G2,G3,H,F,VBAR,F3)
      CALL PF4(ST,R,H,F4)
      RETURN
      END
C * * * * * * * * * * * * * * * * * * * * * * * * * * * * * * * * * *
      SUBROUTINE PF1(ST,RC,R,H,F1)
      F1 = ST + ( H + R * ST ) / ( RC + R )
      RETURN
      END
C * * * * * * * * * * * * * * * * * * * * * * * * * * * * * * * * * *
      SUBROUTINE PF2(ST,RC,R,G1,G2,G3,H,F2)
      T1 = G2 * G3 * R / RC
      T2 = R * G1 * ST / H
      F2 = RC * ( T1 - T2 ) / ( RC + R )
      RETURN
      END
```

```
C * * * * * * * * * * * * * * * * * * * * * * * * * * * * * * * * *
      SUBROUTINE PF3(ST,RC,U,R,G1,G2,G3,H,F,VBAR,F3)
      T1 = F * U / (8.0 * VBAR)
      T2 = ( G2 * H ) / ( RC + R )
      T22 = G1 * RC * ST / ( G3 * ( RC + R ) )
      RN = 1.0 / SQRT(F)
      T3 = ( R * ST + H ) / H
      T33 = G3 * R * U / ( H * VBAR )
      T4 = ( T2 - T22 ) * ( T3 - T33 ) / ( 2.0 * RN + 1.0 )
      F3 = T4 - T1
      RETURN
      END
C * * * * * * * * * * * * * * * * * * * * * * * * * * * * * * * * *
      SUBROUTINE PF4(ST,R,H,F4)
      T = R * ST / H
      F4 = 1.0 + T
      RETURN
      END
C * * * * * * * * * * * * * * * * * * * * * * * * * * * * * * * * *
      SUBROUTINE EVAL(A,B,C,RJ,RJM1,SUM)
C        THIS SUBROUTINE EVALUATES THE ANALYTICAL SOLUTION OF   *
THE C          CONTINUITY EQUATION AS THE PROGRAM BEGINS A NEW   *
C        SECTION.   THE GENERAL FORM OF THE INTEGRAL IS          *
C        GIVEN BY:                                               *
C              I = INTEGRAL( X *SQRT( C*(A*X + B)/(X + C) ) )    *
C     WHERE:                                                     *
C        X = RADIAL COORDINATE,  R(J)                            *
C        A = TRANSVERSE BED SLOPE,  ST                           *
C        B = MEAN FLOW DEPTH, H                                  *
C        C = RADIUS OF CURVATURE, RC                             *
C        T = TRANSFORMED COORDINATE, DEFINED AS:                 *
C          = SQRT( C * (A * X + B) / (X + C) )                   *
C          = SQRT( RC * ( R(J) * ST + H ) / ( R(J) + RC ) )      *
C  RJ,RJM1 = UPPER AND LOWER INTEGRATION LIMITS, RESPECTIVELY    *
C      SUM = FINAL EVALUATION OF THE INTEGRAL                    *
C * * * * * * * * * * * * * * * * * * * * * * * * * * * * * * * * *
      T2 = SQRT( C * ( A * RJ + B ) / ( RJ + C ) )
      T1 = SQRT( C * ( A * RJM1 + B ) / ( RJM1 + C ) )
      SUM = 0.0
      TT = A * C
      IF(TT .NE. 0.0) GO TO 70
      WRITE(6,60) A
   60 FORMAT(/,5X,'ZERO TRANSVERSE BED SLOPE ST = ',E20.8,/)
      STOP
   70 CONTINUE
      IF(TT .GT. 0.0) GO TO 100
      RIA = ATAN( T2 / SQRT(-TT) ) - ATAN( T1 / SQRT(-TT) )
      RIA = RIA / SQRT( -TT )
      GO TO 150
  100 CONTINUE
      RIA2 = ABS( ( T2 - SQRT( TT ) ) / ( T2 + SQRT( TT ) ) )
```

```
      RIA1 = ABS( ( T1 - SQRT( TT ) ) / ( T1 + SQRT( TT ) ) )
      RIA = ( ALOG(RIA2) - ALOG(RIA1) ) / ( 2.0 * SQRT( TT ) )
  150 CONTINUE
      FAC2 = ( T2**2 - TT )
      FAC1 = ( T1**2 - TT )
      S1 = ( T2 / FAC2**2 ) - ( T1 / FAC1**2 )
      S1 = S1 * ( TT - B ) / 4.0
      S2 = ( T2 / FAC2 ) - ( T1 / FAC1 )
      S2 = S2 * ( 5.0 * TT - B ) / ( 8.0 * TT )
      S3 = -1.0 * ( 3.0 * TT + B ) * RIA / ( 8.0 * TT )
      SUM = 2.0 * ( TT - B ) * ( S1 + S2 + S3 ) * C**2
      RETURN
      END
```

INPUT FILE: SEGDAT

1.56	0.505	8.0	.00104	0.40	2.65	1.1E-05		4
1	137	273	409	545				
43.0	0.0	67.5	1.416	3.276	0.032	0.30		136
38.7	67.5	135.0	1.416	3.276	0.032	0.30		136
-34.83	135.0	202.5	1.416	3.276	0.032	0.30		136
-31.347	202.5	270.0	1.416	3.276	0.032	0.30		136

OUTPUT FILE: OUTT

```
MATHEMATICAL MODEL FOR THE PREDICTION OF
THE VELOCITY FIELD IN RIVER FLOW


*******************************************************************************


VALUES FOR VBAR, H, W, SCL, POR, SG, RMU, NSEG :
  1.560    0.505    8.000  0.10400E-02  0.400  2.650  0.110E-04   4

STCTION NUMBERS WHERE NEW SEGMENTS BEGIN ARE :
   1      137      273      409      545
*******************************************************************************
DOWNSTREAM STEPS =   545  RADIAL STEPS =    17  CENTER AT M =     9
RADIAL POSITIONS STORED AT J = 1    5    9   13   17
RESULTS OUTPUT EVERY     2  SECTIONS
D/S AND RADIAL OUTPUT FREQUENCY IS     1    1   STEPS

RELATIVE ERROR CRITERIA FOR V AND UBAR ARE    0.00100   0.01000
MAXIMUM ITERATIONS    20  PRINTED EACH    10 ITERATIONS
PROGRAM OPTIONS FOR UBAR, MOMENTUM FORM, DIRECTION ARE     3    2    2

INITIAL NUMBER OF SUBINTERVALS FOR SIMPSON RULE =     0
MAX NUMBER OF U-V ITERATIONS IS =    20
DIMENSION OR NUMBER OF SECTIONS TO BE TABULATED IS =      6
AND ARE AT SECTIONS:
       1       69       205       341       477       545

SEDIMENT POWER LAW OF THE FORM  QS = A * ( V )**B
 WITH A, B =       0.1080      4.0000

*******************************************************************************
DISCHARGE =        6.3024 DARCY-WEISBACH F =   0.555483E-01
POWER-LAW N =   0.42429190E+01 RADIAL STEP =   0.5000E+00
LEFT & RIGHT BANK AT R =   0.4000E+01 -0.4000E+01
SHEAR VELOCITY   0.129991E+00  FROUDE NO =   0.387014E+00
N-TERM GIVEN BY   0.103775E+01
QS =    0.639620E+00 ENG TONS/DAY

*******************************************************************************


                   NONDIMENSIONAL QUANTITIES :
TWO GRAVITY TERMS FOR -VERT-, -HOR- ARE   0.667648E+01  0.105766E+03
DEPTH =   0.631250E-01 LEFT AND RIGHT BANKS AT    0.500000E+00 -0.500000E+00
RADIAL STEP   0.625000E-01
*******************************************************************************
*******************************************************************************


NEW SEGMENT --- IMPORTANT PARAMETERS GIVEN AS
FOR SECTION I =     1  RC =   0.430000E+02
```

SEGMENT LOCATION BETWEEN 0.000000E+00 0.675000E+02
ALPHA, BETA = 1.4160 3.2760 THETAC, D50 = 0.0320 0.3000
NUMBER OF SECTIONS BETWEEN S1 & S2 IS 136

COMPUTED VARIABLES FOR THE NEW SEGMENT GIVEN BY

RESTAR, VSTARC, RATIO = 0.116313E+02 0.408905E-01 0.317901E+01
DENSIMETRIC FROUDE = 0.682460E+01
G1, G2, G3 = 0.7181779E-01 0.6249260E+00 0.3922577E+00

****

NONDIMENSIONALIZED QUANTITIES GIVEN BY

RC, S1, S2 = 0.537500E+01 0.000000E+00 0.843750E+01 D50 0.194901E-02
INTERVAL BETWEEN SECTIONS DS = 0.6204044E-01

****

INLET SECTION V =

0.1050030E+01	0.1043364E+01	0.1036822E+01	0.1030402E+01	0.1024100E+01
0.1017912E+01	0.1011835E+01	0.1005865E+01	0.1000000E+01	0.9942364E+00
0.9885712E+00	0.9830016E+00	0.9775252E+00	0.9721394E+00	0.9668416E+00
0.9616295E+00	0.9565008E+00			

Q, QT, ETA = 0.10000000E+01 0.10010936E+01 0.99890757E+00

ETA-MODIFIED V-VELOCITIES WITH UNIT DISCHARGES

J = 1	V = 0.10488832E+01	VA = 0.31250000E-01	VQ = 0.32777600E-01
J = 2	V = 0.10422237E+01	VA = 0.62500000E-01	VQ = 0.65138981E-01
J = 3	V = 0.10356894E+01	VA = 0.62500000E-01	VQ = 0.64730585E-01
J = 4	V = 0.10292764E+01	VA = 0.62500000E-01	VQ = 0.64329773E-01
J = 5	V = 0.10229809E+01	VA = 0.62500000E-01	VQ = 0.63936308E-01
J = 6	V = 0.10167997E+01	VA = 0.62500000E-01	VQ = 0.63549981E-01
J = 7	V = 0.10107291E+01	VA = 0.62500000E-01	VQ = 0.63170567E-01
J = 8	V = 0.10047662E+01	VA = 0.62500000E-01	VQ = 0.62797889E-01
J = 9	V = 0.99890757E+00	VA = 0.62500000E-01	VQ = 0.62431723E-01
J = 10	V = 0.99315012E+00	VA = 0.62500000E-01	VQ = 0.62071882E-01
J = 11	V = 0.98749113E+00	VA = 0.62500000E-01	VQ = 0.61718196E-01
J = 12	V = 0.98192763E+00	VA = 0.62500000E-01	VQ = 0.61370477E-01
J = 13	V = 0.97645724E+00	VA = 0.62500000E-01	VQ = 0.61028577E-01
J = 14	V = 0.97107732E+00	VA = 0.62500000E-01	VQ = 0.60692333E-01

```
J = 15 V =   0.96578526E+00 VA =  0.62500000E-01 VQ =  0.60361579E-01
J = 16 V =   0.96057892E+00 VA =  0.62500000E-01 VQ =  0.60036182E-01
J = 17 V =   0.95545578E+00 VA =  0.31250000E-01 VQ =  0.29857993E-01
NEW VALUE OF QT WITH MODIFIED V =   0.10000000E+01

QS =   0.642432E+00 ENG TONS/DAY   QS/QSACT =    0.100440E+01


I =  1 VALUES FOR UBAR =
   0.0000000E+00  0.3613871E-01  0.6641153E-01  0.9111969E-01  0.1105051E+00
   0.1248353E+00  0.1343290E+00  0.1392268E+00  0.1397205E+00  0.1360422E+00
   0.1283485E+00  0.1168347E+00  0.1016711E+00  0.8302411E-01  0.6104374E-01
   0.3588059E-01  0.7671790E-02


END OF INLET SECTION


******************************************************************************

 FOR SECTION I =     3 ST =   0.527754E-02 UCL =   0.134543E-01
 SATISFACTORY ITERATION      ERRV2 =   0.226433E-03 ERRU2 =   0.417332E-02
 NUMBER OF ITERATIONS KOUNT =    2
 RELATIVE DIFFERENCE OF QT TO Q IS   0.4611015E-03

 CENTERLINE POSITION S =   0.124081E+00 WITH RC =   0.537500E+01
 NEWEST Q =   0.99998546E+00  WITH ETA =   0.1000461E+01
 SEDIMENT DISCHARGE =    0.64231E+00  QS/QSACT =    0.10042E+01

  NUMBER OF ITERATIONS FOR UB, Q, UV ARE      2    2    3
 NEW VALUES FOR UBAR GIVEN BY

   0.0000E+00  0.2017E-01  0.3617E-01  0.4863E-01  0.5781E-01  0.6392E-01
   0.6716E-01  0.6771E-01  0.6576E-01  0.6147E-01  0.5500E-01  0.4648E-01
   0.3606E-01  0.2386E-01  0.1001E-01 -0.5390E-02 -0.2222E-01
 ETA-MODIFIED MOMENTUM VALUES FOR V GIVEN BY
   0.1020E+01  0.1044E+01  0.1038E+01  0.1031E+01  0.1025E+01  0.1019E+01
   0.1013E+01  0.1007E+01  0.1001E+01  0.9946E+00  0.9888E+00  0.9830E+00
   0.9773E+00  0.9716E+00  0.9661E+00  0.9606E+00  0.9552E+00


 FOR SECTION I =     5 ST =   0.986028E-02 UCL =   0.251373E-01
 SATISFACTORY ITERATION      ERRV2 =   0.191607E-03 ERRU2 =   0.489446E-02
 NUMBER OF ITERATIONS KOUNT =    2
 RELATIVE DIFFERENCE OF QT TO Q IS   0.4338026E-03

 CENTERLINE POSITION S =   0.248162E+00 WITH RC =   0.537500E+01
 NEWEST Q =   0.99998736E+00  WITH ETA =   0.1000434E+01
 SEDIMENT DISCHARGE =    0.64227E+00  QS/QSACT =    0.10041E+01

  NUMBER OF ITERATIONS FOR UB, Q, UV ARE      2    2    3
```

```
NEW VALUES FOR UBAR GIVEN BY

  0.0000E+00  0.1002E-01  0.3331E-01  0.4443E-01  0.5249E-01  0.5772E-01
  0.6035E-01  0.6057E-01  0.5857E-01  0.5453E-01  0.4862E-01  0.4097E-01
  0.3174E-01  0.2106E-01  0.9033E-02 -0.4213E-02 -0.1858E-01
ETA-MODIFIED MOMENTUM VALUES FOR V GIVEN BY
  0.1008E+01  0.1044E+01  0.1039E+01  0.1033E+01  0.1027E+01  0.1020E+01
  0.1014E+01  0.1008E+01  0.1002E+01  0.9960E+00  0.9900E+00  0.9841E+00
  0.9783E+00  0.9725E+00  0.9668E+00  0.9611E+00  0.9555E+00
```

VALUES FOR UBAR

R	J = 1	69	205	341	477	545
-0.500	0.0000E+00	0.0000E+00	0.0000E+00	0.1182E-02	0.1787E-03	0.6042E-04
-0.438	0.3614E-01	0.1441E-02	0.2029E-03	-0.8245E-03	-0.1618E-03	-0.6320E-04
-0.375	0.6641E-01	0.2746E-02	0.4165E-03	-0.2621E-02	-0.4552E-03	-0.1663E-03
-0.313	0.9112E-01	0.3708E-02	0.6065E-03	-0.4209E-02	-0.7049E-03	-0.2498E-03
-0.250	0.1105E+00	0.4359E-02	0.7592E-03	-0.5599E-02	-0.9135E-03	-0.3150E-03
-0.188	0.1248E+00	0.4754E-02	0.8690E-03	-0.6791E-02	-0.1082E-02	-0.3628E-03
-0.125	0.1343E+00	0.4934E-02	0.9356E-03	-0.7704E-02	-0.1209E-02	-0.3931E-03
-0.063	0.1392E+00	0.4928E-02	0.9622E-03	-0.8563E-02	-0.1294E-02	-0.4064E-03
0.000	0.1397E+00	0.4760E-02	0.9521E-03	-0.9112E-02	-0.1335E-02	-0.4031E-03
0.063	0.1360E+00	0.4449E-02	0.9090E-03	-0.9404E-02	-0.1329E-02	-0.3830E-03
0.125	0.1283E+00	0.4012E-02	0.8358E-03	-0.9406E-02	-0.1271E-02	-0.3467E-03
0.188	0.1168E+00	0.3464E-02	0.7352E-03	-0.9072E-02	-0.1160E-02	-0.2963E-03
0.250	0.1017E+00	0.2817E-02	0.6090E-03	-0.8335E-02	-0.9956E-03	-0.2344E-03
0.313	0.8302E-01	0.2002E-02	0.4594E-03	-0.7101E-02	-0.7822E-03	-0.1653E-03
0.375	0.6104E-01	0.1269E-02	0.2805E-03	-0.5257E-02	-0.5311E-03	-0.9562E-04
0.438	0.3588E-01	0.3879E-03	0.9738E-04	-0.2756E-02	-0.2573E-03	-0.3515E-04
0.500	0.7672E-02	-0.5553E-03	-0.1121E-03	0.0000E+00	0.0000E+00	0.0000E+00

I	R = -0.5000	-0.2500	0.0000	0.2500	0.5000
1	0.0000E+00	0.1105E+00	0.1397E+00	0.1017E+00	0.7672E-02
2	0.0000E+00	0.4359E-02	0.4760E-02	0.2817E-02	-0.5553E-03
3	0.0000E+00	0.7592E-03	0.9521E-03	0.6090E-03	-0.1121E-03
4	0.1102E-02	-0.5599E-02	-0.9112E-02	-0.8335E-02	0.0000E+00
5	0.1787E-03	-0.9135E-03	-0.1335E-02	-0.9956E-03	0.0000E+00
6	0.6042E-04	-0.3150E-03	-0.4031E-03	-0.2344E-03	0.0000E+00

VALUES FOR U

R	J = 1	69	205	341	477	545
-0.500	0.0000E+00	0.6610E-01	0.6988E-01	-0.1453E+00	-0.1940E+00	-0.1979E+00
-0.438	0.0000E+00	0.7370E-01	0.7577E-01	-0.1445E+00	-0.1881E+00	-0.1913E+00
-0.375	0.0000E+00	0.7968E-01	0.8156E-01	-0.1430E+00	-0.1819E+00	-0.1845E+00
-0.313	0.0000E+00	0.8411E-01	0.8719E-01	-0.1409E+00	-0.1755E+00	-0.1775E+00
-0.250	0.0000E+00	0.8793E-01	0.9268E-01	-0.1383E+00	-0.1688E+00	-0.1704E+00
-0.188	0.0000E+00	0.9148E-01	0.9804E-01	-0.1353E+00	-0.1619E+00	-0.1631E+00
-0.125	0.0000E+00	0.9488E-01	0.1033E+00	-0.1319E+00	-0.1548E+00	-0.1556E+00
-0.063	0.0000E+00	0.9817E-01	0.1084E+00	-0.1282E+00	-0.1476E+00	-0.1480E+00
0.000	0.0000E+00	0.1014E+00	0.1135E+00	-0.1242E+00	-0.1401E+00	-0.1402E+00
0.063	0.0000E+00	0.1044E+00	0.1184E+00	-0.1199E+00	-0.1324E+00	-0.1322E+00
0.125	0.0000E+00	0.1074E+00	0.1233E+00	-0.1153E+00	-0.1245E+00	-0.1241E+00

0.188	0.0000E+00	0.1103E+00	0.1281E+00	-0.1104E+00	-0.1164E+00	-0.1159E+00
0.250	0.0000E+00	0.1131E+00	0.1327E+00	-0.1051E+00	-0.1081E+00	-0.1075E+00
0.313	0.0000E+00	0.1159E+00	0.1373E+00	-0.9912E-01	-0.9958E-01	-0.9900E-01
0.375	0.0000E+00	0.1185E+00	0.1418E+00	-0.9192E-01	-0.9091E-01	-0.9045E-01
0.438	0.0000E+00	0.1210E+00	0.1463E+00	-0.8247E-01	-0.8209E-01	-0.8191E-01
0.500	0.0000E+00	0.1235E+00	0.1506E+00	-0.7012E-01	-0.7326E-01	-0.7360E-01

VALUES FOR V

R	J					
	1	69	205	341	477	545
-0.500	0.1049E+01	0.8691E+00	0.8498E+00	0.9641E+00	0.1085E+01	0.1100E+01
-0.438	0.1042E+01	0.9311E+00	0.8757E+00	0.9805E+00	0.1078E+01	0.1090E+01
-0.375	0.1036E+01	0.9643E+00	0.8988E+00	0.9937E+00	0.1070E+01	0.1079E+01
-0.313	0.1029E+01	0.9801E+00	0.9193E+00	0.1004E+01	0.1060E+01	0.1067E+01
-0.250	0.1023E+01	0.9888E+00	0.9376E+00	0.1011E+01	0.1050E+01	0.1054E+01
-0.188	0.1017E+01	0.9948E+00	0.9543E+00	0.1017E+01	0.1039E+01	0.1040E+01
-0.125	0.1011E+01	0.9996E+00	0.9695E+00	0.1021E+01	0.1026E+01	0.1025E+01
-0.063	0.1005E+01	0.1004E+01	0.9837E+00	0.1023E+01	0.1012E+01	0.1009E+01
0.000	0.9989E+00	0.1007E+01	0.9970E+00	0.1024E+01	0.9971E+00	0.9924E+00
0.063	0.9932E+00	0.1010E+01	0.1009E+01	0.1024E+01	0.9807E+00	0.9741E+00
0.125	0.9875E+00	0.1013E+01	0.1021E+01	0.1022E+01	0.9627E+00	0.9545E+00
0.188	0.9819E+00	0.1015E+01	0.1032E+01	0.1019E+01	0.9428E+00	0.9334E+00
0.250	0.9765E+00	0.1016E+01	0.1043E+01	0.1012E+01	0.9207E+00	0.9107E+00
0.313	0.9711E+00	0.1018E+01	0.1053E+01	0.1000E+01	0.8961E+00	0.8862E+00
0.375	0.9658E+00	0.1019E+01	0.1062E+01	0.9751E+00	0.8688E+00	0.8600E+00
0.438	0.9606E+00	0.1020E+01	0.1071E+01	0.9238E+00	0.8384E+00	0.8323E+00
0.500	0.9555E+00	0.1020E+01	0.1080E+01	0.8330E+00	0.8046E+00	0.8044E+00

I	R				
	-0.5000	-0.2500	0.0000	0.2500	0.5000
1	0.1049E+01	0.1023E+01	0.9989E+00	0.9765E+00	0.9555E+00
2	0.8691E+00	0.9888E+00	0.1007E+01	0.1016E+01	0.1020E+01
3	0.8498E+00	0.9376E+00	0.9970E+00	0.1043E+01	0.1080E+01
4	0.9641E+00	0.1011E+01	0.1024E+01	0.1012E+01	0.8330E+00
5	0.1085E+01	0.1050E+01	0.9971E+00	0.9207E+00	0.8046E+00
6	0.1100E+01	0.1054E+01	0.9924E+00	0.9107E+00	0.8044E+00

VALUES FOR HL

R	J					
	1	69	205	341	477	545
-0.500	0.1000E+01	0.6851E+00	0.6475E+00	0.1386E+01	0.1435E+01	0.1436E+01
-0.438	0.1000E+01	0.7245E+00	0.6916E+00	0.1338E+01	0.1381E+01	0.1381E+01
-0.375	0.1000E+01	0.7638E+00	0.7356E+00	0.1289E+01	0.1326E+01	0.1327E+01

-0.313	0.1000E+01	0.8032E+00	0.7797E+00	0.1241E+01	0.1272E+01	0.1272E+01
-0.250	0.1000E+01	0.8426E+00	0.8238E+00	0.1193E+01	0.1218E+01	0.1218E+01
-0.188	0.1000E+01	0.8819E+00	0.8678E+00	0.1145E+01	0.1163E+01	0.1163E+01
-0.125	0.1000E+01	0.9213E+00	0.9119E+00	0.1096E+01	0.1109E+01	0.1109E+01
-0.063	0.1000E+01	0.9606E+00	0.9559E+00	0.1048E+01	0.1054E+01	0.1054E+01
0.000	0.1000E+01	0.1000E+01	0.1000E+01	0.1000E+01	0.1000E+01	0.1000E+01
0.063	0.1000E+01	0.1039E+01	0.1044E+01	0.9518E+00	0.9456E+00	0.9456E+00
0.125	0.1000E+01	0.1079E+01	0.1088E+01	0.9035E+00	0.8912E+00	0.8911E+00
0.188	0.1000E+01	0.1118E+01	0.1132E+01	0.8553E+00	0.8368E+00	0.8367E+00
0.250	0.1000E+01	0.1157E+01	0.1176E+01	0.8071E+00	0.7824E+00	0.7822E+00
0.313	0.1000E+01	0.1197E+01	0.1220E+01	0.7588E+00	0.7280E+00	0.7278E+00
0.375	0.1000E+01	0.1236E+01	0.1264E+01	0.7106E+00	0.6736E+00	0.6734E+00
0.438	0.1000E+01	0.1276E+01	0.1308E+01	0.6624E+00	0.6192E+00	0.6189E+00
0.500	0.1000E+01	0.1315E+01	0.1352E+01	0.6142E+00	0.5648E+00	0.5645E+00

VALUES FOR (UBAR + U)

R	J					
	1	69	205	341	477	545
-0.500	0.0000E+00	0.6610E-01	0.6788E-01	-0.1441E+00	-0.1938E+00	-0.1978E+00
-0.438	0.3614E-01	0.7534E-01	0.7597E-01	-0.1453E+00	-0.1882E+00	-0.1913E+00
-0.375	0.6641E-01	0.8243E-01	0.8198E-01	-0.1456E+00	-0.1824E+00	-0.1847E+00
-0.313	0.9112E-01	0.8782E-01	0.8780E-01	-0.1451E+00	-0.1762E+00	-0.1778E+00
-0.250	0.1105E+00	0.9229E-01	0.9344E-01	-0.1439E+00	-0.1697E+00	-0.1707E+00
-0.188	0.1248E+00	0.9624E-01	0.9890E-01	-0.1421E+00	-0.1630E+00	-0.1635E+00
-0.125	0.1343E+00	0.9982E-01	0.1042E+00	-0.1397E+00	-0.1561E+00	-0.1560E+00
-0.063	0.1392E+00	0.1031E+00	0.1094E+00	-0.1360E+00	-0.1488E+00	-0.1484E+00
0.000	0.1397E+00	0.1061E+00	0.1144E+00	-0.1333E+00	-0.1414E+00	-0.1406E+00
0.063	0.1360E+00	0.1089E+00	0.1193E+00	-0.1293E+00	-0.1337E+00	-0.1326E+00
0.125	0.1283E+00	0.1114E+00	0.1241E+00	-0.1247E+00	-0.1258E+00	-0.1245E+00
0.188	0.1168E+00	0.1138E+00	0.1288E+00	-0.1195E+00	-0.1175E+00	-0.1162E+00
0.250	0.1017E+00	0.1159E+00	0.1333E+00	-0.1134E+00	-0.1091E+00	-0.1077E+00
0.313	0.8302E-01	0.1179E+00	0.1378E+00	-0.1062E+00	-0.1004E+00	-0.9917E-01
0.375	0.6104E-01	0.1178E+00	0.1421E+00	-0.9718E-01	-0.9144E-01	-0.9054E-01
0.438	0.3588E-01	0.1214E+00	0.1464E+00	-0.8523E-01	-0.8235E-01	-0.8194E-01
0.500	0.7672E-02	0.1229E+00	0.1505E+00	-0.7012E-01	-0.7326E-01	-0.7360E-01

VALUES FOR SQRT((UBAR+U)**2+V**2)

R	J					
	1	69	205	341	477	545
-0.500	0.1049E+01	0.8716E+00	0.8527E+00	0.9740E+00	0.1102E+01	0.1118E+01
-0.438	0.1043E+01	0.9341E+00	0.8790E+00	0.9912E+00	0.1094E+01	0.1107E+01
-0.375	0.1038E+01	0.9678E+00	0.9025E+00	0.1004E+01	0.1085E+01	0.1095E+01
-0.313	0.1033E+01	0.9840E+00	0.9234E+00	0.1014E+01	0.1075E+01	0.1082E+01
-0.250	0.1029E+01	0.9931E+00	0.9423E+00	0.1022E+01	0.1064E+01	0.1068E+01

-0.188	0.1024E+01	0.9995E+00	0.9594E+00	0.1027E+01	0.1051E+01	0.1053E+01
-0.125	0.1020E+01	0.1005E+01	0.9751E+00	0.1031E+01	0.1038E+01	0.1037E+01
-0.063	0.1014E+01	0.1009E+01	0.9898E+00	0.1032E+01	0.1023E+01	0.1020E+01
0.000	0.1009E+01	0.1013E+01	0.1004E+01	0.1033E+01	0.1007E+01	0.1002E+01
0.063	0.1002E+01	0.1016E+01	0.1017E+01	0.1032E+01	0.9898E+00	0.9831E+00
0.125	0.9958E+00	0.1019E+01	0.1029E+01	0.1030E+01	0.9708E+00	0.9626E+00
0.188	0.9889E+00	0.1021E+01	0.1040E+01	0.1026E+01	0.9501E+00	0.9406E+00
0.250	0.9817E+00	0.1023E+01	0.1051E+01	0.1019E+01	0.9271E+00	0.9171E+00
0.313	0.9746E+00	0.1025E+01	0.1062E+01	0.1006E+01	0.9017E+00	0.8918E+00
0.375	0.9677E+00	0.1026E+01	0.1072E+01	0.9799E+00	0.8736E+00	0.8647E+00
0.438	0.9612E+00	0.1027E+01	0.1081E+01	0.9277E+00	0.8424E+00	0.8363E+00
0.500	0.9555E+00	0.1027E+01	0.1090E+01	0.8359E+00	0.8080E+00	0.8078E+00

VALUES FOR VELOCITY VECTOR ANGLES

R				I		
	1	69	205	341	477	545
-0.500	0.0000E+00	0.4349E+01	0.4701E+01	-0.8501E+01	-0.1013E+02	-0.1019E+02
-0.438	0.1986E+01	0.4626E+01	0.4958E+01	-0.8430E+01	-0.9905E+01	-0.9956E+01
-0.375	0.3669E+01	0.4886E+01	0.5211E+01	-0.8330E+01	-0.9674E+01	-0.9713E+01
-0.313	0.5059E+01	0.5120E+01	0.5456E+01	-0.8227E+01	-0.9433E+01	-0.9462E+01
-0.250	0.6165E+01	0.5332E+01	0.5691E+01	-0.8099E+01	-0.9182E+01	-0.9201E+01
-0.188	0.6999E+01	0.5526E+01	0.5917E+01	-0.7954E+01	-0.8921E+01	-0.8932E+01
-0.125	0.7570E+01	0.5702E+01	0.6135E+01	-0.7792E+01	-0.8649E+01	-0.8652E+01
-0.063	0.7889E+01	0.5865E+01	0.6344E+01	-0.7612E+01	-0.8366E+01	-0.8363E+01
0.000	0.7962E+01	0.6015E+01	0.6546E+01	-0.7414E+01	-0.8071E+01	-0.8063E+01
0.063	0.7800E+01	0.6153E+01	0.6741E+01	-0.7195E+01	-0.7764E+01	-0.7751E+01
0.125	0.7405E+01	0.6280E+01	0.6927E+01	-0.6954E+01	-0.7443E+01	-0.7428E+01
0.188	0.6785E+01	0.6398E+01	0.7111E+01	-0.6688E+01	-0.7107E+01	-0.7093E+01
0.250	0.5944E+01	0.6508E+01	0.7286E+01	-0.6393E+01	-0.6757E+01	-0.6746E+01
0.313	0.4887E+01	0.6609E+01	0.7456E+01	-0.6063E+01	-0.6390E+01	-0.6385E+01
0.375	0.3617E+01	0.6704E+01	0.7621E+01	-0.5691E+01	-0.6008E+01	-0.6011E+01
0.438	0.2139E+01	0.6791E+01	0.7781E+01	-0.5271E+01	-0.5610E+01	-0.5623E+01
0.500	0.4600E+00	0.6872E+01	0.7935E+01	-0.4812E+01	-0.5202E+01	-0.5228E+01

VALUES FOR UNIT SEDIMENT DISCHARGES

R				I		
	1	69	205	341	477	545
-0.500	0.7742E+00	0.3650E+00	0.3336E+00	0.5526E+00	0.8062E+00	0.9377E+00
-0.438	0.7547E+00	0.4807E+00	0.3762E+00	0.5912E+00	0.8637E+00	0.9031E+00
-0.375	0.7359E+00	0.5530E+00	0.4174E+00	0.6237E+00	0.8377E+00	0.8666E+00
-0.313	0.7179E+00	0.5902E+00	0.4567E+00	0.6495E+00	0.8089E+00	0.8285E+00
-0.250	0.7005E+00	0.6115E+00	0.4943E+00	0.6695E+00	0.7776E+00	0.7891E+00
-0.188	0.6837E+00	0.6264E+00	0.5304E+00	0.6845E+00	0.7440E+00	0.7484E+00
-0.125	0.6675E+00	0.6386E+00	0.5652E+00	0.6951E+00	0.7085E+00	0.7066E+00

-0.063	0.6519E+00	0.6490E+00	0.5990E+00	0.7016E+00	0.6712E+00	0.6639E+00
0.000	0.6368E+00	0.6580E+00	0.6320E+00	0.7043E+00	0.6322E+00	0.6203E+00
0.063	0.6223E+00	0.6658E+00	0.6642E+00	0.7033E+00	0.5916E+00	0.5759E+00
0.125	0.6082E+00	0.6725E+00	0.6958E+00	0.6905E+00	0.5493E+00	0.5310E+00
0.188	0.5946E+00	0.6781E+00	0.7267E+00	0.6889E+00	0.5053E+00	0.4856E+00
0.250	0.5815E+00	0.6827E+00	0.7567E+00	0.6718E+00	0.4596E+00	0.4400E+00
0.313	0.5688E+00	0.6864E+00	0.7860E+00	0.6408E+00	0.4124E+00	0.3945E+00
0.375	0.5565E+00	0.6892E+00	0.8145E+00	0.5783E+00	0.3645E+00	0.3498E+00
0.438	0.5446E+00	0.6913E+00	0.8422E+00	0.4659E+00	0.3160E+00	0.3069E+00
0.500	0.5330E+00	0.6926E+00	0.8689E+00	0.3079E+00	0.2681E+00	0.2678E+00

APPENDIX C: NOTATION

NOTATION

a	Constant used in sediment-transport formula
A	Constant in quadratic equation
b	Constant used in sediment-transport formula
B	Constant in quadratic equation
C	Constant in quadritic equation
d	Local flow depth
d_c	Centerline flow depth
D_{50}	Median bed-material size
f	Darcy-Weisbach friction factor
F	Arbitrary variable
$F_1,\ldots$	Dimensionless functions
F_r	Froude number
g	Gravitational constant
$g_1,\ldots$	Dimensionless functions
h	Local bed elevation
h_c	Centerline bed elevation
H	Local water-surface elevation
$i,\ldots$	Streamwise grid locations
I	Streamwise index for section numbers
$j,\ldots$	Transverse grid locations
J	Transverse index for section numbers
M	Number of transverse grid points
n	Exponential parameter used in power-law velocity distribution

N	Number of streamwise grid points
p	Bed-material porosity
q_t	Total-load discharge per unit width
Q_t	Total-load discharge
Q	Total water discharge
r	Transverse coordinate
r_i	Radius of curvature at inside bank
r_0	Radius of curvature at outside bank
$r_j,\ldots$	Radial grid locations
R_c	Centerline radius of curvature
s	Streamwise coordinate
s_o	Origin of streamwise coordinate
$s_i,\ldots$	Streamwise grid locations along channel centerline
S_c	Streamwise water-surface slope along channel centerline
S_T	Transverse bed slope
t	Integral function
$T,T_1,\ldots$	Integral functions
u	Local secondary-flow velocity
u_*	Local shear velocity
U	Local secondary-flow velocity at water surface
U_c	Secondary-flow velocity at channel centerline
$\overline{U}$	Mass-shift velocity
v	Local streamwise velocity
V	Depth-averaged streamwise velocity
V_c	Depth-averaged velocity at channel centerline

$\overline{V}$	Area-averaged streamwise velocity
W	Channel width
y	Vertical coordinate
y_b	Bed-layer thickness
α	Proportionality constant for bed-layer thickness
β	Proportionality constant for bed-shear stresses
θ_c	Critical shear-stress parameter
ρ	Fluid mass density
ρ_s	Sediment mass density
τ_o	Streamwise bed-shear stress = τ_{os}
τ_{or}	Transverse bed-shear stress
ϕ	Streamwise angular coordinate